Master Thesis, Department of Geosciences

Ground temperature response to winter warm events in Svalbard

A periglacial landform comparison

Sarah Marie Strand

UNIVERSITY OF OSLO

FACULTY OF MATHEMATICS AND NATURAL SCIENCES

Ground temperature response to winter warm events in Svalbard

A periglacial landform comparison

Sarah Marie Strand

Master Thesis in Geosciences

Physical Geography, Hydrology, and Geomatics

Department of Geosciences

Faculty of Mathematics and Natural Sciences

University of Oslo

May 2016

This thesis was conducted and completed on Svalbard, as part of a guest master student contract at the University Centre in Svalbard (UNIS).

Cover photo: Longyeardalen, showing icy ground conditions following an extreme rain-on-snow event in December 2015 and January 2016. Photo by Ole Humlum.

Abstract

The Svalbard archipelago is subject to winter warm events, where daily mean air temperature exceeds 0°C. These warm events occur when low pressure systems direct air northwards across the Nordic Seas towards the west coast of Spitsbergen (Svalbard's largest island). If the advected air is moist, rain-on-snow (ROS) events result. In this thesis, ground temperatures and meteorological data are coupled to assess the impact of ROS and warm events on periglacial landform ground temperatures. The four landforms chosen for analysis – a loess terrace, solifluction sheet, blockfield, and strandflat – are representative of the varied terrain and ground materials on Svalbard.

Analysis of winter meteorological data from the Longyearbyen area between 1958 and 2015 shows that mean winter (November through April) air temperatures are increasing. While there is no clear trend in winter rainfall (ROS amount), the five rainiest winters of the 1958-2015 record have occurred since 1994. Winter rainfall and the number of days of rain during winter bear some correlation to winter thawing degree days (TDD). Three winters during the investigated ground temperature series had major ROS events (>10 mm). A comparison of 2014-2015 winter air temperatures at the landform locations indicates that winter air temperatures rarely exceed 0°C at higher elevations, which precludes precipitation falling as rain in the winter at these sites.

Warm events result in increased ground temperatures. The thermal disturbance is observed down to 2 m depth in the loess terrace and solifluction sheet, 1 m depth in the blockfield, and 5 m depth in the strandflat. The depth of warm event propagation is dependent on the thermal properties of the substrate, in addition to snow cover. This study shows that the largest ROS events impact shallow ground temperatures more than dry warm events, as liquid water can collect at the ground surface and freeze, releasing latent heat. Neither ROS nor warm events individually impact seasonal or annual ground temperatures; winter ground temperatures are primarily controlled by air temperature and the duration and depth of snow cover. However, the combined effect of multiple warm events can impact mean winter ground temperatures, and may contribute to the observed permafrost warming trend in these landforms.

Acknowledgements

First, I would like to acknowledge my supervisors Hanne Christiansen and Ole Humlum for their guidance throughout my master program and this project. Hanne was incredibly helpful in making arrangements so that I could complete my entire MSc degree on Svalbard, and welcomed me as her student after one brief meeting – for this I am eternally grateful. I would also like to thank Hanne for helping me improve as a scientist, for taking interest in my future career path, and for supporting me during the past two years. I thank Ole for his consistently cheerful demeanor, enthusiasm for teaching, and willingness to discuss my meteorology questions.

Financially, my stay on Svalbard was made possible by the Fulbright Program and the U.S.–Norway Fulbright Foundation. I am also grateful for my past teachers who have each played a part in getting me to where I am today. Special appreciation is extended to members of the Tufts EOS Department and the Svalbard REU, who fostered my interest in the geosciences.

I am deeply appreciative to the people who make Longyearbyen and UNIS such a warm (in the figurative sense) environment to live and learn. As a student employee of the UNIS Library, I have had the pleasure of working with four fantastic women (Ann-Louise, Berit, Cathrine, and Jule) who are incredibly knowledgeable, caring, and fun to be around. Thanks for making the library such an enjoyable work environment. The burgeoning scientists on the old 3rd floor corridor also deserve praise; thanks for bettering long hours in the office and my life in general. Extra thanks are extended to Graham (unfortunately on the 2nd floor) for fielding my frequent questions and giving excellent feedback and advice. Zoe, thanks for our bicontinental friendship and your ability to talk me through anything. I would also like to acknowledge those that have shared coffee breaks or beers at Friday Gathering with me; you have shaped my time at UNIS thus far in a wonderful way.

Lastly, I am ever grateful for my family and friends back in the U.S. who have accepted my move to the high Arctic in stride. (I hope to see more of you up here in the near future.) Thank you for encouraging me to follow my dreams and for supporting me wherever that may be.

Table of Contents

1. Introduction

1.1. Motivation

Permafrost occurrence and ground thermal regime depends largely on major trends in climate (Lachenbruch and Marshall 1986; Williams and Smith 1989). However, the relationship between meteorology and ground temperatures is complex and depends on a number of site-specific factors (Williams and Smith 1989; French 2007). Near-surface ground temperatures exhibit periodic variation with the seasons, but superimposed on this pattern are shorter-term fluctuations resulting from changes in site characteristics and local weather (Williams and Smith 1989). This thesis investigates the impact of short-term air temperature fluctuations, in the form of winter warm events, on ground temperatures in Svalbard.

Svalbard (Figure 1.1) is a particularly relevant location to study the impact of warm events on ground temperatures because (i) permafrost is generally continuous where glaciers are absent, and (ii) Svalbard is subject to significant winter air temperature fluctuations (Humlum et al. 2003). Each winter on Svalbard is punctuated by a few warm events of varying magnitude, length, and moisture content. In this thesis, winter warm events are defined as a day or consecutive days of positive daily mean air temperature. When rain falls during these warm events, water can percolate to the bottom of the snowpack, increasing temperatures at the ground surface as this water freezes and releases latent heat (Westermann et al. 2011). Ground temperature modelling and a related sensitivity analysis by Etzelmüller et al. (2011) indicated ground temperatures at sediment-covered sites in Nordenskiöld Land (west-central Spitsbergen, Svalbard) are more sensitive to changes in winter temperatures than to changes in summer temperatures, making an analysis of winter meteorological fluctuations particularly relevant.

Numerous studies have investigated the thermal state of Svalbard permafrost sites on a yearly or multi-year basis (Harris et al. 2003; Isaksen et al. 2007b; Christiansen et al. 2010), but few have examined how meteorological fluctuations, on the scale of days to weeks, effect ground temperatures. Some papers have addressed specific winter warm events and rain-on-snow (ROS) occurrence on Svalbard (Hansen et al. 2014; Isaksen et al. 2007a; Westermann et al. 2011; Christiansen et al. 2013; Eckerstorfer and Christiansen 2012; Putkonen and Roe 2003), but the long-term meteorological and ground temperature data series available for Spitsbergen have not previously been used to compare events or landform response. ROS events in the circumpolar Arctic are predicted to increase in

frequency during the remainder of the 21st century (Rennert et al. 2009), so there is a specific need to understand how this sort of meteorological event impacts the ground.

1.2. Objectives and hypotheses

This thesis grew out of a desire to utilize and couple the high temporal resolution ground temperature and meteorology data available for Spitsbergen. By using these data sets in tandem, the impact of winter warm events on near-surface ground temperatures can be assessed at the daily scale. To better understand ROS events, the three rainiest winters occurring during the ground temperature data series (2009-2015) are focused on. The main objectives of the thesis overall are to:

- Identify and characterize winter ROS and warm events in the meteorological record from central Svalbard, focusing on those occurring in the last decade;
- Ascertain how deep these warm events can be detected in ground temperatures, and how this depth varies in four different landforms;
- Compare the impact of winter warm events with and without rain on ground temperatures;
- Determine if winter ROS and warm events on the scale of days to weeks impact ground temperatures on a longer scale (i.e. for the rest of the season or hydrologic year).

Previous conclusions in the Svalbard ROS event literature (Hansen et al. 2014; Westermann et al. 2011) are tested as hypotheses. These hypotheses are investigated in the four landforms to assess the impact of ROS events in Svalbard's heterogeneous landscape.

- Strong winter rain events impact ground temperatures, and do so most significantly when snow depth is high and a large quantity of rain falls over a short period (Westermann et al. 2011).
- Winter rain events constrain ground surface temperature near 0°C for prolonged periods (Westermann et al. 2011; Hansen et al. 2014).
- Extreme warm events with rain cause substantial increase in permafrost temperatures, with ground temperature response lasting weeks to months after the event (Hansen et al. 2014; Isaksen et al. 2000).

The validity of these hypotheses is addressed in the discussion in addition to the conclusions and perspectives section.

1.3. Thesis structure

This thesis is divided into eight chapters. Chapters 1 and 2 introduce the project and provide the necessary scientific background, respectively. Chapter 3 explains the geography, climate, and geology of Svalbard, focusing on western Spitsbergen. This chapter also introduces the relevant literature specific to Svalbard. The location and characteristics of the four main study sites are described in Chapter 4. Chapter 5 outlines how the meteorological and ground temperature data was obtained and processed. Chapters 6 and 7, the results and discussion, address the meteorological and ground temperature data and how these data sets relate to one another. Chapter 8 presents the conclusions and implications of the project and proposes areas of further research.

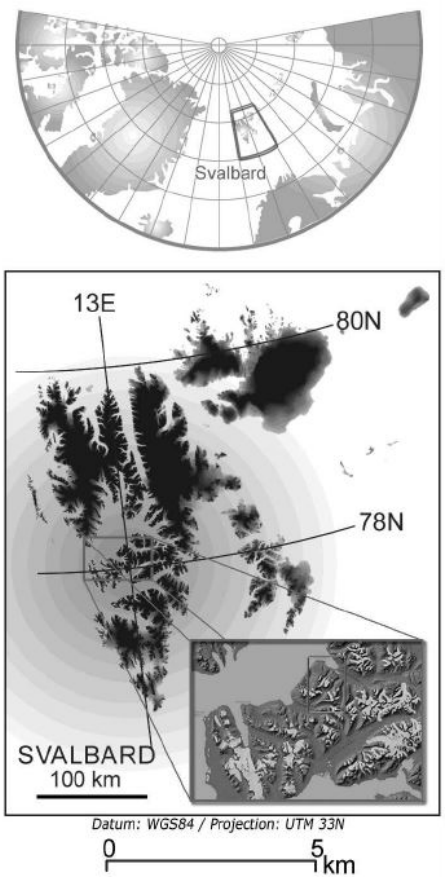

Figure 1.1. Svalbard's Arctic location (top) and its main islands (bottom). The map inset shows Nordenskiöld Land in west-central Spitsbergen, where the focus sites of this thesis are located. From Eckerstorfer and Christiansen (2011).

2. Scientific background

2.1. Permafrost and ground temperatures

2.1.1. Definitions and description

Permafrost is ground that remains at or below 0°C for at least two consecutive years (Harris et al. 1988; French 2007; Williams and Smith 1989). This definition is based entirely on temperature, making the presence of water or ice irrelevant for the technical classification of permafrost. However, water and ice are common constituents of permafrost and play a major role in shaping permafrost terrain. Permafrost is frozen when the ground material has pore water existing as ice (Harris et al. 1988). All permafrost is cryotic, as this term refers to material that is at or below 0°C (Harris et al. 1988). The aforementioned terminology, which differentiates between the state and temperature of the ground, is important because water contained in soil and rock does not necessarily freeze at 0°C. Fine-grained material promotes the adsorption of water, allowing a thin film of water to persist between soil particles and interstitial ice at temperatures below 0°C (French 2007). Capillarity also increases with decreasing soil particle size. This process confines water to progressively smaller spaces, lowering the water's free energy, and necessitating lower temperatures for freezing (Williams and Smith 1989; French 2007). Additionally, the presence of dissolved salts depresses the freezing point of water; this effect increases with the concentration of dissolved salts. These processes can operate at the top of permafrost, making it thaw and freeze annually (i.e. seasonally active) while remaining cryotic (French 2007).

The top layer of ground overlying permafrost is known as the active layer, because this layer undergoes annual freezing and thawing (Harris et al. 1988; French 2007). Unlike the definition of permafrost, the definition of the active layer is based on ground state (i.e. frozen or unfrozen), not temperature. This means the uppermost section of permafrost may be included in the measurement of the active layer if the freezing point of water is depressed, allowing a thin layer of cryotic material to remain unfrozen (French 2007). Active layer thickness is primarily controlled by summer temperatures (Hinkel and Nicholas 1995; Romanovsky and Osterkamp 1997; French 2007), but is also impacted by factors like site wetness, vegetation, and cloud cover (Kudryavtsev et al. 1977; Walker et al. 2003; Christiansen and Humlum 2008). Active layer thickness exhibits interannual variation and varies on the local scale (Brown et al. 2000).

2.1.2. Ground thermal regime

Ground temperatures – both in the active layer and underlying permafrost – are determined by the balance between heat exchange at the ground surface and heat flow from the Earth's interior, represented by the geothermal gradient. Thus, ground temperature at any depth, as well as permafrost thickness, can be estimated from the ground-surface temperature and the geothermal gradient (Williams and Smith 1989). Entirely accurate ground temperatures and permafrost thicknesses are difficult to model because of site-specific factors, and regional aspects like past climate, climate stability, the presence of large water bodies, and geothermal activity (French 2007). Ground temperature data are commonly presented in a diagram showing minimum and maximum ground temperatures (Figure 2.1) or in a mean annual temperature profile (Figure 2.2); these are used to define and characterize ground thermal regime. This prior sort of figure is sometimes called a trumpet curve given the shape of the minimum and maximum temperature lines (Andersland and Ladanyi 2004). The minimum and maximum temperature lines meet at the depth of zero annual amplitude. This depth, which is typically close to or greater than 10 m, is where seasonal temperature variations cease to propagate and ground temperature is constant throughout the year (Williams and Smith 1989). Permafrost temperature measurements at this depth are valuable for studying long-term climatic changes, as high-frequency noise is "filtered out" by the overlying ground (Lachenbruch and Marshall 1986). In this thesis, the uppermost ground temperatures are used, since the high-frequency noise resulting from winter warm events is the focus of this study.

Mean annual temperature profiles of the uppermost meters of ground give valuable information regarding the relationship between air temperature, surface cover (like snow and vegetation), and ground temperatures (Figure 2.2). The surface offset, or difference between mean annual air temperature (MAAT) and mean annual ground surface temperature (MAGST), arises from snow and vegetation cover (French 2007). In the winter, snow insulates, making the ground surface temperature higher than the air; in the summer, vegetation cools the ground surface by shading it from solar radiation. However, since summer in permafrost environments is relatively short and vegetation is relatively limited, the insulating effect of snow dominates and MAGST is usually higher than MAAT (Smith and Riseborough 2002; French 2007). The thermal offset, or difference between MAGST and the temperature at the top of permafrost (TTOP), is dependent on the air thawing index, vegetation effect, and the ratio of thermal conductivity arising from the difference of thawed and frozen ground material (Smith and Riseborough 2002; French 2007). In bedrock, this ratio approaches unity,

eliminating the thermal offset (Smith and Riseborough 2002). In most mineral soils, this ratio ranges from 0.6 to 0.9 depending on water content (Smith and Riseborough 2002). If climate and the ground's thermal conductivity are constant, the mean ground temperature below the top of permafrost will be linear, gently warming with depth due to the geothermal gradient (Williams and Smith 1989). Permafrost temperatures that warm towards the surface imply climatic change or other alterations of surface conditions (Williams and Smith 1989). Warm surface temperatures, departing from linear permafrost temperature profiles, have been observed in a number of Arctic boreholes and are attributed to climate warming (Lachenbruch and Marshall 1986; Isaksen 2007b; Christiansen et al. 2010; Smith et al. 2010; Osterkamp 2007) and increased snowfall (Smith et al. 2010; Osterkamp 2007). Given the relatively long length of winter in permafrost environments, winter meteorology has the potential to alter annual and multi-annual ground thermal regime; permafrost can warm without change in summer conditions if milder winters and/or substantial snow cover prevails (Osterkamp 2007).

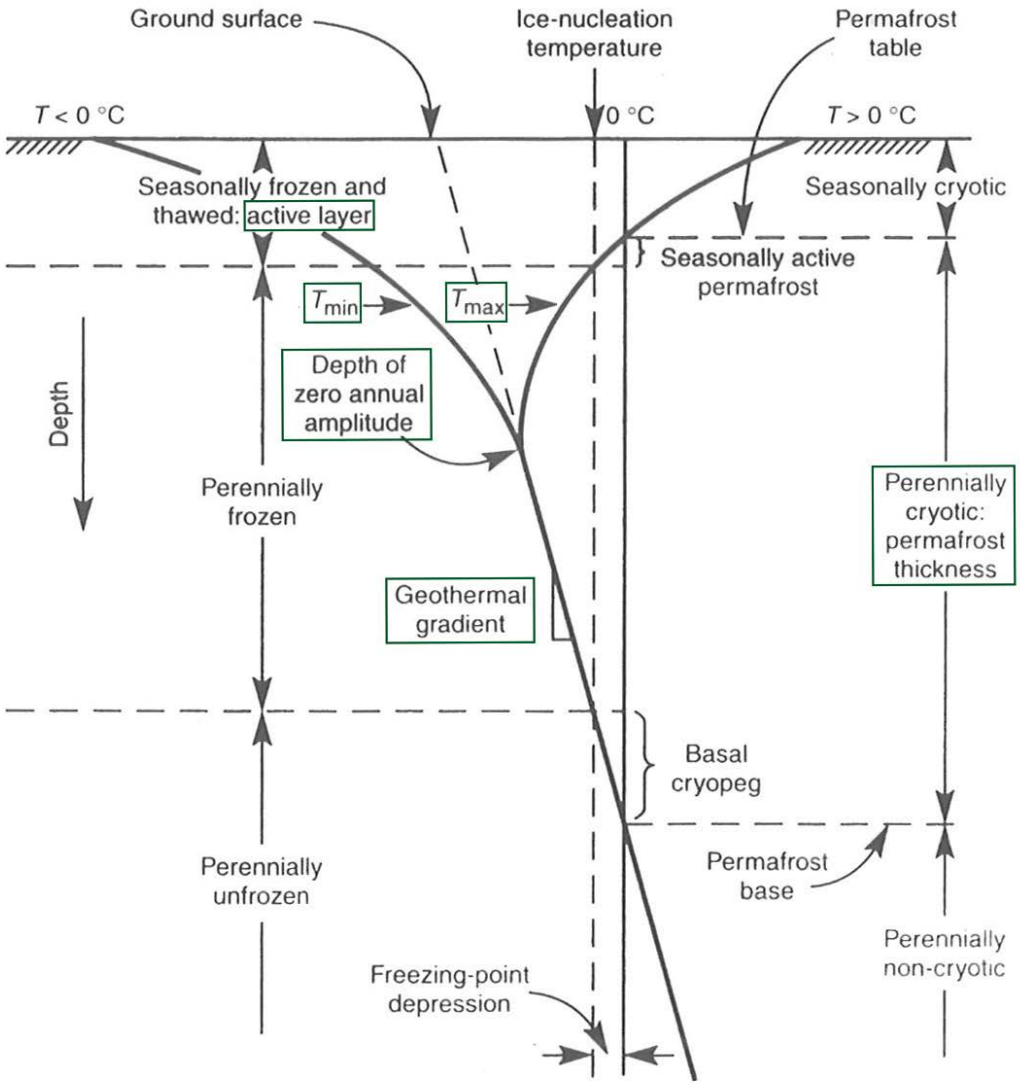

Figure 2.1. Idealized ground temperature profile, with the annual minimum and maximum temperature lines (T_{min} and T_{max}), depth of zero annual amplitude (ZAA), active layer, permafrost thickness, and geothermal gradient highlighted. A projected mean annual ground temperature above the depth of zero annual amplitude is indicated with a dotted line. Adapted from French (2007).

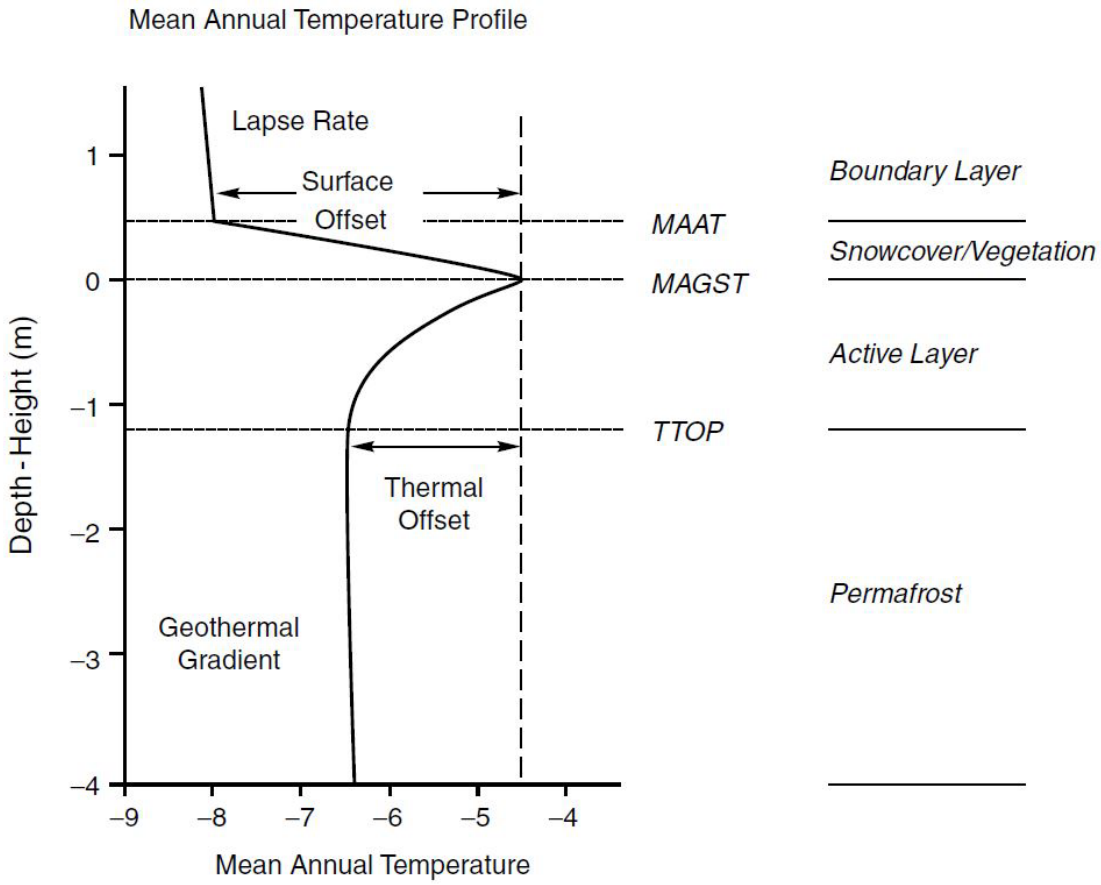

Figure 2.2. A schematic mean annual temperature profile of the upper ground in a permafrost region, which illustrates the typical relationship between mean annual air temperature (MAAT), mean annual ground surface temperature (MAGST), and the temperature at the top of permafrost (TTOP). The surface offset and thermal offset are also depicted. From Smith and Riseborough (2002).

2.2. Rain-on-snow events

Rain-on-snow (ROS) events are frequently mentioned in scientific literature, but their overall occurrence and impact are mainly studied on a case-by-case basis. Taken literally, any rain falling on snow constitutes a ROS event. Small quantities of rain freeze close to the snow surface (Westermann et al. 2011), but if enough rain falls, water will wet sections of the snowpack and reach the ground surface. At the wetting front, which is the transitional zone between wet snow and dry snow, temperature is isothermal and near 0°C (Conway and Benedict 1994). In order for the wetting front to progress spatially through the snowpack, areas of wetted snow must reach 0°C and liquid water must form a continuous film through the wetted snow's pore spaces (Westermann et al. 2011; Colbeck 1979). Water infiltration in snow is a highly non-uniform process, with water flowing through vertical channels (sometimes referred to as "flow fingers") that typically occupy less than 50% of the snowpack (Conway and Benedict 1994) (Figure 2.3). The downward penetration of water in a snowpack is impeded by buried snow crusts and ice layers (Conway and Benedict 1994); increased snowpack heterogeneity and layering leads to increased water absorption and retention (Singh et al. 1997). These processes make water infiltration in snow a difficult process to model and quantify.

Modelling by Westermann et al. (2011) "illustrates that rain events only have strong impact on the soil temperatures if water percolates to the bottom of the snow pack." These authors describe a threshold of liquid precipitation, above which rain will percolate to the bottom of the snowpack. For a 1 m snowpack at -5°C, with an assumed maximum volumetric water content of 0.01, this threshold of liquid precipitation is estimated to be 20 mm (Westermann et al. 2011). This threshold is dependent on snow pack characteristics like temperature and water capacity, which are impacted by snow stratigraphy (Westermann et al. 2011; Singh et al. 1997). Putkonen et al. (2009) define major ROS events as having 10 mm of rain or more, based on the ability of this amount of water to "percolate well into the snowpack," making the snow denser as percolated water freezes. In this thesis, 10 mm of rain or more is considered to constitute a major ROS event, as only one day during the investigated meteorological data series had rainfall exceeding 20 mm. The impact of ROS events in regards to rainfall amount is addressed in the discussion, Section 7.1.4.

If water does percolate through the snowpack, it pools at the frozen ground surface and begins to freeze. During the freezing process, latent heat is released, warming the ground surface as well as the overlying snow (Putkonen and Roe 2003; Rennert et al. 2009; Westermann et al. 2011). Given a sufficiently thick snowpack, it takes weeks for the ice layer to freeze, constraining ground surface

temperatures to 0°C during this time (Putkonen and Roe 2003). The resulting ground ice layers are significant from the ecological perspective, as they hinder ungulates' ability to graze (Putkonen et al. 2009; Grenfell and Putkonen 2008; Rennert et al. 2009). ROS events have been linked to reindeer, caribou, elk, and muskox deaths across the Arctic (Putkonen and Roe 2003). ROS events can also act as a trigger for wet snow and slush avalanches; this has occurred in Spain, Iceland, Switzerland, New Zealand, the USA, Svalbard, and Norway (Furdada et al. 1999; Decaulne and Sæmundsson 2006; Baggi and Schweizer 2009; Conway et al. 2009; Stimberis and Rubin 2011; Eckerstorfer and Christiansen 2012; Jaedicke et al. 2013).

During the 20th century, precipitation in the Arctic and boreal regions has increased approximately 1.4% per decade, with the greatest increases in participation occurring in fall and winter (McBean 2005). While precipitation is increasing, the fraction falling as snow is decreasing (McBean 2005). Groisman et al. (2003) found a significant increase in the number of rain-on-snow events in western Russia between 1950 and 2000; rain-on-snow events in western Canada decreased during this period, though this is attributed to snow cover retreat. Climate models indicate Arctic precipitation will increase over the course of the 21st century, with precipitation increasing up to 35% in the high Arctic by 2071-2090 (Kattsov and Källén 2005). This increase in precipitation, specifically in the Arctic, is explained by a warmer atmosphere causing increased moisture transport to high latitudes (Kattsov and Källén 2005). Rennert et al. (2009) propose that ROS events will occur in more areas of the Arctic and at a higher frequency in the future, though they also suggest these events will decrease in some areas (like coastal Norway) due to decreasing snow extent. Rain-on-snow can be detected through passive microwave satellite data, synthetic aperture radar, and scatterometry (Grenfell and Putkonen, 2008; Hopsø, 2013; Bartsch 2010). Further remote sensing of ROS events will hopefully lead to increased understanding of event frequency, distribution, and impact (Grenfell and Putkonen, 2008; Hopsø, 2013).

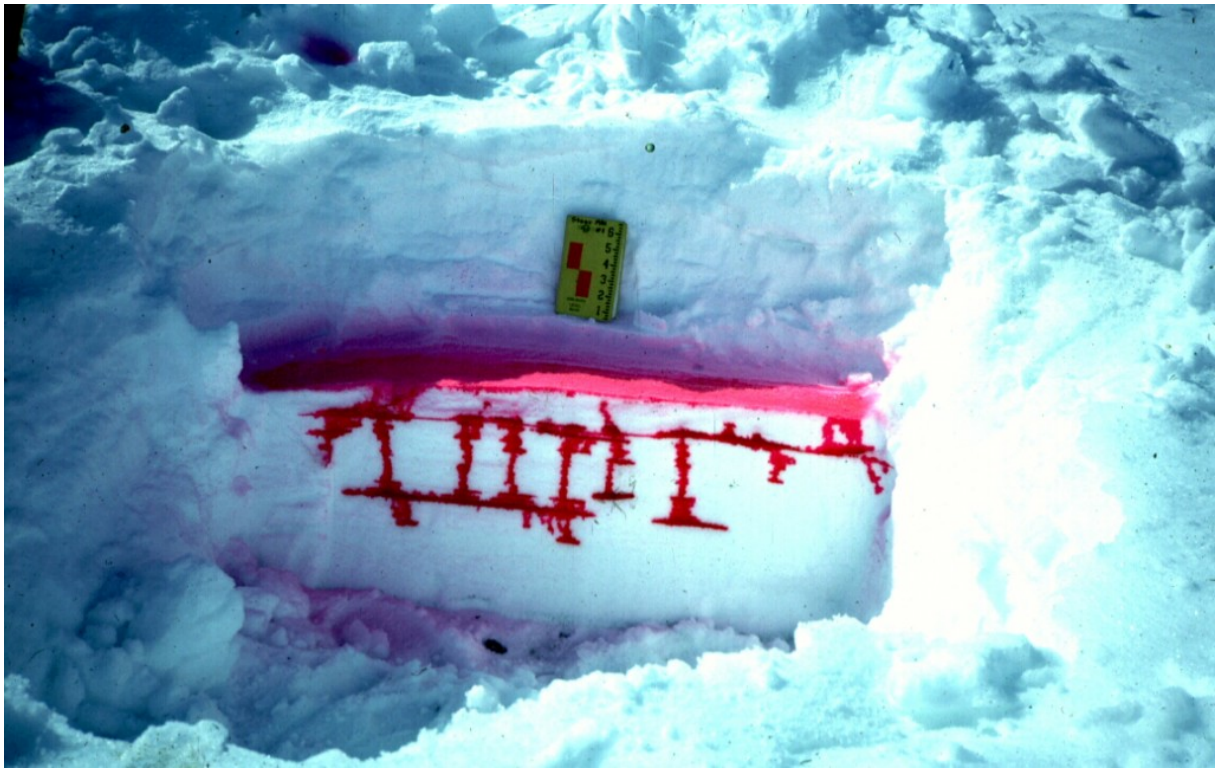

Figure 2.3. Percolation of dyed liquid in a snow pit near Resolute, Nunavut, Canada. Vertical “flow fingers” are visible between horizontal layers within the snowpack that impede downward percolation and promote lateral liquid flow. The scale on the notebook is in inches, and the notebook is 7 inches tall. Photo by Philip Marsh.

3. Regional background

3.1. Svalbard geography and geology

Svalbard is an Arctic archipelago lying east of Greenland and approximately halfway between the Norwegian mainland and the North Pole (Figure 1.1). Spitsbergen, the largest island, accounts for 62% of the archipelago's 60,667 km^2 total area (Dallmann 2015). Rocks from every geologic period since the Archaean can be found on Svalbard (Dallmann 2015). The oldest rocks are found in the western and northern parts of the archipelago; one sample from the Atomfjella mountain range in northeast Spitsbergen was dated to be 2.7 billion years old (Dallmann 2015). Svalbard's latitude has shifted due to plate tectonics from approximately 40°S at the beginning of the Cambrian (ca. 540 Ma) to its present latitudinal range, 74-81°N. The archipelago's environmental setting has also changed drastically throughout geologic history, and includes periods of shallow- and open-marine conditions, orogeny, uplift, volcanism, and glaciation.

Though Svalbard's geologic history stretches into deep time, the archipelago's current morphology was largely shaped by Quaternary glaciations (Ingólfsson 2011; Dallmann 2015). Numerous fjords were carved into the archipelago, created primarily by the active ice streams that existed in the region. Currently, approximately 59% of Svalbard is covered by ice, with the largest ice caps located in eastern Spitsbergen and Svalbard's eastern islands (Dallmann 2015). Permafrost is continuous where glaciers are absent, meaning 90-100% of ice-free ground on Svalbard is underlain by permafrost, which is less than 100 m thick near the coasts and more than 500 m thick in the highlands (Humlum et al. 2003). Svalbard's permafrost terrain exhibits a wide range of periglacial landforms such as ice wedge polygons, patterned ground, rock glaciers, and pingos. These landforms are mainly found on raised beaches and in broad, sediment-filled valleys which characterize central Spitsbergen. Plateau mountains with blockfields are also common in central Spitsbergen, and form from the sandstones, shales, and siltstones that dominate the area south of central Isfjorden. Mountains in the west and north of the island are steep and jagged, comprised of more resistant rock types (Dallmann 2015).

3.2. Quaternary history and permafrost development

During the Quaternary period (2.6 Ma to present), Svalbard was repeatedly covered by the Svalbard-Barents Sea Ice Sheet. Ice rafted debris (IRD) and fine sediment successions found in marine cores indicate this ice sheet initially built-up 3.6-2.4 Ma, and likely covered Svalbard's mountains before advancing towards, but not to, the shelf edge approximately 2.7 Ma (Knies et al. 2009; Butt et al. 2000). IRD fluctuations imply ice retreated back to Svalbard's coastline around 2.4 Ma, and then expanded to the shelf edge ~1.7-1.5 Ma (Knies et al. 2009; Vorren et al. 2011). Changes in clay mineral assemblages in the Fram Strait during this period are proposed as evidence for intensified glacial erosion on Svalbard (Knies et al. 2009). Glaciation intensified around 1.0 Ma, and parts of the Svalbard-Barents Sea Ice Sheet became marine-based; submarine landforms indicate ice reached beyond the shelf edge at this time (Butt et al. 2002; Knies et al. 2009). Vorren et al. (2011) propose eight full-scale glaciations during the Middle Pleistocene (0.78-0.12 Ma) based on debris flows in the Bjørnøya trough mouth fan. Ice reached the shelf break during the Last Glacial Maximum (LGM) between 19 and 15 ^{14}C ka BP (Figure 3.1), and then deglaciation began (Landvik et al. 1998). Climate warming at the transition to the Holocene caused rapid ice sheet decay, and Svalbard's coasts and fjords were ice-free by approximately 10 ^{14}C ka BP (Landvik et al. 1998; Ingólfsson and Landvik 2013).

Figure 3.1. A reconstruction of ice cover around the Svalbard archipelago during the LGM, overlaid on an overview map of modern conditions. Arrows indicate the flow direction of ice streams. From Vorren et al. (2011).

The extent and style of past glaciation partially dictates where permafrost is found today. Extensive permafrost in Siberia is attributed to the absence of ice during the Late Pleistocene, which created cold, sub-aerial conditions and allowed for the formation of deep and continuous permafrost (French 2007). In contrast, the repeated thick ice cover Svalbard experienced during the Quaternary limited permafrost formation. Svalbard's main fjords and associated valleys were occupied by fast flowing ice streams during the LGM (Landvik et al. 2014; Vorren et al. 2011). Any pre-existing permafrost would have been thawed under these ice streams, as the permafrost would have been warmed from the top by frictional heat generated by basal sliding and from the bottom by geothermal heat (Humlum et al. 2003). However, not all permafrost was necessarily eliminated during the LGM. Landvik et al. (2005; 2014) have proposed that the ice covering areas between ice streams (the inter-fjord areas) was less active and periodically cold-based, meaning permafrost could have been preserved. Permafrost, especially when thick and ice-rich, can persist subglacially for thousands of years (Waller et al. 2012). Humlum et al. (2003) propose that high elevation permafrost on Svalbard may date back to the Middle Pleistocene; this is particularly probable where coastal nunataks may have existed (Landvik et al. 1998).

The absolute dating of permafrost is challenging and requires analysis of cryostratigraphy and incorporated material; methods include radiocarbon dating of organics, oxygen isotope analysis of ice bodies, and optically stimulated luminescence (OSL) dating of sediments. Analysis of a 60 m core from lower Adventdalen in central Spitsbergen has shown that the valley was inundated after deglaciation, followed by a period of rapid delta progradation from 6.1 to 4.6 ka (Gilbert 2014). This period marks the earliest possible onset of permafrost development in Adventdalen, as it is when the valley bottom became sub-aerially exposed (Gilbert 2014). This is supported by the dating of three pingos in lower Adventdalen, where the youngest pingo (<140±20 a BP) is adjacent to the modern fjord in the Adventdalen delta and the oldest (<6980±70 a BP) is the furthest inland of the three (Yoshikawa and Nakamura 1996). The pingos are believed to have formed quickly after relative sea level decline exposed the area and allowed for permafrost development (Yoshikawa and Nakamura 1996). The upper meters of permafrost in Adventdalen are syngenetic, meaning the permafrost formed concurrently with sedimentation (Gilbert 2014). Below this, permafrost is epigenetic, having formed after the deposition of the host material (Gilbert 2014; French 2007).

3.3. Spitsbergen's climate and meteorology

3.3.1. Climate and currents

According to the Köppen climate classification system, Spitsbergen has a polar-tundra climate, meaning the mean air temperature of the warmest month is less than 10°C, but at least one month has a mean air temperature exceeding 0°C (Hanssen-Bauer et al. 1990). Within Spitsbergen, inland sites exhibit a more "continental" climate, with summer air temperatures 1-2°C higher and winter air temperatures 2-5°C lower than at the coast (Førland et al. 2009). Serreze and Barry (2014) use Isfjord Radio as an example of a maritime Arctic climate, where winter air temperatures are substantially higher than those of other Arctic sites of similar latitude. A major factor in western Svalbard's relative warmth is the West Spitsbergen Current (WSC); the WSC is the northernmost extension of ocean currents carrying warm, saline Atlantic water through the Nordic Seas (Walczowski and Piechura 2011). The WSC limits sea ice formation in the Fram Strait, permitting intense ocean-atmosphere heat exchange in the winter, making air temperatures during this season milder (Walczowski and Piechura 2011).

Air currents over the Nordic Seas are determined by the position and strength of the Icelandic low pressure system and the Siberian high pressure system, which extends over the central Arctic Ocean towards northern Greenland (Hanssen-Bauer et al. 1990). When the Siberian high extends to the southwest (over continental Europe), southerly winds dominate the Nordic Seas, causing advection of warm, moist air to Svalbard via cyclones and polar lows (Humlum et al. 2003; Tsukernik et al. 2007) (Figure 3.2). These storms bring cloudiness, precipitation, and increased wind speeds to Svalbard (Przybylak 2003; Serreze and Barry 2014; Zahn and Storch 2010). This situation is typical in autumn and early winter, when the contrast between the Icelandic low and Siberian high is greatest (Serreze et al. 1997). As a result of this seasonality, the west-central coast of Spitsbergen experiences distinct seasonality in precipitation; maximum precipitation occurs during autumn and early winter (September-January) and minimum precipitation occurs in spring and early summer (late April, May and June) (Serreze and Barry 2014). Since Svalbard exists in the border zone between air masses, the weather is unstable overall (Hanssen-Bauer et al. 1990). Tsukernik et al. (2007) describe the Icelandic low region as "one of the most synoptically active and variable areas of the planet, especially during winter."

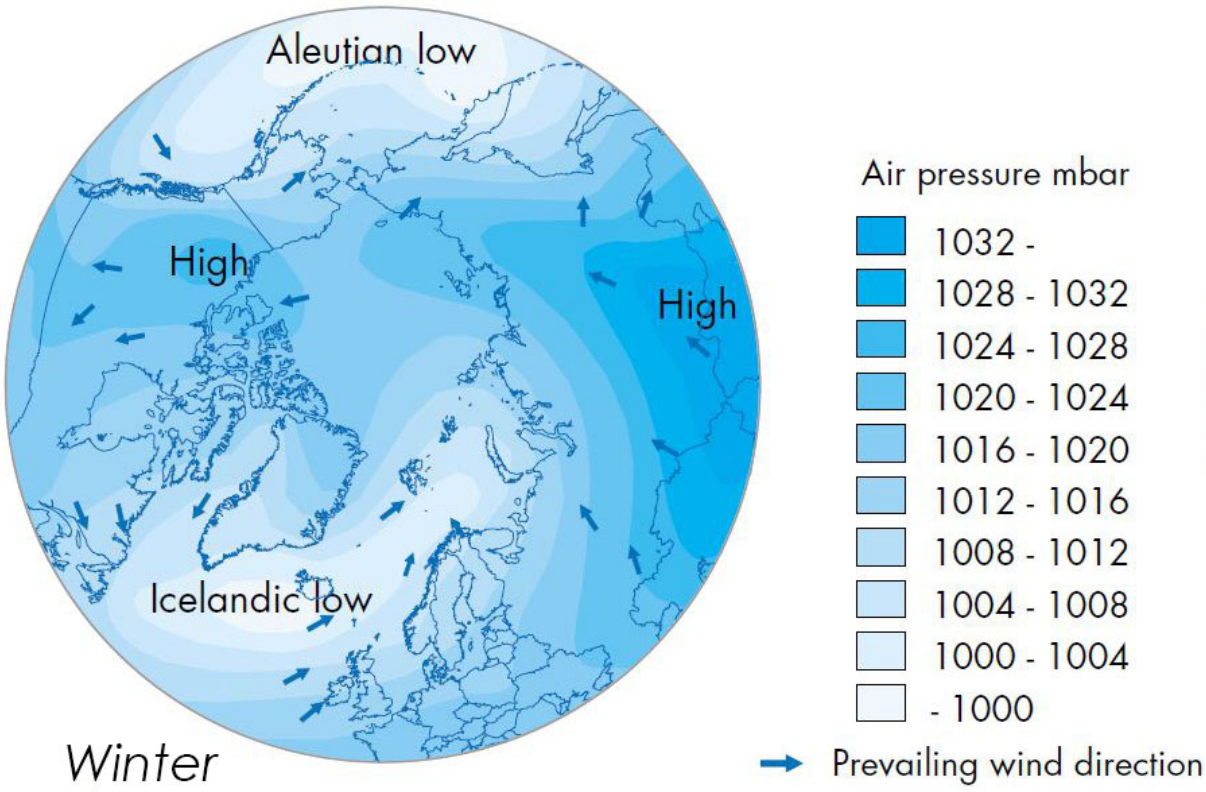

Figure 3.2. Average atmospheric sea-level air pressure in winter over the North Atlantic and Arctic Oceans. The prevailing winds surrounding the Icelandic low bring warm, moist air to Svalbard. Adapted from Arctic Council (2001).

3.3.2. Air temperatures

The average annual air temperature at the Svalbard Lufthavn (Svalbard Airport) was -6.7°C during 1961-1990, and -4.6°C during 1981-2010 (Førland et al. 2011). Mean annual air temperature has increased 2.5°C at Svalbard Airport from 1912-2011, as assessed by a linear trend (Førland et al. 2011). However, air temperature has not consistently increased during this entire period; widespread cooling occurred in the Arctic from 1946 to 1965 (McBean 2005) and this is reflected in annual air temperature trends from Svalbard (Førland et al. 2011) (Figure 3.3). From 1966 to 2011, warming has occurred during all seasons at all Svalbard weather stations except Bjørnøya (Førland et al. 2011), the southernmost island in the archipelago. In the last 30 years Svalbard has experienced the greatest increase in air temperatures (~4°C) of all areas in Europe (Nordli et al. 2014). From 1989 to 2012, winter (December, January, February) and spring (March, April, May) temperatures have increased the most, 2.9°C and 3.9°C respectively, when assessed by a linear trend (Nordli et al. 2014; Førland et al. 2011). Statistically, the winter trend has lower significance; this arises from air temperature exhibiting greater variation in winter compared to the other seasons (Nordli et al. 2014). The average winter

temperature on the west coast of Spitsbergen is approximately -10°C, and in the summer, temperatures rarely exceed 15°C (Førland et al. 2009). Regional climate models indicate that the archipelago will warm 3-8°C between the periods 1961-1990 and 2071-2100, with mean annual air temperature increasing 0.6°C per decade and mean winter air temperature increasing 0.9°C per decade (Førland et al. 2009; Førland et al. 2011). The greatest increases in temperatures are expected in eastern Svalbard, specifically Nordaustlandet and Edgeøya (Førland et al. 2009).

In general, temperatures are colder in north-east Svalbard and at higher altitudes. The mean annual lapse rate in Longyeardalen from 2001-2010 was 0.0062°C m^{-1}, though this lapse rate was seen to increase in May and June and reverse during winter temperature inversions, which mainly occur when sea ice is present (Etzelmüller et al. 2011; Christiansen et al. 2013). Ice-temperature feedbacks are an important component of the climate system in this area, with diminishing sea ice playing a critical role in warming on Svalbard and across the Arctic (Screen and Simmonds 2010; Førland et al. 2009). The absence of sea ice leads to increased absorption of solar radiation, summer ocean heating, and atmosphere-ocean heat exchange; these processes lead to relatively mild and humid terrestrial conditions (Screen and Simmonds 2010; Førland et al. 2009).

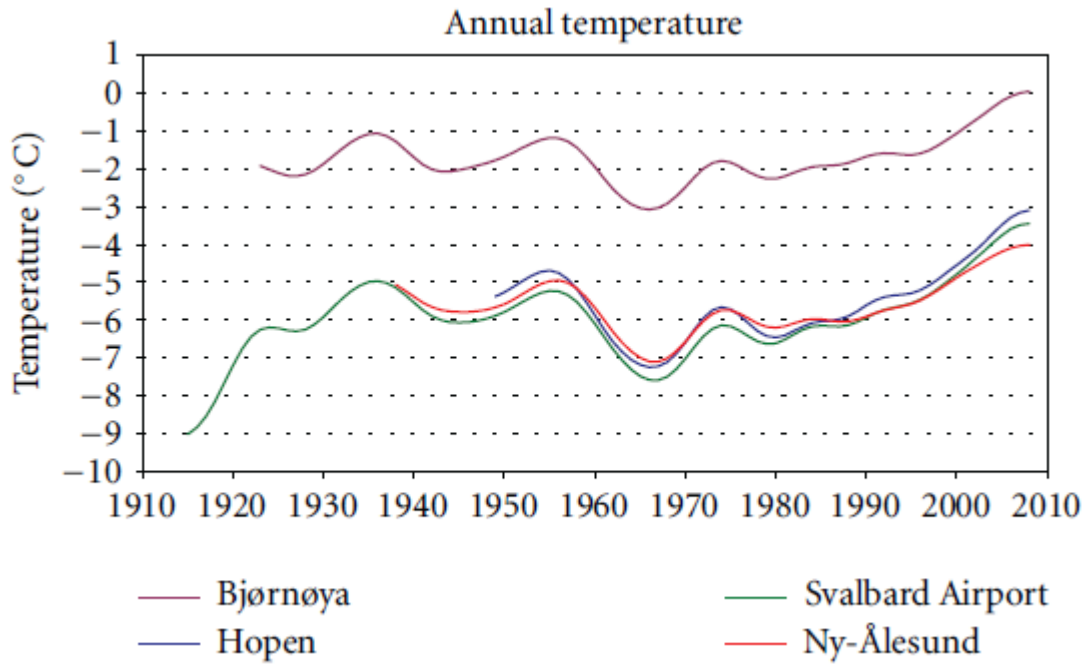

Figure 3.3. Annual temperature development at weather stations in the Svalbard region. Figure and caption from Førland et al. 2011.

3.3.3. Precipitation

Surface temperatures are closely linked with a number of climatic elements, including precipitation. Climatic warming causes an increase of atmospheric water vapor (O'Gorman and Schneider 2009), which in turn causes an increase in poleward vapor transport (Held and Soden 2006) and a general intensification of the hydrologic cycle (Wetherald and Manabe 1975). Thus, moisture transport to high latitudes increases with rising temperatures, and precipitation increases in polar areas (Kattsov and Källén 2005). Given the aforementioned increase in temperature on Svalbard during the past century, an increase in precipitation is expected. Precipitation has increased 2.7% per decade at Svalbard Lufthavn during the period 1912-2001 (Førland and Hanssen-Bauer 2003). However, precipitation is quite limited at this site overall. Between 1961-1990, the annual precipitation at Svalbard Lufthavn was 190 mm – the lowest of any Norwegian meteorological station (Førland and Hanssen-Bauer 2003). The average annual precipitation at both Isfjord Radio (western Spitsbergen) and Ny-Ålesund (northern Spitsbergen) is more than double that of Longyearbyen (Humlum 2002; Førland et al. 2011). Long-term patterns in precipitation are unique for each meteorological station on Svalbard, which Førland et al. (2011) attribute to precipitation varying on a smaller spatial scale than temperature in the high Arctic. Regional climate model simulations show a 40% increase in precipitation in north-eastern Svalbard, and a 12% increase in the Longyearbyen area up to year 2100 (Førland et al. 2011). These precipitation increases will occur during all seasons, but the largest increase is predicted to occur during spring.

On Spitsbergen, the inner fjords receive the least precipitation, and mountain areas receive the most; this is attributed to orographic precipitation (Førland et al. 2009). In Nordenskiöld Land, where all of this thesis' study sites are located, this pattern is manifested in the Longyearbyen/Adventdalen area receiving the least precipitation and mountains near the west coast receiving the most (Humlum 2002). Precipitation increases with altitude on Spitsbergen, but an exact vertical precipitation gradient is not known and likely varies with locality; estimates for precipitation increase per 100 m in altitude gained range from 5-25% (Førland et al. 2009; Humlum 2002).

3.3.4. Wind

Wind is another critical aspect of meteorology on Svalbard, especially since the landscape lacks vegetation. On Spitsbergen, wind is typically funneled by fjords and valleys, blowing towards the coast (Førland et al. 2009). At unconfined sites, like plateau tops, wind speeds are generally lower and reflect the regional airflow from the south-east to the north-west (Christiansen et al. 2013). Isfjorden locally

strengthens winds, making Isfjord Radio a particularly windy meteorological station; over half of all days between November and March have a maximum wind speed greater than 14 m/s (Førland et al. 2009). In the Longyearbyen area, the highest wind speeds occur during late autumn and early winter, which coincides with peak cyclone activity (Christiansen et al. 2013; Serreze et al. 1997). Between 2000 and 2010 (hydrological years), the average annual wind speed at Svalbard Lufthavn was 4.97 m/s (Christiansen et al. 2013). Maximum wind speeds are projected to increase over the ocean between Svalbard and Novaya Zemlya in the coming century, whereas projected changes in wind conditions over Svalbard are small and uncertain (Førland et al. 2009).

The interaction of wind with terrain governs snow distribution in central Spitsbergen, and preferentially deposits snow in regional catchments and leeward areas (Farnsworth 2013). Modelling by Schirmer et al. (2011) has shown qualitative snow distribution patterns can be reproduced given terrain, wind speed, and total available precipitation parameters. However, the model failed to reproduce accurate snow depths, which is attributed to the nonlinear relationship between snow redistribution and wind speed. The precipitation distribution around Ny-Ålesund is strongly dependent on wind direction, with up to 60% more precipitation occurring on the glacier Austre Brøggerbreen than in Ny-Ålesund (which is immediately adjacent) during southerly winds (Førland et al. 1997). Ground temperatures are largely affected by wind distribution of snow, as this process plays a role in determining snow thickness, density, and timing, all of which impact insulation of the ground (Farnsworth 2013). Wind can also directly impact ground temperatures; blocky debris, which covers numerous mountains in Spitsbergen, can be ventilated by high wind speeds. This process can alter active layer temperatures, as a continuous air exchange with the atmosphere is maintained (Humlum 1997; Juliussen and Humlum 2008).

It must be noted that wind also effects other meteorological measurements. On windy days, falling snow is frequently diverted away from the opening of measurement gauges, creating a significant undercatch problem; this is less of an issue for more aerodynamic raindrops (Fassnacht 2004). Conditions on Spitsbergen are frequently windy, so a correction factor can be applied (i.e. multiplied) to gauge measurements. In Ny-Ålesund, the correction factors of 1.15 for rain and 1.85 for snow were determined (Førland and Hanssen-Bauer 2000). Førland and Hanssen-Bauer (2000) also explained how these correction factors impact the observed precipitation increase over the last century at Svalbard meteorological stations. Since temperature has also increased over this period, the fraction of

precipitation falling as snow has presumably decreased, meaning gauge undercatch has decreased as well. Thus, the observed precipitation increase is partially due to a decrease in undercatch error.

3.3.5. Rain-on-snow events

Rennert et al. (2009) describe Svalbard as an ideal setting to study ROS, as event magnitude is relatively large in this location and there are reliable meteorological stations scattered throughout the archipelago. These same authors predict an increase in ROS frequency in Svalbard in the coming half-century, based on the output of a general circulation climate model. Regional climate model results show that the amount of precipitation falling as snow between December and February in south-west Spitsbergen will decrease in the coming century (Førland et al. 2009), which implies there will be an increase in rain during these months. A decrease in the fraction of precipitation falling as snow has already been observed at Svalbard Lufthavn during the latest decades (Førland and Hanssen-Bauer 2003).

ROS events on Svalbard occur when low pressure systems direct warm and moist winter storms northwards across the Nordic Seas towards the west coast of Spitsbergen (Putkonen and Roe 2003). Putkonen and Roe (2003) determined that ROS events on Spitsbergen are five times more likely during extreme positive phases of the North Atlantic Oscillation (NAO), which exacerbates the pressure differences and promotes the cyclone activity previously described in Section 3.3.1. Spitsbergen ROS events described in the literature have occurred during the winters of 1994, 1996, 2006, 2007, 2010, 2011, and 2012 (Kohler and Aanes 2004; Putkonen and Roe 2003; Isaksen et al. 2007a; Westermann et al. 2011; Eckerstorfer and Christiansen 2012; Hansen et al. 2014). The events in 1996, 2006, and 2007 all confined ground surface temperatures close to 0°C for multiple weeks, due to pooled rain slowly refreezing at the ground surface (Putkonen and Roe 2003; Westermann et al. 2011). The events in 2010, 2011, and 2012 are particularly well documented. Three-quarters of the 68.7 mm of precipitation that fell in the Longyearbyen area during January 2010 was rain, resulting in wet snow avalanches and thick ground surface ice cover in Adventdalen (Eckerstorfer and Christiansen 2012; Christiansen et al. 2013). In March 2011, 30.4 mm of rain fell in three days; during this time temperature and wind speed reached 4.2°C and 32 m/s respectively (Eckerstorfer and Christiansen 2012). This event also spawned a wet snow avalanche cycle (Eckerstorfer and Christiansen 2012). On 30 January 2012, 98 mm of rain fell in Ny-Ålesund, which is approximately 25% of mean annual precipitation in this location (Hansen et al. 2014). On the same day in Longyearbyen, 25.9 mm of rain fell and daily mean temperature was 4.0°C (Hansen et al. 2014). Other ROS events have occurred since winter 2012, but information about their meteorology and the resulting biological and physical effects has not been published.

4. Study Sites

4.1. Site selection

The majority of Svalbard permafrost data comes from field sites that are easily accessible from Longyearbyen, the largest settlement of the archipelago. The four boreholes focused on in this thesis are located within Nordenskiöld Land (Figure 4.1), which is bounded by Isfjorden in the north and Van Mijenfjorden in the south. Longyearbyen, Barentsburg, and Svea – Svalbard's main settlements and mining areas – are located in this region. Because of this, weather and avalanche forecasts are made specifically for Nordenskiöld Land. All the investigated boreholes, except for Breinosa, were drilled as part of the International Permafrost Association's Thermal State of Permafrost (TSP) project during the 2007-2008 International Polar Year. The Breinosa borehole was drilled the following year by LNS Spitsbergen and Store Norske for geological surveying, and then was instrumented for thermal monitoring by the University Centre in Svalbard (UNIS).

The four boreholes (Table 4.1) were chosen for their long time series (since 2008) and high density of thermistors near the ground surface. The sites are close enough to utilize meteorological data from the same station (Svalbard Lufthavn), but have unique characteristics that allow for comparison across a number of different factors. Specifically, the chosen sites allow for the investigation of ground temperature response to warm events at low vs. high elevations and maritime vs. relatively continental sites. In addition, each borehole is located in a different type of periglacial landform and thus has a unique substrate and sedimentology: the Old Auroral Station 2 borehole is located in a loess terrace overlying fluvial and marine sediments; the Endalen borehole is located in a diamicton solifluction sheet; the Breinosa borehole is located in a blockfield; and the Kapp Linné 1 borehole is located in strandflat bedrock. This range of landforms is representative of the varied terrain and ground materials on Svalbard, spanning from fine-grained to coarse-grained sediments, and bedrock. Each site's ground temperature data and metadata can be obtained from NORPERM, a permafrost database established as part of the TSP project and maintained by the Geological Survey of Norway (NGU) (NORPERM 2016). From this point forwards, the boreholes will primarily be referred to by the landforms that contain them, though the headings in the following section contain the common borehole names in parenthesis, as these names indicate location and are used in literature and the NORPERM database.

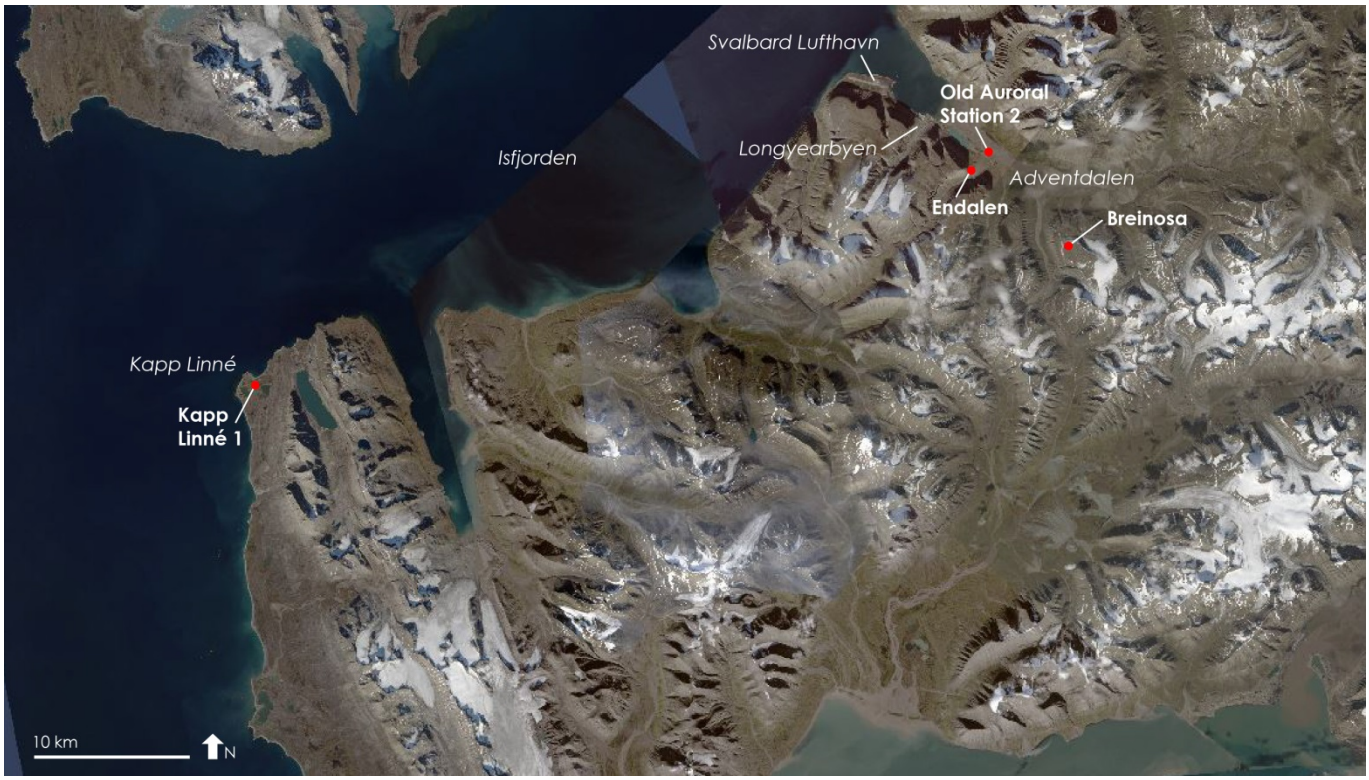

Figure 4.1. Location of the study boreholes (red dots with borehole name) within Nordenskiöld Land, west-central Spitsbergen (see Figure 1.1 for the location of Nordenskiöld Land within Svalbard). Geographic areas of interest mentioned in the text are written in italic. The background is stitched satellite photos, available from the Norwegian Polar Institute (2016) Svalbardkartet.

Borehole name/ID, Landform	Longitude	Latitude	Elevation (m a.s.l.)	Borehole depth (m)	Landform/ ground material	Start date	Instrumentation	Sensor depths (m)
Old Auroral Station 2/AS-B-2, Loess terrace	15°50'05"E	78°12'05"N	9	10	Loess terrace. Ice at 3-4 m depth, marine sediment below 6 m	30.07.2008	GeoPrecision	0, 0.25, 0.5, 0.75, 1, 2, 3, 5, 7, 9.85
Endalen/EN-B-1, Solifluction sheet	15°46'54"E	78°11'26"N	53	20	Solifluction slope. 6 m diamicton above 1.7 m crushed bedrock; solid bedrock below	16.09.2008	Campbell w/YSI thermistors	0, 0.25, 0.5, 0.75, 1, 1.5, 2, 2.5, 3, 4, 5, 6, 7, 8, 9, 10, 12, 15, 19
Breinosa/E-2009, Blockfield	16°04'01"E	78°08'35"N	677	335	12 m weathered material above bedrock	07.03.2009	GeoPrecision	0, 0.25, 0.5, 1, 2, 3, 4, 5, 7, 10
Kapp Linné 1/KL-B-1, Strandflat (bedrock)	13°38'05"E	78°03'21"N	20	30	Strandflat, bedrock	23.09.2008	Campbell w/YSI thermistors	0, 0.25, 0.5, 0.75, 1, 1.5, 2, 2.5, 3, 4, 5, 6, 7, 8, 9, 10, 12, 15, 20, 25, 29

Table 4.1. Metadata for the four focus boreholes, obtained from NORPERM (2016) and Christiansen et al. (2010).

4.2. Site descriptions

4.2.1. Loess terrace (Old Auroral Station 2)

The Old Auroral Station 2 borehole is located in a loess terrace on the southern side of Adventelva (Advent River), approximately 5 km east of Longyearbyen (Figure 4.2). The borehole is roughly 60 m away from the active stream bank and 180 m away from a cluster of buildings that were used for aurora research prior to 2008. The ground surface is relatively flat and has patchy vegetation consisting of *Salix herbacea* L. (snowbed willow), sedges, and mosses (Bryant 1982). The upper 4 m of the loess terrace consists of aeolian-deposited, horizontally laminated sandy silt (Bryant 1982). In the upper 2 m, grain size distribution is relatively homogeneous and the most abundant grain sizes are fine sand and silt (Langhamer 2009). During drilling, clean ice was encountered between 3 and 4 m depth – this was likely part of an ice wedge (Christiansen et al. 2010). Below 4 m there are delta top and fluvial sands and silts overlying delta front deposits. These sediments were deposited during the middle Holocene when the Adventdalen fjord-head delta prograded; this progradation was caused by forced regression arising from isostatic sea level change (Gilbert 2014). During the summer, the ground surface is dry. A Circumpolar Active Layer Monitoring (CALM) grid lies next to the borehole, and in September 2015 the maximum active layer thickness was 105 cm. Winds are funneled and strengthened by the topography of Adventdalen, resulting in a thin (<30 cm) winter snow cover (NORPERM 2016). Between 25 January and 22 March 2013, average snow depth at this landform was 18 cm (Farnsworth 2013).

4.2.2. Solifluction sheet (Endalen)

Endalen is a tributary valley of Adventdalen, with its opening just south of the location of the Old Auroral Station 2 borehole (Figure 4.2). The borehole is located in a solifluction sheet on an east-facing slope at the entrance of Endalen (Figure 4.3). Vegetation in this area is dominated by dwarf shrubs and mosses (Elberling 2007). The solifluctuion sheet is located at the base of a 457 m plateau mountain; the 30-40° upper slopes are scree-covered with bedrock outcrops (Harris et al. 2011). Roughly 250 m upslope from the borehole, there is a break in slope where the rocky terrain transitions into the solifluction sheet with an approximately 7° slope (Harris et al. 2011). The active layer is approximately 1 m thick at this site, and is composed of frost-susceptible sandy silt diamicton with sandstone clasts and ice lenses (Harris et al. 2011). Drilling elsewhere in the solifluction sheet revealed that ground ice content is approximately 45% by volume around 90 cm depth; this ice-rich section indicates the

transient layer, which is the zone of contact between the active layer and top of permafrost (Harris et al. 2011; French 2007). The upper 6 m of the borehole is diamicton interspersed with ice lenses. From 6 to 7.7 m depth there is a zone of crushed bedrock, which overlies solid bedrock comprised of sandstones, siltstones, and shale from the Middle Jurassic (NORPERM 2016; Etzelmüller et al. 2011). Since the site is at the base of a leeward slope, given Adventdalen's strong south-easterly winds in winter (Christiansen 2005), moderate snow cover (between 30 and 80 cm) builds up around the area in the winter. Between 2006 and 2009, maximum winter snow depth at the solifluction sheet was between 45 and 60 cm. Between 25 January and 22 March 2013, average snow depth was 38 cm (Farnsworth 2013). Both the timing of snow cover and the thickness of the snowpack exhibit significant interannual variation at this location (Harris et al. 2011). The summer ground surface is moist, as water percolates into the solifluction sheet from melting snow patches both atop and upslope from this landform. This contrasts with the loess terrace, which is well-drained and thus exhibits a relatively dry ground surface in the summer.

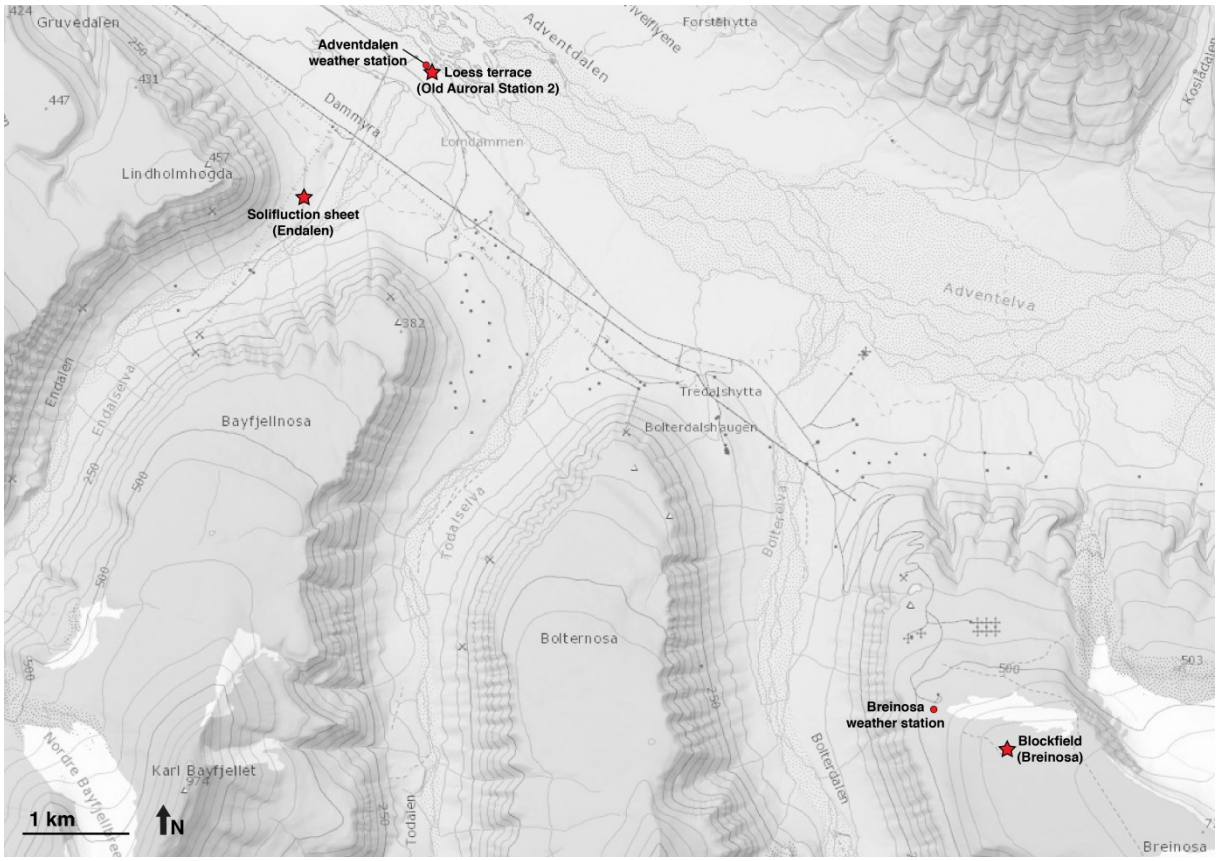

Figure 4.2. Detailed map of the Adventdalen area boreholes. The landforms/borehole sites are marked with stars. The small dots show the location of two weather stations. The basemap is available from the Norwegian Polar Institute (2016) Svalbardkartet.

Figure 4.3. The Endalen site, with a circle indicating the location of the solifluction sheet monitoring station, which is adjacent to the borehole. The photograph is looking northwest, and shows the steep scree upper slope and vegetated solifluction sheet. From Harris et al. (2011).

4.2.3. Blockfield (Breinosa)

The blockfield is located on top of Breinosa, a flat-topped mountain approximately 15 km east of Longyearbyen on the southern side of Adventdalen. The highest portion of the mountain is covered by the Foxfonna ice cap. The unglaciated summit area is covered by blockfields and has seasonal snowfields. The borehole is located in one of these blockfields, on the northern tip of the summit plateau just upslope from the terminus of the nearest road (Figure 4.2). More snow collects around this borehole than at the loess terrace, as the Breinosa borehole is located in a small depression a few meters across (Figure 4.4). Snow depth measurements have not been made at this site, but digital photogrammetry experiments conducted elsewhere on Breinosa indicate that snow reliably accumulates in terrain hollows (Cimoli 2015). The upper 12 m of the borehole consists of coarse weathered material, below which is solid bedrock (NORPERM 2016). Though the entire borehole is 335 m deep, the casing is 16.3 m long and is closed at the bottom to prevent water intrusion. There is an active mine extending into Breinosa; temperatures recorded in the main mine corridor during 2003-2004 indicate permafrost is between 100 and 300 m thick within this mountain (Christiansen et al. 2005). The mine corridor traverses under the east side of the summit plateau, while the borehole is located on the west side of the summit plateau (Christiansen et al. 2005).

Figure 4.4. Downloading data from the blockfield borehole instrumentation in autumn 2015, after some of the season's first snow. The small depression the borehole sits in is indicated by fewer rocks protruding through the snow in this area (bottom left corner of the photo). The thermistor string used for temperature measurements can be seen in front of the yellow borehole casing. Photo by Sarah Strand.

4.2.4. Strandflat (Kapp Linné 1)

The strandflat borehole is located at Kapp Linné, a promontory on the west coast of Spitsbergen at the southern mouth of Isfjorden. This site is approximately 50 km west-southwest of the Longyearbyen area and location of the other boreholes. Strandflats are erosional, coastal rock platforms found at relatively high latitudes (Benn and Evans 2010). The strandflat at Kapp Linné is comprised of marine terraces, beach ridges, bedrock outcrops, small lakes, and bogs. Small polygons (5-15 m) can be found in the sand and gravel beach deposits; both ice wedges and soil wedges exist in the area as well (Watanabe et al. 2013). The borehole is drilled into pre-Devonian schist and carbonate bedrock, which is weathered in the upper 30 cm. The active layer was 2.5 m at this borehole between September 2008 and September 2009; this is thicker than the active layer at any of the Adventdalen area boreholes. The relatively thick active layer is due to the higher thermal diffusivity of rock compared to that of organics and sediments (Christiansen et al. 2010). Kapp Linné is the site of Isfjord Radio, where meteorological measurements are made. As is mentioned in Section 3.3, Isfjord Radio is frequently wet and windy, with winter air temperatures approximately 3°C warmer than those at Svalbard Lufthavn (Nordli et al. 2014). Wind minimizes snow accumulation in the low-relief strandflat area, making winter snow thickness less than 30 cm (NORPERM 2016; Watanabe et al. 2013).

5. Methods

5.1. Meteorological data

This project concerns the impact of warm events on ground temperatures during the winter period. Warm events are defined as a day or consecutive days with positive daily mean air temperature. Winter is defined as 1 November through 30 April. During this period, ground temperatures are typically below 0°C. Snow cover begins to form in October, and is reliable at sea level by November. Maximum snow depths are typically reached in April, and in May the snow begins to melt (Eckerstorfer and Christiansen 2011). Hereafter, winter refers to November-April, unless noted otherwise. When possible, winters are referred to by both calendar years they are comprised of for clarity (ex. 2008-2009 winter). In situations where multiple winters are being compared or appear in a single figure, winters are referred to by the year in which they end.

Data for the identification and analysis of winter warm events and rain-on-snow events was obtained from eKlima, a climate and meteorological database hosted by the Norwegian Meteorological Institute (eKlima 2016). The long-term winter record (1958–2015) presented is a composite of data from two weather stations. Between 1958 and 1975, data are sourced from the Longyearbyen manual weather station. The Longyearbyen station was located where the governor's office is currently situated. In 1964, the radiation screen and precipitation gauge were moved 61 m and 68 m, respectively, which reduced the station elevation from 38 m to 37 m. The 1958–1975 data series is homogeneous (Nordli et al. 1996). From 1976 to the present, data from the Svalbard Lufthavn station was used; this station is located near the southern shore of outer Adventfjorden and has an elevation of 28 m (Figure 4.1). The sensors at the Svalbard Lufthavn station were moved 150 m in October 2010 to prevent thermal influences from airport activity (Nordli et al. 2014). The old Longyearbyen station and the modern Svalbard Lufthavn station are separated by 3.8 km of coastline. The Svalbard Lufthavn station is approximately 50 km from Kapp Linné (Figure 4.1).

The Longyearbyen weather station was located on a small plateau above the valley floor, and temperatures at this location are slightly warmer than temperatures at Svalbard Lufthavn. When the homogenized, extended Svalbard Airport temperature series (1898–2012) was created, the Longyearbyen series was adjusted no more than -1.5°C for incorporation into the principal Svalbard Airport series (Nordli et al. 2014). The composite Longyearbyen-Svalbard Lufthavn 1958–2015 series used here is therefore not homogeneous, but still allows for a basic assessment of long-term winter

meteorology trends, given the relatively small difference in site temperature and location. The two separate Longyearbyen and Svalbard Lufthavn meteorological series were used in thesis over the homogenized Svalbard Airport temperature series because of the need for precipitation data to determine rain-on-snow events.

Daily mean air temperatures and daily precipitation totals were used for climate analysis of winters during the entire 1958-2015 period. For each winter, the average temperature, rain sum, and accumulated thawing degree-days (TDD) were calculated. TDD are dependent on the duration and magnitude of warming and are connected with active layer thickness (Brown et al. 2000; Åkerman and Johansson 2008; Smith et al. 2009), sea ice thickness (Su and Wang 2012), and sea ice extent (Drobot et al. 2008). TDD values were obtained by summing positive daily mean air temperature values during each winter. It should be noted that between 2012 and 2015, nine days are missing a daily mean air temperature value. Inaccuracies in the calculated average winter temperatures and TDD caused by the missing data are considered negligible. Mean annual air temperatures (MAAT) were calculated by averaging the daily mean air temperatures for each calendar year.

Winter rain sum values must be viewed as estimates, because there is not reliable information regarding what precipitation fell as rain vs. wet snow. During some periods, precipitation type was recorded at the stations. However, these observations are not cohesive or reliable throughout the entire data set, so the rain sum has been calculated as the sum of precipitation values on days with a mean air temperature equal to or higher than the threshold temperature. The threshold temperature refers to the temperature where the probability for liquid and solid precipitation is equal (Førland and Hanssen-Bauer 2003). The threshold temperature is 1.96°C for the original Longyearbyen station, and 1.70°C for the Svalbard Lufthavn station (Førland and Hanssen-Bauer 2003). Using these threshold temperatures largely eliminates accidental counting of wet snow as rain, which greatly increases precipitation totals. Less than 10% of snow events at Svalbard Lufthavn occur during air temperatures above 0°C (Førland and Hanssen-Bauer 2003), so snow is unlikely to be incorporated into the rain sum totals. Mixed precipitation like sleet and freezing rain may be counted in the rain sums. Though this method does not report daily rain sum with complete accuracy, it easily allows for the identification of winter days with relatively large quantities of rainfall.

In order to quantify air temperature difference between the landform locations and Svalbard Lufthavn, air temperature data from four weather stations was compared for the 2014-2015 winter. eKlima was used to obtain daily mean air temperatures for Svalbard Lufthavn and Isfjord Radio, which

is located on Kapp Linné approximately 800 m north-northwest of the strandflat borehole (Figure 4.1). In Adventdalen, there is a weather station adjacent to the loess terrace site (Figure 4.2); air temperature at this station is measured hourly at 2 m above ground level. The Breinosa weather station is approximately 800 m downslope from the blockfield borehole and measures air temperature every 5 minutes at 3.7 m above ground level (Figure 4.2). Daily mean air temperatures for Adventdalen and Breinosa were calculated by averaging temperature measurements each day at each site. Data from these two stations is available online from UNIS at http://www.unis.no/resources/weather-stations-and-web-cameras/. This comparison was only made for one winter because data are not available from Isfjord Radio before September 2014.

5.2. Ground temperature data

The loess terrace, solifluction sheet, and strandflat boreholes were drilled in spring 2008 with a hammer drill rig (NORPERM 2016; Christiansen et al. 2010), shown in Figure 5.1. Following drilling, PVC tubing was installed to house the thermistor strings (Figure 5.2). GeoPrecision thermistor strings, which are installed in the loess terrace and blockfield boreholes, have an accuracy of ±0.2°C. YSI thermistor strings, which are installed in the solifluction sheet and strandflat boreholes, have ±0.05°C accuracy after ice bath calibration (Juliussen et al. 2010; NORPERM 2016). Temperatures are recorded hourly in the loess terrace and blockfield, and every six hours in the solifluction sheet and strandflat. At the loess terrace and blockfield, the thermistor string is connected to a data logger which is affixed to the borehole cap; the thermistor string hangs freely within the borehole casing (Figure 4.4). At the solifluction sheet and strandflat, Campbell data loggers are used; these loggers are positioned a few meters away from the boreholes in sealed containers. The uppermost section of the thermistor string and casing connects the top of the borehole to the logger (Figure 5.2).

Temperature data are downloaded at least once a year from each borehole. The ground temperature raw data files are imported into Microsoft Excel and then examined for erroneous data, or spikes in the ground temperature series. These spikes result from unscrewing the borehole cap, which opens the casing to the atmosphere, and/or removing the thermistor string from the borehole. These actions are most easily identified by sudden increase in temperature at the deepest thermistors, as this increase in temperature would not occur naturally. After the data have been checked, they are uploaded to the NORPERM and Global Terrestrial Network for Permafrost (GTN-P) databases. In this thesis, data were processed in spreadsheet format and plotted using Golden Software's Grapher (version 11).

Seven full winters (2009-2015) of borehole data were examined for each site, except for the blockfield. This borehole was not drilled and instrumented until March 2009, and thus lacks data from the 2008-2009 winter (NORPERM 2016). The solifluction sheet has an incomplete data series for the 2012-2013 winter, as ground temperature data are unavailable from 21.03.2013 to 02.05.2013. Otherwise, the ground temperature series are continuous. In the results, all data from selected winters are plotted for chosen depths within the upper 5 m. The depths were selected for each site based on how far intra-seasonal temperature variations penetrate into the ground. Plotting temperature at all available depths would reduce figure comprehension and was not necessary to address the objectives presented in Section 1.2.

In Section 6.2.6, mean winter ground temperature profiles are presented for each landform from the ground surface to 3 m depth. Temperature measurements from deeper depths were not incorporated because of the phase lag that occurs between maximum annual temperature at the ground surface and at depth (Isaksen et al. 2001). Thus, temperature measurements from greater depths would not be representative of winter temperatures, but rather temperatures that occurred in earlier seasons. In Section 6.2.7, mean annual ground temperatures at 10 m depth are presented by hydrologic year, which is defined as 1 September through 31 August.

Figure 5.1. The drill rig used during the 2007-2008 IPY campaign, shown here at the strandflat (Kapp Linné 1) site. Isfjord Radio, the site of meteorological measurements in this area, can be seen in the background. Photo by Håvard Juliussen, taken from NORPERM (2016).

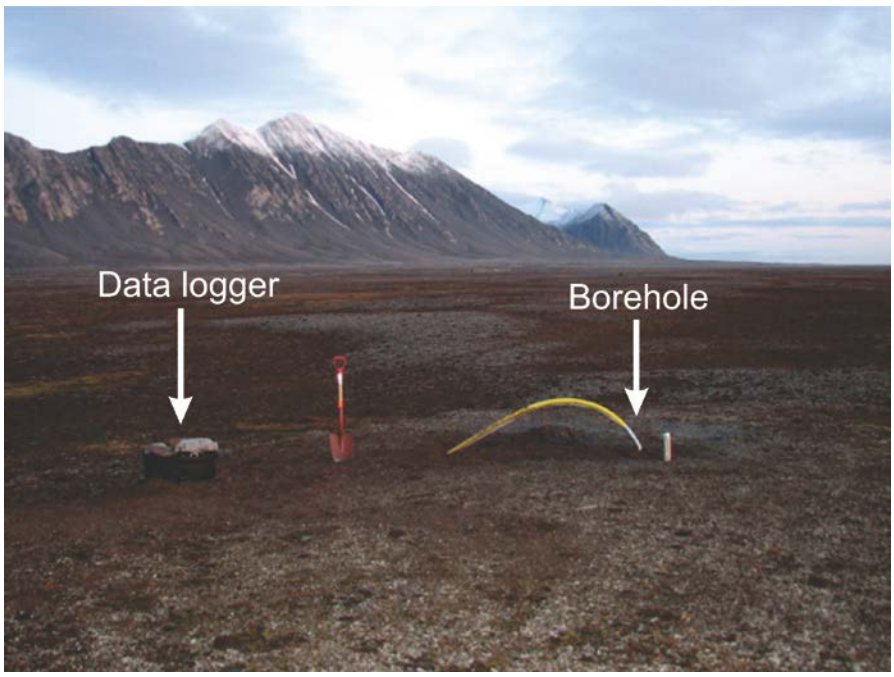

Figure 5.2. The strandflat borehole after drilling, showing the Campbell data logger container and the yellow borehole casing exiting the top of the borehole. Photo by Håvard Juliussen, taken from NORPERM (2016).

6. Results

6.1. Meteorological data

6.1.1. Overview

The Longyearbyen area 1958-2015 meteorology record is investigated to distinguish patterns and/or trends in rain-on-snow occurrence. Some previous literature has addressed rain-on-snow in the Svalbard meteorological record (Hansen et al. 2011; Eckerstorfer and Christiansen 2012), but only since 1980. The meteorology of the four warmest winters during the ground temperature series (2009-2015) is presented in detail. Major ROS events (>10 mm) occurred during three of these winters. The meteorology data during the ground temperature series is sourced from Svalbard Lufthavn, as this station provides the most complete record with the most parameters. However, meteorology does differ between the borehole locations; air temperature measured adjacent to three of the landforms is available for the 2014-2015 winter, and is presented in Section 6.1.4 to quantify air temperature difference between the landform locations and Svalbard Lufthavn. Snow conditions vary significantly between the landforms (described in Chapter 4), so snow depth measurements from Svalbard Lufthavn indicate relative snowpack development rather than absolute snow thickness at any of the sites.

6.1.2. Longyearbyen winters, 1958-2015

During the 1958-2015 period, winter mean air temperatures in Longyearbyen show an increasing trend. The linear trendline depicted in Figure 6.1 corresponds to an increase of 0.9°C per decade, and a total increase in mean winter temperature of 5.1°C between 1958 and 2015. Winter TDD over the same period do not exhibit a linear trend and have high variability, with a mean of 15.0 and standard deviation of 13.4. Except for one particularly warm winter in 1960, the years with the highest TDD values all occur in the past two decades. The 2005-2006 winter had both the highest mean temperature and TDD value of 79.4. The winter ending in 1981 did not have any daily mean air temperatures above 0°C, and thus has a TDD value of 0.

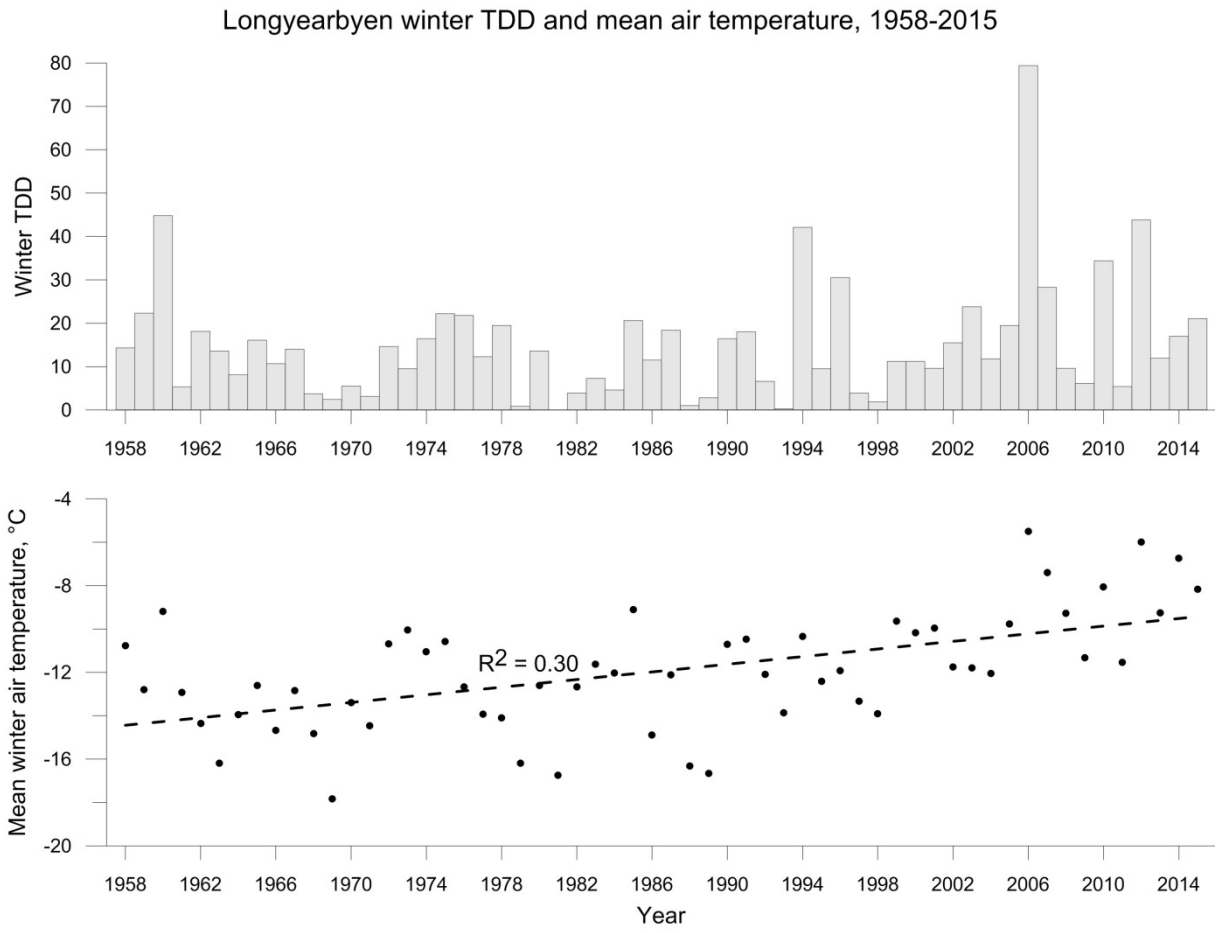

Figure 6.1. Longyearbyen winter TDD and mean winter air temperature from 1958-2015. Data pre-1976 comes from the old Longyearbyen station and data post-1976 comes from Svalbard Lufthavn; data from eKlima (2016).

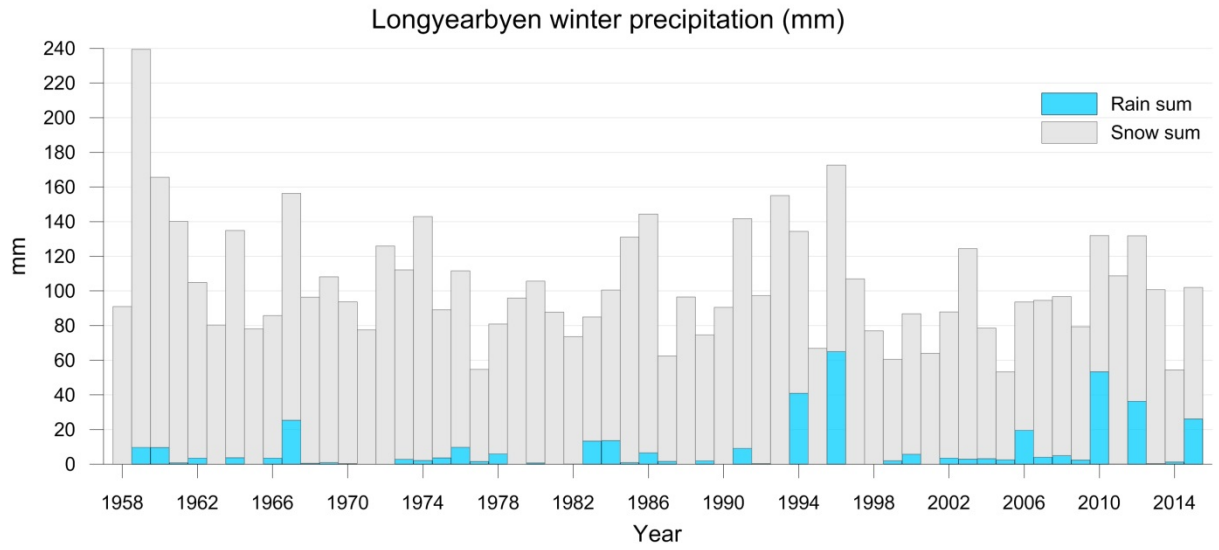

Figure 6.2. Longyearbyen winter precipitation, divided into rain and snow, from 1958 to 2015. Data pre-1976 comes from the old Longyearbyen station and data post-1976 comes from Svalbard Lufthavn; data from eKlima (2016).

There is no statistically significant linear trend in total winter precipitation or winter rain sum within the 1958-2015 period (Figure 6.2). It must be stressed that this result is entirely dependent on the investigated timescale, and does not preclude trends in these parameters in longer time series. Between 1958 and 2015, the average winter precipitation was 103.8 mm, with a standard deviation of 33.8 mm. The average winter rain sum was 7.0 mm with a standard deviation of 13.1 mm. The five rainiest winters have occurred since 1994. There is poor correlation between total winter precipitation and the winter rain sum ($R^2 = 0.18$); winters with high overall precipitation do not necessarily have high rainfall. Within the years of the ground temperature series (2009-2015), 2010, 2012, and 2015 were the rainiest winters, with 53.4 mm, 36.3 mm, and 26.2 mm of rain respectively. The other winters – 2009, 2011, 2013, and 2014 – were relatively dry, with their winter rain sums ranging between 0.2 mm and 2.4 mm (Table 6.1).

Winter rain sum exhibits greater correlation with TDD ($R^2 = 0.32$) than with winter mean air temperature ($R^2 = 0.12$). TDD is linked to winter rain sum in that both of these parameters are calculated from daily mean air temperatures greater than 0°C. Since all the investigated winter mean air temperatures are below 0°C, winter mean air temperature does not indicate how many above 0°C days might have occurred. Given the stronger connection between TDD and winter rain sum, and thus rain-on-snow events, this parameter has been compared with the others in Figure 6.3. Winter TDD and winter mean air temperature display a somewhat linear trend ($R^2 = 0.43$), with greater variability in this relationship occurring as winter mean air temperature and TDD increase. Winter TDD and total precipitation are not correlated ($R^2 = 0.07$). A cluster of data points is bounded by the limits of approximately 20 TDD and 120 mm total precipitation; more than half of the data points plot in this region. A similar clustering can be observed in the winter TDD vs. winter rain sum plot, as most winters have TDD values less than 20 and rain sums less than 10 mm. Winter TDD and the number of days of rain are linearly correlated ($R^2 = 0.71$). Since the number of days of rain was only reported as integers, the plot exhibits a somewhat stepped appearance, with increase in the number of days of rain corresponding to a leftward shift in the related TDD values.

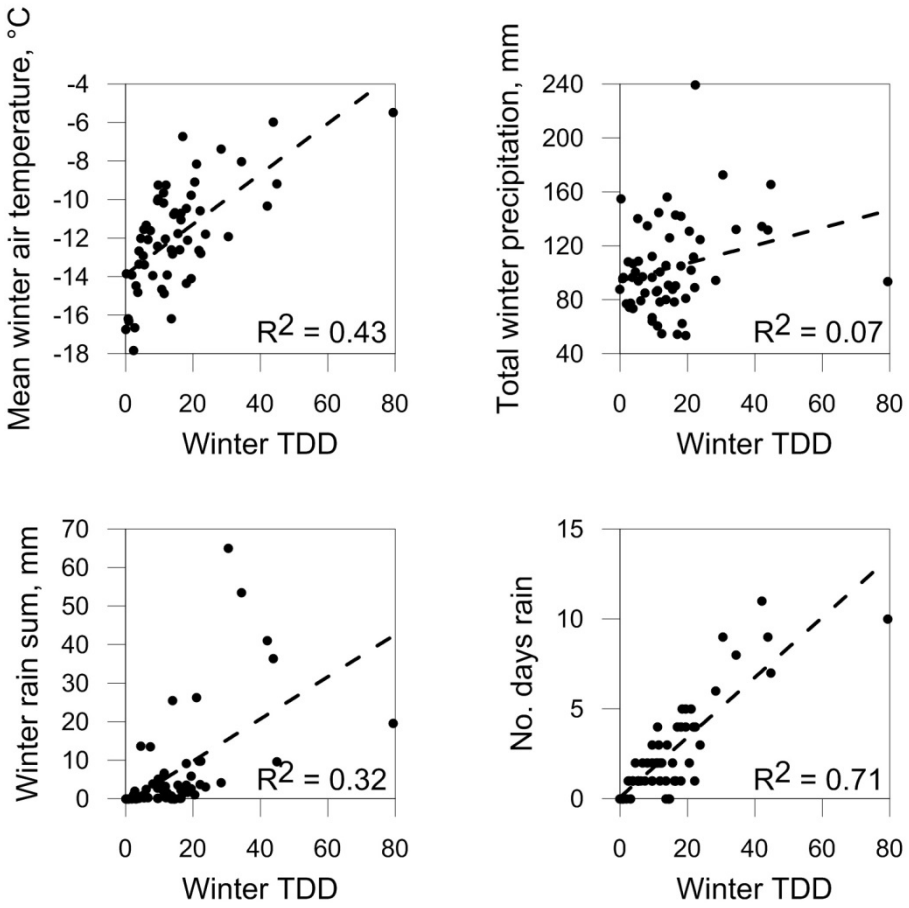

Figure 6.3. 1958 to 2015 winter TDD compared to winter mean air temperature, total winter precipitation, winter rain sum, and number of days of rain. There are 57 data points in each plot.

6.1.3. Longyearbyen winter meteorology, 2009-2015

As was previously mentioned, 2009-2010, 2011-2012, and 2014-2015 were the rainiest winters during the ground temperature series. The rain sums of these winters are greater than those of all other winters in the 1958 to 2015 meteorological series, except for 1994 and 1996. Winter 2011-2012 was the second rainiest and the warmest since 2009, with a winter mean air temperature of -6.0°C (Table 6.1). This winter also had the highest TDD value of 43.8 and the most days of rain, 9. The winter with the second highest TDD value, 2010, had the largest rain sum (53.4 mm) and 8 days of rain. The third rainiest winter, 2014-2015, had the third highest TDD value and the third most days of rain. This winter had a mean air temperature of -8.2°C, which is 0.5°C warmer than the 2009-2015 winter mean air temperature. The second warmest winter, 2014, was dry in terms of both total precipitation and rain sum. Winter 2010-2011 was the coldest and had the smallest amount of rain and TDD value. The 2009-2015 period was warmer and had more rain than the 1958-2015 winter mean; all parameter

means were greater during the 2009-2015 period except for total precipitation, which was 2.5 mm less than the 1958-2015 winter mean.

Since this thesis is focused on the impact of rain-on-snow events, the detailed meteorology of the relatively rainy 2009-2010, 2011-2012, and 2014-2015 winters is presented below (Figure 6.4). All of these winters had major (>10 mm) ROS events. The 2014-2015 winter is also included, as this winter is utilized in the discussion section to differentiate the impact of warm events with and without rain (Figure 6.5). This winter was warm (mean air temperature = -6.7°C), but only had 1.3 mm of rain. Detailed winter meteorology figures were made for all winters between 2009 and 2015; those that do not appear in this section can be found in Appendix A.

The 2009-2010 winter started off warm in comparison to the other winters; during November and December there were 11 days with a mean air temperature above 0°C. 2.4 mm of rain fell on 27 November; this rain occurred in the middle of three consecutive days with above 0°C mean air temperatures. The wind immediately before and during this rain event came from the west and was ~6 m/s on average. On 11 December, 11.3 mm of rain fell. Snow depth decreased by 7 cm between the onset of rain and three days afterwards. During the second half of January, 43.8 mm of rain fell and there were 8 days with mean air temperatures greater than 0°C. From 15-17 January, air temperature hovered

Winter	Mean air temperature	TDD	Total precip. (mm)	Rain sum (mm)	No. days rain
2008-2009	-11.3	6.1	79.4	2.4	1
2009-2010	-8.1	34.4	132.0	53.4	8
2010-2011	-11.5	5.4	108.7	0.2	1
2011-2012	-6.0	43.8	131.8	36.3	9
2012-2013	-9.3	11.9	100.7	0.3	1
2013-2014	-6.7	17.0	54.5	1.3	4
2014-2015	-8.2	21.1	102.0	26.2	5
2009-2015 winter means	-8.7	20.0	101.3	17.2	4
1958-2015 winter means	-11.9	15.0	103.8	7.0	3

Table 6.1. Winters 2009-2015 by parameter.

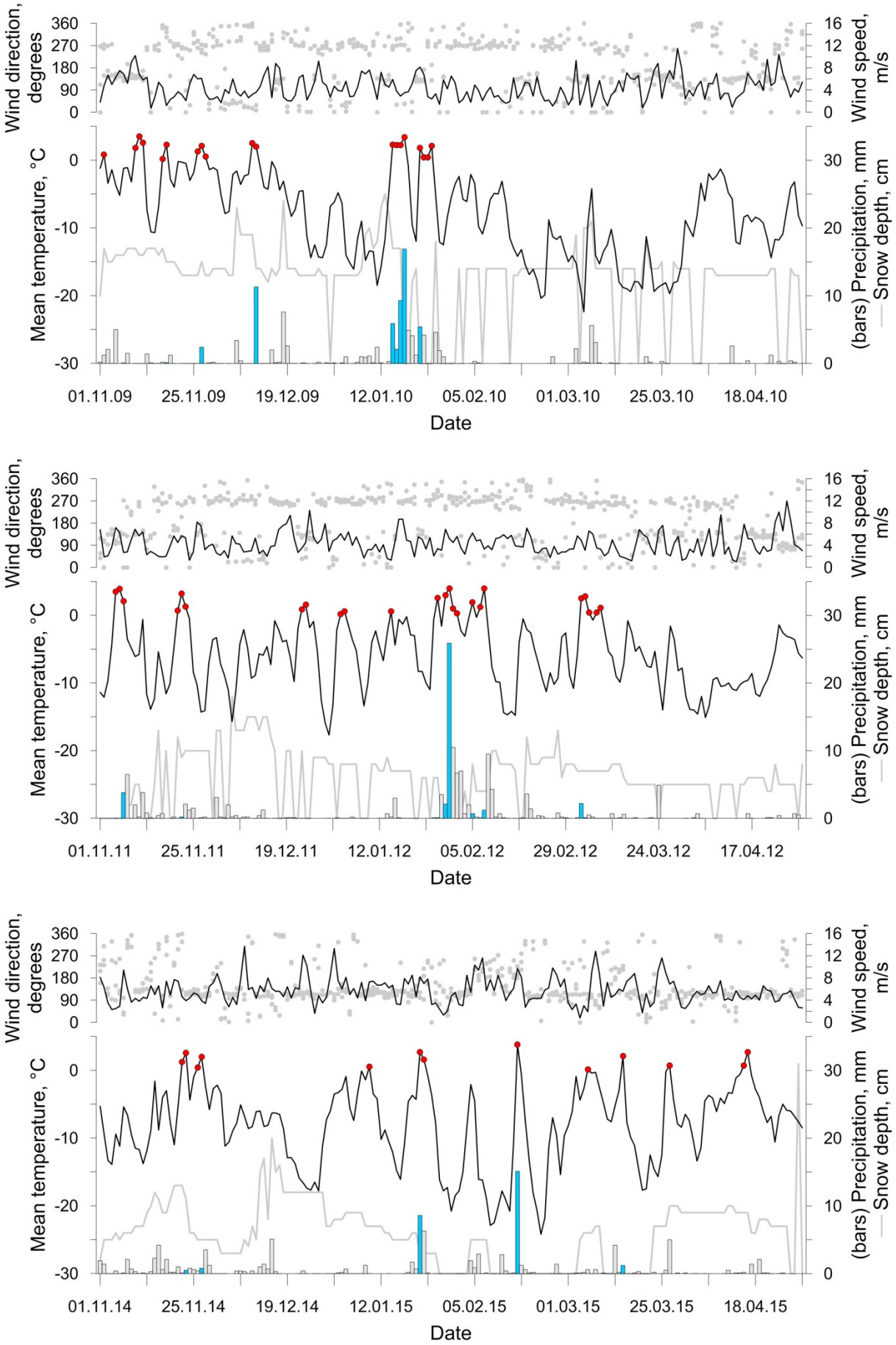

Figure 6.4. Meteorology for winters 2009-2010 (top), 2011-2012 (middle), and 2014-2015 (bottom). Red dots indicate when daily mean air temperature exceeded 0°C, blue bars indicate rain, and gray bars indicate snow. Gray dots indicate wind direction measured at 06, 12, and 18 Coordinated Universal Time (UTC).

around 2.2°C and daily rain sums were between 2.1 mm and 9.3 mm. On 18 January, the daily mean air temperature was 3.4°C and 16.9 mm rain fell. The beginning of these four days of consecutive rain coincided with a small peak in wind speed of 5.9 m/s. Snow depth decreased from 22 cm the day before the rain started to 0 cm on 19 January. Air temperature became negative following the rain, and approximately 10 cm of snow fell between 19-21 January. Then, air temperature rapidly increased and 5.4 mm of rain fell on 22 January; snow depth was reduced back to 0 cm on this date. This rain also coincided with a relative peak in wind speed. After 25 January, daily mean air temperatures were below 0°C and snow depth was approximately 14 cm for the remainder of the winter.

The 2011-2012 winter had an initially cold start (daily mean air temperature <-10°C) followed by 3.8 mm of rain on 7 November. Snow depth was 0 cm at this time at Svalbard Lufthavn, so this rain did not occur as rain-on-snow near sea level. However, this might have been a ROS event at other locations. This winter had 24 days with a mean air temperature above 0°C (the most of any winter examined), occurring during 8 warm events. Though there were a number of warm days during the first half of the winter, rain-on-snow did not occur until late January. On 30 January, 25.9 mm rain fell and daily mean air temperature was 4.0°C; these values are higher than those of any other winter day in the investigated period. This extreme day of rain was immediately preceded by a relative peak in average wind speed of 6.9 m/s. The two week period from 27 January to 8 February was generally warm and wet; the average of daily mean air temperatures during this time was 0.8°C and 60.7 mm of rain fell in total. Snow depth was 6-7 cm before the rain event and decreased to 0 cm afterwards. Another warm event occurred 4-9 March, when 5 of the 6 days had a daily mean air temperature above 0°C. However, this warm spell was not accompanied by much moisture; 2.3 mm rain fell over two days. The remainder of March and April were cold (average of daily mean air temperatures = 8.1°C) with very little precipitation (9.8 mm snow in total).

Instead of having a few multi-day warm events like the aforementioned winters, the 2014-2015 winter was characterized by spikes in air temperature. Days with a mean air temperature above 0°C occurred individually or in pairs. Two small rain events (0.5 and 0.8 mm) occurred 3 days apart in late November. 8.6 mm of rain fell on 22 January; this was accompanied by a daily mean air temperature of 2.7°C and an average wind speed of 8.2 m/s. Temperatures decreased and remained below 0°C until 16 February, when daily mean air temperature was 3.8°C and 15.1 mm rain fell. On this day average wind speed was 9.7 m/s. After this event, temperature decreased rapidly, reaching a daily mean air temperature of -24.2°C on 22 February. Another small rain event occurred on 15 March, when 1.2 mm

of rain fell. Daily snow depth was relatively low during this winter (mean snow depth = 5.9 cm), and was 0 cm for multiple days surrounding the 16 February and 15 March rain events. This winter had a dominant southeast wind direction (mode of measured wind directions = 109°), in contrast to the 2009-2010 and 2011-2012 winters, which had a more bimodal wind direction distribution, with both westerly and southeasterly winds. These latter winters also had a greater number of 0° wind direction values.

The 2013-2014 winter (Figure 6.5) will be used as a reference year, to compare the aforementioned rain-on-snow events to winter warm events without rain. This winter had 5 short-lived (one or two day) warm events and a 6 day warm event 9-14 February. During this period daily mean air temperature peaked at 3.6°C and snow depth was 4-5 cm. This warm event did not correspond with a relative peak in wind speed, as many of the other warm and wet periods in other winters did. The dominant winter wind direction was west-southwest (mode of measured wind directions = 249°), though a more bimodal wind direction distribution is visible in November, March, and April, when southeasterly winds were also frequent.

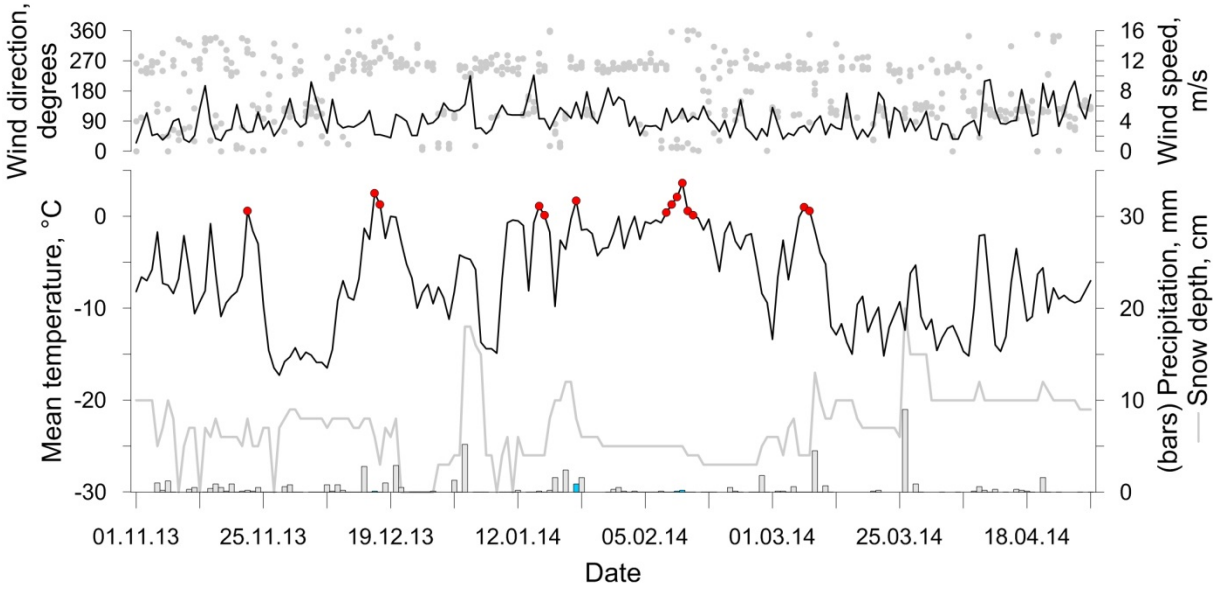

Figure 6.5. Meteorology the 2013-2014 winter. Red dots indicate when daily mean air temperature exceeded 0°C, blue bars indicate rain, and gray bars indicate snow. Gray dots indicate wind direction measured at 06, 12, and 18 Coordinated Universal Time (UTC).

6.1.4. Landform location air temperature comparison

Mean winter air temperature in central Spitsbergen decreases as distance from the coast and elevation increase. Isfjord Radio, which is located on the coast 800 m north-northwest of the strandflat borehole, experienced the mildest 2014-2015 winter with the highest mean winter air temperature (-6.4°C) and minimum winter air temperature (-18.1°C) (Table 6.2). During winter warm events, air temperature at Isfjord Radio, Svalbard Lufthavn, and Adventdalen (measured next to the loess terrace) was similar, though temperatures at Isfjord Radio were 1°C to 2°C lower during some temperature maxima. Air temperature in Adventdalen closely followed air temperature at Svalbard Lufthavn, except during temperature minima, when air temperature in Adventdalen was up to 5.6°C lower than at Svalbard Lufthavn. Adventdalen had slightly lower mean, maximum, and minimum winter air temperature than Svalbard Lufthavn. Breinosa was the coldest location, with a mean winter air temperature of -12.0°C and no positive air temperatures during winter 2014-2015. Winter air temperature at Breinosa was 2.5°C lower than in Adventdalen, on average, but air temperature was lower in Adventdalen than at Breinosa during three air temperature minima (12 November 2014, 27 December 2014, and 22 February 2015). The comparison of Adventdalen and Breinosa air temperatures yields an approximate lapse rate of 0.005°C m^{-1} during the 2014-2015 winter.

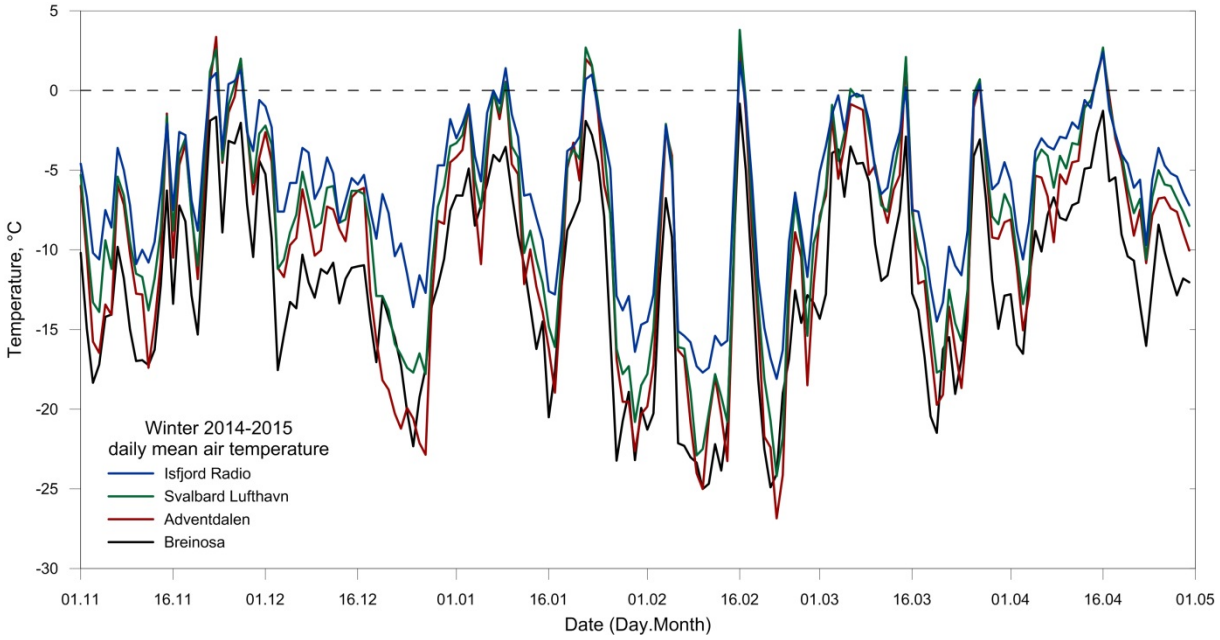

Figure 6.6. Daily mean air temperature during winter 2014-2015 at Isfjord Radio, Svalbard Lufthavn, Adventdalen, and Breinosa. The location of these weather stations is described in Section 5.1 and depicted in Figures 4.1 and 4.2.

Location	Mean winter air temp., °C	Max. winter air temp., °C	Min. winter air temp., °C	TDD
Isfjord Radio	-6.4	2.4	-18.1	13.0
Svalbard Lufthavn	-8.2	3.8	-24.2	21.1
Adventdalen	-9.5	3.4	-26.9	18.7
Breinosa	-12.0	-0.8	-25.0	0.0

Table 6.2. Mean, maximum, and minimum winter air temperature (°C) and TDD at Isfjord Radio, Svalbard Lufthavn, Adventdalen, and Breinosa during the 2014-2015 winter.

6.2. Ground temperature data

6.2.1. Overview

In keeping with the previous sections and the overall aims of this thesis, ground temperatures are presented from the four warmest winters. Three of these winters (2009-2010, 2011-2012, and 2014-2015) had major ROS events, while the relatively dry 2013-2014 winter is included to assess the difference in ground temperature response between warm events with and without rain. Ground temperatures are compared to daily mean air temperature and rain sum from Svalbard Lufthavn, as this is the only weather station that provides precipitation data and a complete air temperature record during the investigated winters. Winter mean ground temperature profiles are presented for the four landforms to assess if warmer and/or wetter winters are reflected in ground thermal regime at the seasonal scale. The winter mean ground temperature profiles also highlight thermal differences between the landforms and the differing impact of winter variability at these locations. Lastly, mean annual ground temperature at 10 m depth is depicted, demonstrating the general warming occurring in the landforms, irrespective of short-term ROS and warm events.

6.2.2. Loess terrace ground temperatures

Ground surface temperature in the loess terrace (Figure 6.7) closely follows daily mean air temperature, temporally and in magnitude. Diurnal variations in ground surface temperature become apparent in March, around the time when direct sunlight reaches the site after the polar night. Both the highest and lowest ground surface temperatures occurred in the 2014-2015 winter; the ground surface temperature ranged from -28.4°C to 3.1°C. In all of the depicted years, temperature at 5 m depth increases slightly

(~0.3°C) until the end of February, at which point temperature begins to decrease. At 3 m, temperature increases slightly until the end of December, at which point it begins to decline. Temperature at the shallower depths increases and decreases intra-seasonally.

Though the 2009-2010 winter started warm, with multiple above 0°C days in November, ground temperatures at 1 and 2 m depth decreased during this month. Temperatures at 1 m increased very slightly (<0.1°C) following the smaller November and December rain events (2.4 mm and 11.3 mm rain respectively). Temperatures at 2 m depth gradually decreased during these months. From 15-25 January, 8 days had a positive mean air temperature and 39.6 mm of rain fell. Ground surface temperature reached 0°C on 17 January and hovered around this value until reaching -1°C on 19 January. Temperature at 1 m began to increase two days after the rain began and increased a total of 2.1°C over 12 days. Temperature at 2 m increased from 22 January to 2 February by 0.3°C.

The 2011-2012 winter started with 3.8 mm rain on 7 November. During the first half of November, ground temperature at 1 m was gradually decreasing and remained constant at 2 m. Temperature at 1 m plateaued briefly during 3 consecutive days of positive mean air temperature, but decreased during and after the 7 November rain. On 30 January, 25.9 mm rain fell during a two week period of mostly positive air temperatures. Ground surface temperature on 30-31 January was positive, reaching 0.4°C both days. Temperature began to increase at 1 m on 28 January, two days after air temperature began to increase. Over the following two weeks, temperature at this depth increased from -3.8°C to -5.1°C. At 2 m, temperature increased by 0.3°C from 1-15 February. Temperature plateaued, but did not increase, at 3 m depth following the event. On 4 March, daily mean air temperature became positive again and there was 2.2 mm of rain. Temperature increased at 1 m depth over the following 10 days by 1.1°C. Temperature at 2 m increased slightly (0.1°C) thereafter, but gradually decreased at 3 and 5 m depth throughout March.

An early cold spell in late November/early December 2013 (daily mean air temperature reached -16.5°C) caused ground temperatures at 1 and 2 m to decrease more rapidly than in the other depicted years. Two days of positive air temperatures in mid-December resulted in a slight increase in ground temperature at 1 and 2 m depth. From 15 January to 15 February, air temperatures were relatively high (average daily mean air temperature = -1.1°C) and generally increasing; this is reflected in temperature at 1m depth, which increased over this period and reached a maximum of -4.5°C on 20 February. On 12 February, ground surface temperature briefly became positive. At 2 m depth, temperature increased very

slightly (0.4°C) following the mild air temperatures. Temperature remained constant or decreased slightly at 3 and 5 m.

At the end of November 2014, there were four days with positive daily mean air temperature and 1.3 mm rain fell in total. This resulted in temperature increase at 1 m depth, but deeper ground temperatures were not impacted. January and February 2015 each had one day of rain. Temperature at 1 and 2 m increased following the increase in air temperature leading up to the 8.6 mm of rain that occurred on 22 January. Temperature increased 1.5°C at 1 m depth and <0.1°C at 2 m. The rain on 16 February was associated with a briefer (approximately one day) spike in air temperature. Temperature at 1 m increased 1.1°C following this event, while temperature at the other depths was still decreasing. Daily mean air temperature reached a seasonal minimum on 22 February and then mainly increased the month afterwards; this longer-term increase in air temperature is reflected in increasing temperatures at 1 and 2 m depth during mid-March.

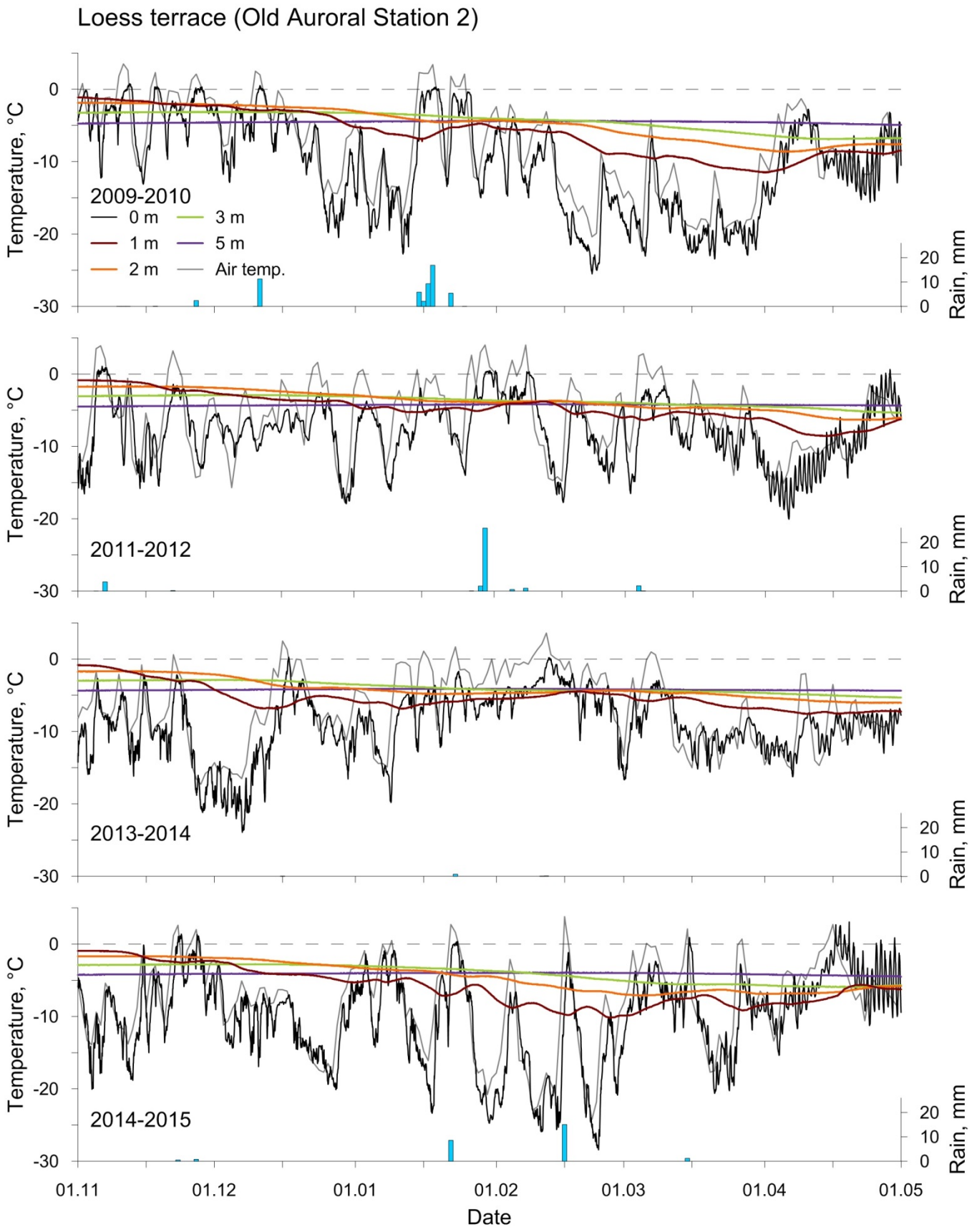

Figure 6.7. Loess terrace ground temperatures from 0-5 m depth; line color indicates depth of temperature measurement. Svalbard Lufthavn daily mean air temperature is plotted in the light gray line. Blue bars indicate daily rain sum.

6.2.3. Solifluction sheet ground temperatures

Ground surface temperature at the solifluction sheet exhibits less variation than ground surface temperature in the loess terrace. Both the maximum and minimum ground surface temperature for the entire data series, 0.5°C and -16.7°C respectively, occurred in November 2014. In general, temperature at 1 m is decreasing during the defined winter period. Temperature at 2, 3, and 4 m depth increases very slightly until mid-winter, when temperatures at these depths begin to decrease as well.

The 11 days with positive daily mean air temperature and two rain events that occurred in November and December 2009 only affected temperature at the surface. During the warm and rainy period which started 15 January 2010, ground surface temperature reached a maximum of -0.7°C on 20 January. Ground temperature at 1 increased from -2.4°C to -1.6°C from 17 to 28 January 2010. Temperature at the lower depths continued to decrease at this time.

Ground temperature, except for at the surface, did not respond to the early November 2011 rain event. Following the 25.9 mm 30 January rain event, ground surface temperature remained between 0°C and -1°C for four days. Temperature at 1 m increased by 0.9°C to -1.6°C after the event. Temperature at 2 m increased slightly (by ~0.1°C) in the two weeks following the event. Ground temperature at 1 m increased by 0.4°C following the warm event at the beginning of March; temperatures at all other depths decreased.

Ground temperatures during the 2013-2014 winter exhibit few fluctuations and are warmer compared to the other investigated winters. Ground surface temperature had a smaller range and was warmer compared to other winters; the minimum and maximum temperatures at the surface were -6.9°C and -0.6°C. Temperature at 1 m decreased for the entire winter except for a brief period in mid-February, when temperature at this depth increased 0.04°C after 6 days of positive daily mean air temperature. Temperature at 2, 3, and 4 m depth began to decrease on 30 December, 12 February, and 17 March, respectively.

The 1, 2, 3, and 4 m ground temperatures were unaffected by the two small rain events occurring late November 2014. Ground surface temperature reached its maximum (0.5°C) the same day as the second small rain event (0.8 mm rain). The two larger rain events, which happened on 22 January and 16 February 2015, only impacted temperature at the ground surface and 1 m. Ground temperature at both 1 m and 2 m increased after an increasing trend in air temperature in early March. Temperature at 1 m increased more rapidly following one warm, rainy day on 15 March.

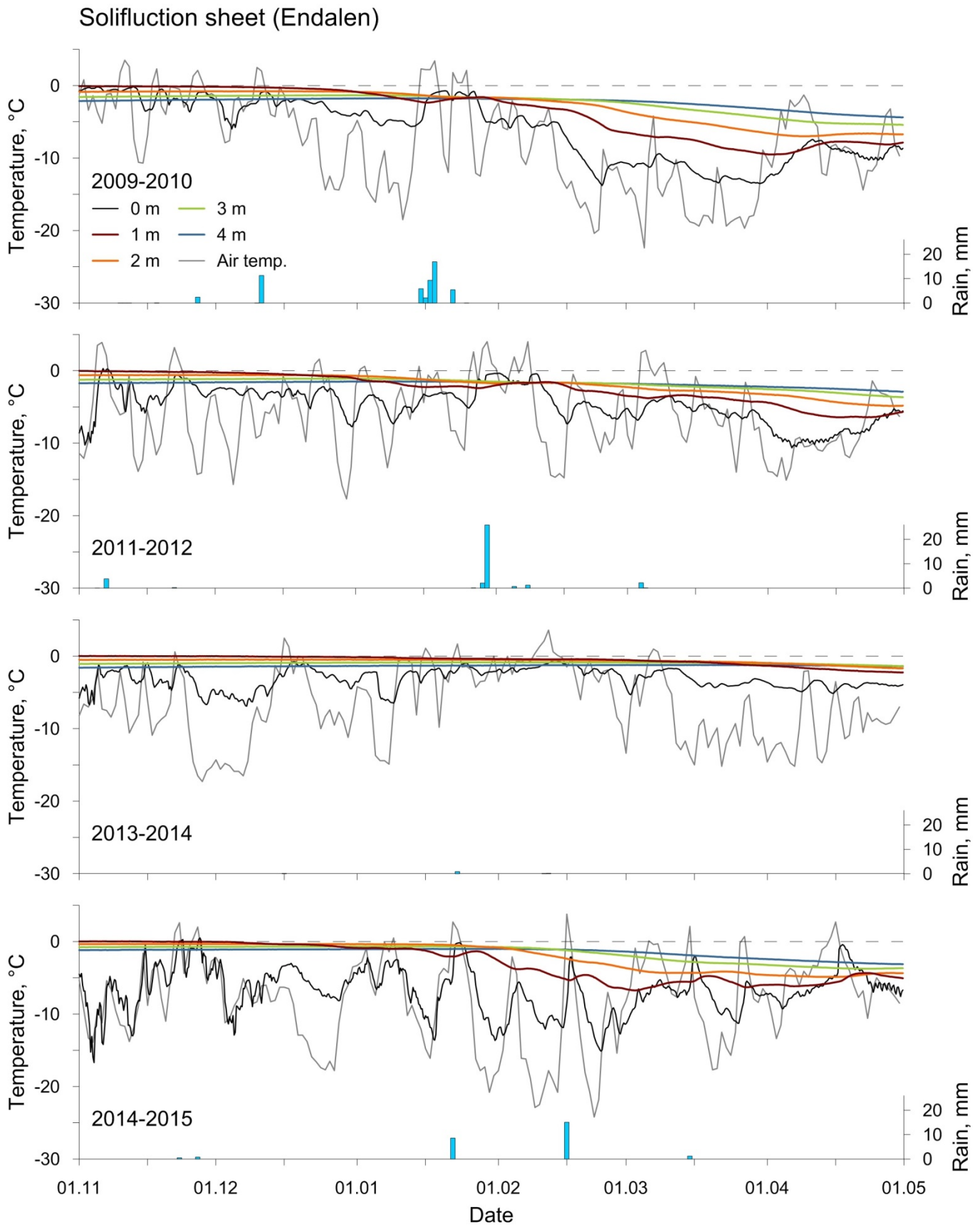

Figure 6.8. Solifluction sheet ground temperatures from 0-4 m depth; line color indicates depth of temperature measurement. Svalbard Lufthavn daily mean air temperature is plotted in the light gray line. Blue bars indicate daily rain sum.

6.2.4. Blockfield ground temperatures

Ground temperatures at the blockfield on Breinosa behave completely differently than temperatures in the other landforms. Except for at the beginning of winter, ground surface temperature is lower than the temperature at 1, 2, and 3 m depth. The ground surface is coldest in this landform; the warmest ground surface temperature measurement in the blockfield was -2.2°C. Overall, the ground surface temperature reflects a dampened air temperature signal, only following multi-day air temperature trends. Unlike the loess terrace and solifluction sheet, temperatures at all depicted depths generally decrease from the onset of winter. Temperature development at 1, 2, and 3 m depth is similar during the four depicted winters.

Temperature at 1 m remained at -6.1°C for two weeks following the 15-25 January 2010 warm and wet period. Temperature at this depth increased slightly (less than thermistor accuracy) as air temperatures began to increase in the second half of April, but otherwise decreased steadily throughout the season. Temperature at 2 and 3 m depth decreased during the entirety of the 2009-2010 winter.

During the 2011-2012 winter, ground temperatures decreased at 2 and 3 m during the entire winter. At 1 m, temperature increased from -6.1 to -6.0°C after the large rain event 30 January and the days with positive air temperature surrounding it. After the small rain event in early March, temperature at 1 m plateaued for approximately one month. During the 15 January to 15 February warm event in 2014, temperature at 2 and 3 m depth plateaued at -6.3°C and -6.2°C, respectively. Temperature at 1 m depth increased from -6.8°C on 26 January to -6.5°C on 3 March 2014. Temperatures at 1, 2, and 3 m depth were mostly decreasing during the 2014-2015 winter. The exception is temperature at 1 m depth during March 2015, which increased from -8.1°C to -7.9°C as daily mean air temperatures began to increase after the season's minimum air temperature in late February. The air temperature spikes that characterized this winter manifest themselves in the ground surface temperature and marginally altered the rate of decrease in temperature at 1 m depth, but did not impact temperatures at deeper depths.

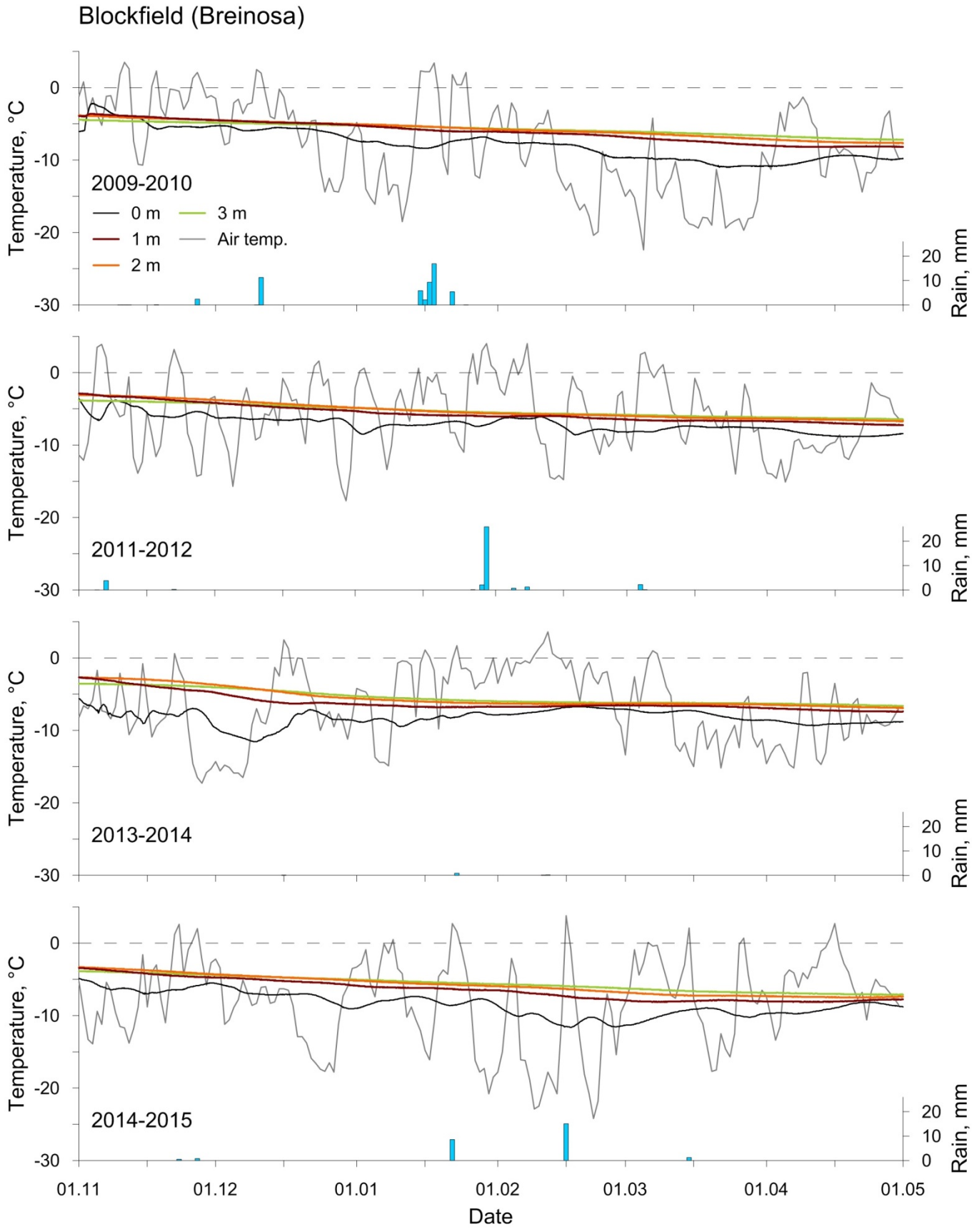

Figure 6.9. Blockfield ground temperatures from 0-3 m depth; line color indicates depth of temperature measurement. Svalbard Lufthavn daily mean air temperature is plotted in the light gray line. Blue bars indicate daily rain sum.

6.2.5. Strandflat ground temperatures

Ground temperatures in the strandflat bedrock exhibit more fluctuations (peaks and troughs) compared to any of the other landforms. Here, ground surface temperature closely mirrors daily mean air temperature. Temperature at 1 m reflects most of the peaks and troughs in daily mean air temperature. The temperature signal at 2 and 3 m depth is attenuated, but is still expressed.

The first rain event of the 2009-2010 winter (2.4 mm on 27 November) caused a small temperature increase at 1 m (0.3°C), while trends at the other depths were unchanged. The ground temperature increased by 1.2°C at 1 m as air temperatures increased leading up to the rain event on 11 December. Temperature at 2 m increased slightly (0.1°C) after the day of rain. Temperature at 1 m began to increase with air temperatures leading up to the 15-25 January warm and wet period; between 13-27 January, temperature at this depth increased from -9.8°C to -3.4°C. Temperature increase began 3 days later at 2 m depth; temperature at this depth increased by 2.3°C. At 3 m depth, temperature increased by 0.4°C, while at 4 m temperature plateaued and at 5 m temperature continued to decrease.

The initial rain event in the 2011-2012 winter (7 November) increased ground surface temperature and temperature at 1 m. Ground surface temperature was -0.0°C on the day of the rain and two days afterwards. Following the next period with positive air temperatures, 21-23 November, temperature at 1 m and 2 m increased, albeit the temperature change at 2 m was smaller than the accuracy of the thermistors. For two weeks starting 26 January 2012, temperatures were mild (average daily mean air temperature = -0.7°C) and 30 mm rain fell in total. Ground surface temperature was between 0 and -1°C between 30 January and 1 February. After this event, temperature increased at all ground depths – 1, 2, 3, 4, and 5 m depth. The magnitude of temperature increase was progressively smaller with depth, ranging from 3.3°C at 1 m to 0.04°C at 5 m. Temperature began to increase at 5 m depth on 12 February, the same day maximum temperature was reached at 2 m depth. Temperature continued to decrease at 6 m depth during and after the event, which is why temperature at this depth is not plotted. The shorter period of positive daily mean air temperatures and rain in early March impacted temperatures at 1, 2, 3, and 4 m depth but not at 5 m.

During and after the 15 January to 15 February 2014 mild period (average daily mean air temperature = -1.1°C), temperatures at all depths between 1 and 5 m increased. Maximum daily mean air temperature was reached on 12 February. The dates maximum temperature was reached at the sensors are as follows: ground surface, 13 February; 1 m, 15 February: 2 m, 18 February; 3 m, 23 February; 4 m, 1 March; 5 m, 5 March. Temperature at 6 m experienced both positive and negative

temperature fluctuations following this event, though they were smaller than the accuracy of the thermistors (<0.02°C).

As described in Section 6.1.3, the 2014-2015 winter was characterized by short-lived, one or two day spikes in temperature. Resultant peaks and troughs in temperature are visible at the ground surface, 1 m, 2 m, and 3 m depth. Spikes in temperature occurred on 22 January, 4 February, and 16 February. The spike on 4 February was not associated with rain, while the other two were. Though the first two spikes in air temperature were of the same magnitude, an increase of 18.8°C and 18.7°C respectively, temperature at 1 m increased 1.3°C more following the spike in temperature associated with rain. The air temperature spike on 16 February was the greatest in magnitude, 26.7°C, and also resulted in the greatest spike in 1 m temperature of 4.5°C.

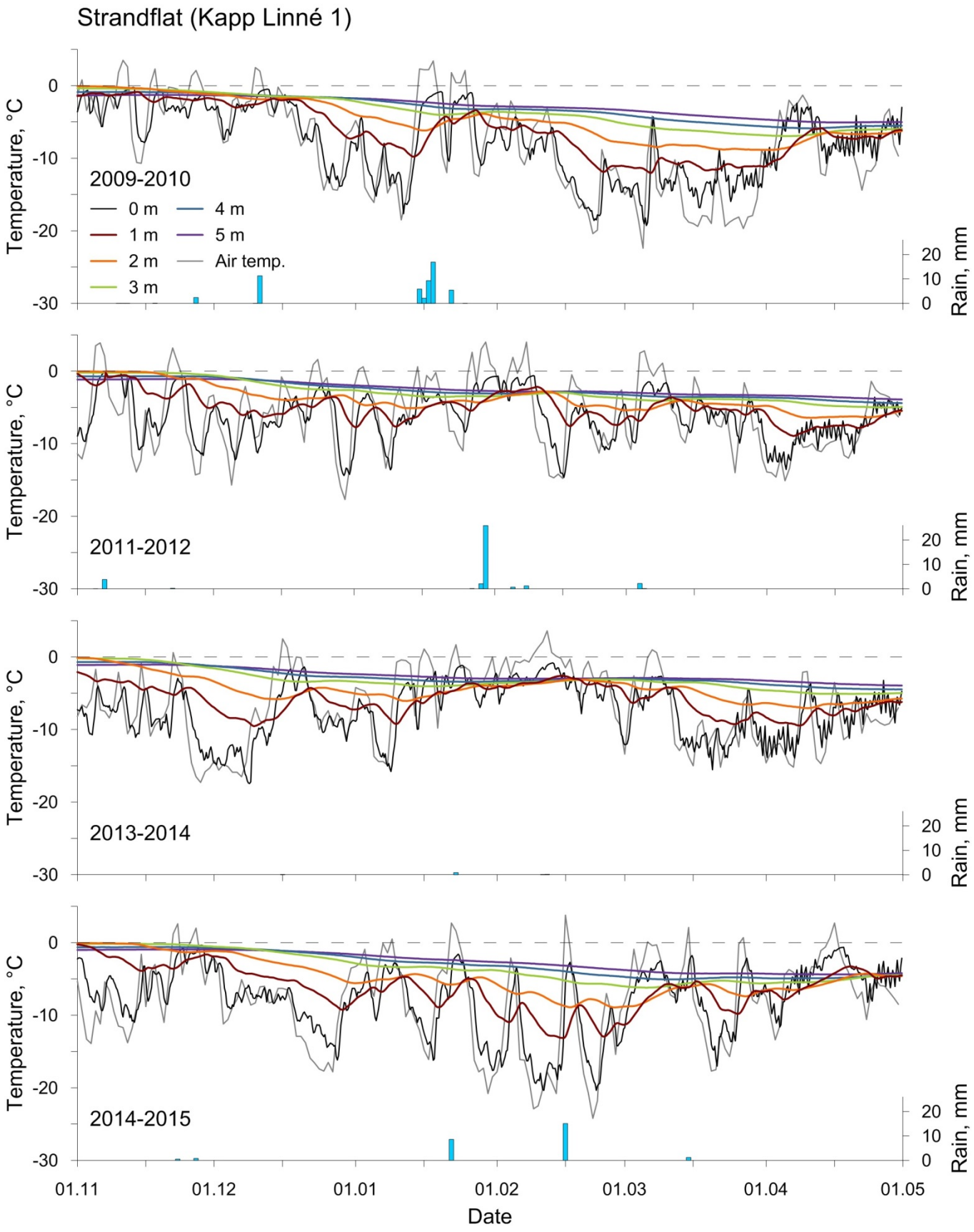

Figure 6.10. Strandflat ground temperatures from 0-3 m depth; line color indicates depth of temperature measurement. Svalbard Lufthavn daily mean air temperature is plotted in the light gray line. Blue bars indicate daily rain sum.

6.2.6. Mean winter ground temperature profiles

The aforementioned results show ground temperature response to winter meteorology, focusing on individual warm and ROS events. To investigate the potential seasonal impact of warm and ROS events, mean winter ground temperature profiles for the upper 3 m at each landform have been created (Figure 6.11). A composite mean winter ground temperature profile is also shown for each landform (dotted lines in Figure 6.11); these profiles were created by averaging winter ground temperature data in the upper 3 m during the entire 2009-2015 period. In the discussion, the mean winter ground temperature profiles are discussed in relation to the corresponding winters' conditions.

Each site has a unique mean winter ground temperature profile, with the loess terrace (Figure 6.11a) and strandflat (Figure 6.11d) sites exhibiting the greatest difference between temperatures near the surface and those at 3 m depth. Based on the composite 2009-2015 mean winter ground temperature profile, the temperature offset between the surface and 3 m depth is 6.3°C at the loess terrace and 4.7°C at the strandflat. The solifluction sheet exhibits the greatest variability between winters (Figure 6.11b). The blockfield exhibits the smallest differences in temperature between both winters and depths (Figure 6.11c). At the blockfield and strandflat sites, the mean winter ground temperature profiles of the four warmest winters during the ground temperature series (2009-2010, 2011-2012, 2013-2014, and 2014-2015) are as warm or warmer than the 2009-2015 average. At the loess terrace and solifluction sheet, the 2009-2010 winter profile was cooler than the 2009-2015 average. The 2011-2012 winter profile was the warmest at all the landforms except the solifluction sheet, where the 2013-2014 profile was significantly warmer than the others.

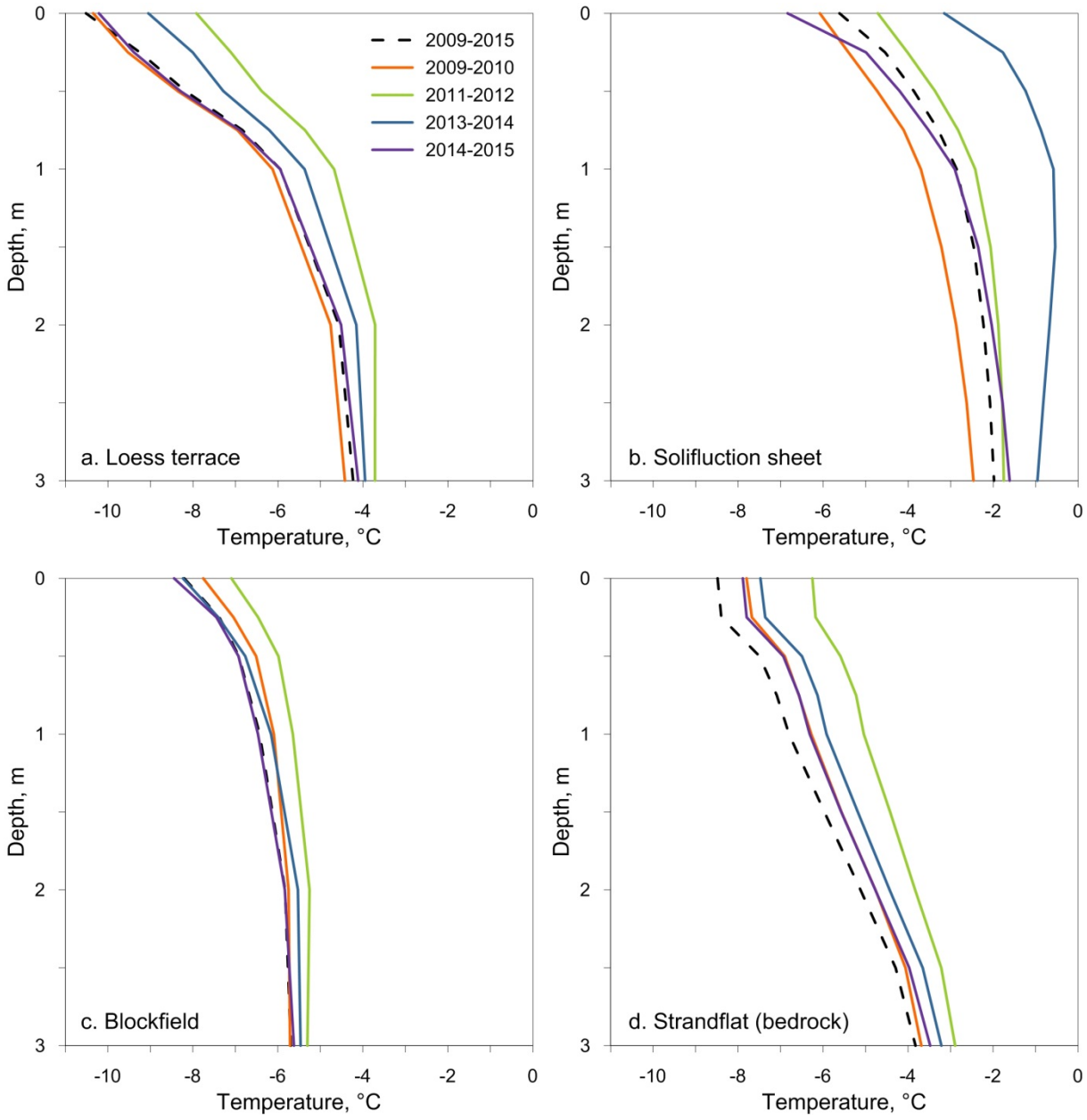

Figure 6.11. Mean winter ground temperature profiles in the upper 3 m at the loess terrace (a), solifluction sheet (b), blockfield (c), and strandflat (d). The black dotted line represents a composite 2009-2015 mean winter ground temperature profile, which was made by averaging the ground temperature data from the seven full winters in the ground temperature series.

6.2.7. Mean annual ground temperatures at 10 m depth

Though the focus of this thesis is the impact of winter ROS and warm events, annual trends in ground temperatures at the studied landforms must also be considered; this puts short-term fluctuations in perspective of any long term changes. Mean annual ground temperature (MAGT) at 10 m depth for each of the landforms is compared in Figure 6.12. The 10 m depth was chosen because this is the deepest measurement depth common to all the boreholes. The depicted timespan, 2010-2015, makes use of the full hydrologic years of data available for each borehole.

From 2010 to 2015, mean annual ground temperature at 10 m depth has increased every year in each studied landform except for the blockfield. Here, 10 m temperature was -5.9°C for both the 2009-2010 and 2010-2011 hydrologic years. Between 2010 and 2015, 10 m temperature at the solifluction sheet increased by 0.9°C; this was the greatest increase in 10 m temperature of the four landforms. MAGT at 10 m at the loess terrace has increased at the most constant rate, with yearly increase ranging between 0.02°C and 0.08°C. The blockfield exhibits the most sporadic warming, with yearly temperature increase at 10 m depth ranging from 0.0°C to 0.2°C. In each landform, temperature at 10 m depth has increased between 0.3°C and 0.9°C over the six year period.

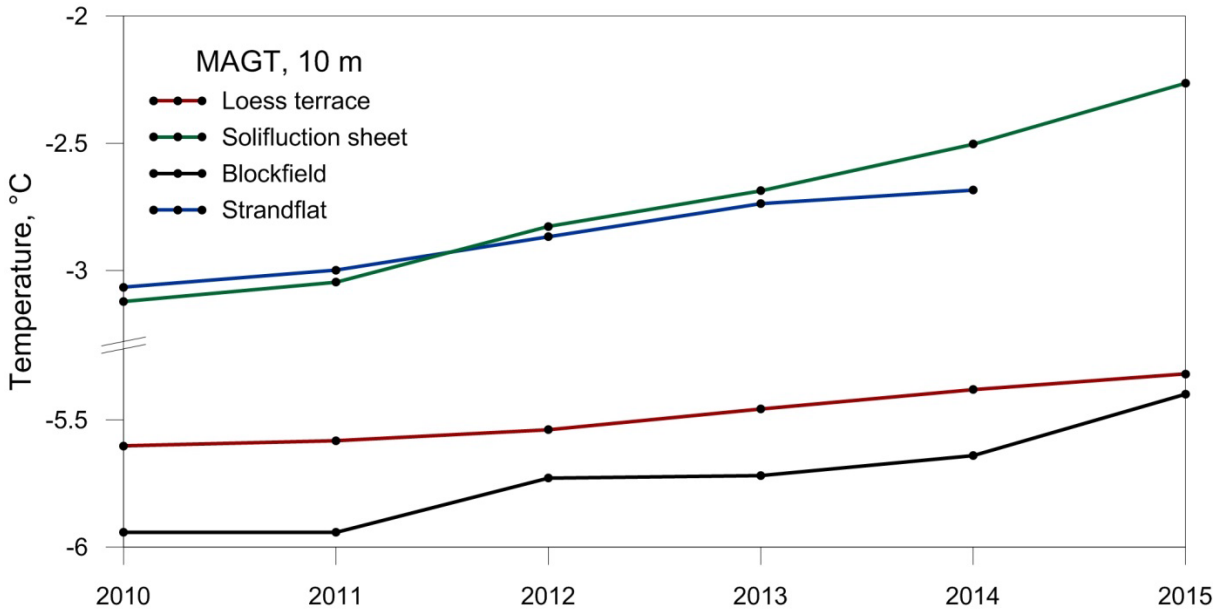

Figure 6.12. Mean annual temperature, calculated by hydrological year (1 September–31 August), at 10 m depth for the four studied landforms. At the loess terrace, temperature is recorded at 9.85 m depth instead of 10 m.

7. Discussion

7.1. Meteorology

This meteorology discussion compares observations of 1958-2015 winter meteorology with the literature. Warm events are considered in the context of atmospheric circulation patterns and their variability. At the end, ROS events and the amount of rainfall required to penetrate through snow cover to the ground surface is examined in the context of known conditions at the study landforms.

7.1.1. Winter air temperatures

Førland et al. (2011) found that average winter air temperature at Svalbard Lufthavn increased 3.4°C from the 1961-1990 standard normal period to the 1981-2010 recent normal period. The increase in average winter air temperature presented in Section 6.1.2 (5.1°C) is higher, but represents the longer 1958-2015 time period. Winter climate regimes in the extended Svalbard Airport series closely resemble annual climate regimes (Nordli et al. 2014), making the comparison of mean winter and mean annual air temperatures relevant. The 1958-2015 period began with relatively low mean annual temperatures and ended with relatively high mean annual air temperatures (Nordli et al. 2014; Førland et al. 2011) (Figure 3.3), making the difference between air temperature at the beginning and end of this series greater than that of Førland et al.'s (2011) 1961-1990 to 1981-2010 normal period comparison. Decadal increase in mean winter air temperature is also sensitive to the time period in which it is calculated, given varying climate regimes. The 1.66°C decadal increase in average winter temperature at Svalbard Lufthavn from 1975-2011 (Førland et al. 2011) is higher than the 1958-2015 decadal increase (0.9°C) presented here because 1975-2011 was a period of overall temperature increase. The 1958-2015 period incorporates a phase of decreasing annual air temperatures from the 1950s to 1960s. The seasonal temperature analysis in this thesis and that of Førland et al. (2011) and Nordli et al. (2014) confirm that winter temperatures are increasing. This winter temperature increase is occurring alongside annual temperature increase, both of which have been attributed to changes in atmospheric circulation patterns and advection (Hanssen-Bauer and Førland 1998; Dickson et al. 2000), in addition to reduction in Arctic sea ice extent (Overland and Wang 2010; Screen and Simmonds 2010).

Accumulated winter TDD do not exhibit a linear trend, but the relative minima and maxima in TDD (Figure 6.1) match with minima and maxima in the annual air temperature development presented by Førland et al. (2011) (Figure 3.3). For example, the 1969 winter had few TDD, followed

by winters with increasing TDD values. This corresponds with the minimum in annual air temperature in Figure 3.3 between 1965 and 1970, which is followed by increasing annual temperatures. If winter air temperatures continue to increase (Nordli et al. 2014; Førland et al. 2011), it seems winter TDD should increase as well. The correlation between winter TDD and mean winter air temperature (R^2 = 0.43) is fair, but neither parameter could be used reliably to predict the other. The absence of a robust correlation is attributed to warm events with relatively short duration, as these events increase TDD without significantly altering mean winter air temperature.

7.1.2. Winter precipitation

No statistically significant linear trend was found in total winter precipitation during the 1958-2015 period (Figure 6.2), though the rainiest winters clustered towards the end of the data series. Førland et al. (2011) found that annual precipitation at Svalbard Lufthavn increased 2% per decade on average, a trend significant at the 1% level. These authors mention that though the long term trend in precipitation is positive, precipitation amount has remained fairly constant during the 1980s and 1990s. In addition, statistically significant increases in winter precipitation (rather than annual) were only found at some Svalbard sites, which did not include Svalbard Lufthavn (Førland et al. 2011). Precipitation at Svalbard Lufthavn is low overall, so small changes in this parameter greatly increase its variability. Precipitation at other areas in Svalbard (i.e. Ny-Ålesund and Bjørnøya) has increased more than at Svalbard Lufthavn (Førland et al. 2011), which is partly due to these areas receiving far more precipitation in general.

A linear correlation between winter rain sum and TDD (R^2 = 0.32) (Figure 6.3) was expected, since higher winter temperatures, and more days with above 0°C daily mean air temperature, result in an increased fraction of precipitation falling as rain. However, this correlation is not strong, which is attributed to the relatively high frequency of warm events without rain. The absence of a linear correlation between total winter precipitation and TDD (R^2 = 0.07) is justified in that the vast majority of winter precipitation falls as snow, which occurs on days with few or no thawing degrees. The linear correlation between number of days rain and TDD (R^2 = 0.71) can be explained using the opposite manner; days with rain must occur on days with thawing degrees. Hansen et al. (2014) plot the number of rain events vs. temperature, which bears resemblance to the number of days rain vs. TDD (Figure 6.3). These authors apply a Poisson distribution to their results, which is likely more representative than a linear function, as the prior is a discrete event probability distribution. The aforementioned correlations indicate that winter rain sum and the number of days of rain are connected to winter TDD,

but high variability in winter meteorology in central Spitsbergen precludes these correlations from being robust. Specifically, the inconsistency of winter warm events in terms of magnitude, duration, and moisture content prohibits the direct connection of these events with mean winter meteorology parameters.

7.1.3. Warm events in the context of climate variability

Warm events on Svalbard occur when low pressure systems direct air northwards across the Nordic Seas towards the west coast of Spitsbergen (described in section 3.3). Atmospheric behavior in the Northern Hemisphere is often described in relation to the North Atlantic Oscillation (NAO) and Arctic Oscillation (AO), which are indices based on sea-level pressure differences. The phases of these indices impact cyclone activity in the Norwegian-Greenland Seas, but NAO influence on storms is limited in the high Arctic (Dickson et al. 2000). Putkonen and Roe (2003) concluded that ROS events on Spitsbergen are five times more likely during extreme positive phases of the NAO. However, Lemke and Jacobi (2011) describe increased meridional atmospheric transport resulting from extremely negative phases of the NAO and AO during the 2009-2010 winter. This winter had the most precipitation and rainfall of the 2009-2015 study period. The winters with the second and third most rainfall (2011-2012 and 2014-2015) both occurred during positive phases of the NAO and AO (NOAA 2016). Overall, the Svalbard Lufthavn 2009-2015 winter meteorology does not reliably relate to the phases of the NAO or AO, which can be attributed to the decreased influence of these indices with increased latitude (Dickson et al. 2000). Winter storminess on Svalbard is best and most simply explained as resulting from increased meridional transport (when warm air from the south reaches Svalbard), which can occur during a variety of NAO and AO phase conditions (Lemke and Jacobi 2011; Dickson et al. 2000).

An interesting pattern arises in the wind direction distribution of the 2009-2015 winters. The three warmest winters, 2009-2010, 2011-2012, and 2013-2014 exhibit a bimodal wind direction pattern with both westerly and southeasterly winds. This is in contrast to the other winters which exhibit a primarily southeast wind direction. The combination of warmer winter air temperatures and westerly winds makes sense, as cyclones and smaller polar lows bring warm air to Spitsbergen from the west (Serreze and Barry 2014). During all the 2009-2015 winters, days with positive mean air temperature were regularly associated with relative peaks in wind speed, but the associated wind directions did not show a clear pattern. It must be acknowledged that the site of Svalbard Lufthavn effects wind directions measured at this location, as topography precludes southerly winds at the airport and favors the westerly and southeasterly wind directions.

Modelling by Zahn and von Storch (2010) indicates polar low frequency will decline in an anthropogenically warmed climate. Given this, Eckerstorfer and Christiansen (2012) hypothesized that fewer low-pressure systems will reach Svalbard, reducing winter rainfall and the resultant wet snow avalanche cycles. However, the modeled decline in polar low frequency is spatially variable across the Arctic. Polar low density distribution on the west coast of Spitsbergen is predicted to remain fairly constant between the 1960-1989 control period and future climate scenarios (Zahn and von Storch 2010), making Eckerstorfer and Christiansen's (2012) hypothesis about decreasing warm event frequency unfounded. Eckerstorfer and Christiansen (2012) also concluded that only a "slow-moving polar low results in periods with positive air temperatures and large amounts of rain on snow." This is contradicted by the spikes in air temperature which characterized the 2014-2015 winter and the 15.1 mm rain event that occurred on 16 February 2015. Rennert et al. (2009) predict an increase in ROS frequency in Svalbard in the coming half-century, based on the output of a general circulation climate model. Irrespective of synoptic conditions, increasing trends in Svalbard air temperature and precipitation will continue to result in an increased fraction of liquid precipitation during winter (Førland and Hanssen-Bauer 2000).

7.1.4. Rainfall amount during ROS events

Westermann et al. (2011) determined that 20 mm of rain was required to reach the ground through a 1 m snowpack at -5°C, with an assumed maximum volumetric water content of 0.01. The assumed snow pack temperature of -5°C fits with snow observations in the valleys surrounding Longyearbyen (Farnsworth 2013), and the assumption of a 0.01 volumetric water content is reasonable given observations and models in snow science literature (Bartelt and Lehning 2002). However, snow depth at the studied landforms does not reach 1 m. Maximum snow depth at the blockfield and solifluction sheet is closer to 0.5 m, while snow depth at the loess terrace and strandflat does not exceed 30 cm (NORPERM 2016; Farnsworth 2013; Harris et al. 2011). Given these thinner snow depths, the assumption could be made that less than 20 mm of rain is required to reach the ground surface at these landforms. However, stabilization of ground surface temperature near 0°C, which is indicative of rainwater refreezing, occurred at three of the landforms (loess terrace, solifluction sheet, and strandflat) only after the two largest rain events: 4 days of rain totaling 34.2 mm in January 2010 and 2 days of rain totaling 28 mm in January 2012. Other major ROS events with less rain, like the individual day of 15.1 mm rain in February 2015, resulted in peaks in ground surface temperature, but not extended periods near 0°C. Stabilization of ground surface temperature near 0°C never occurred at the blockfield,

indicating water does not reach the blockfield surface during winter. This is unsurprising since low winter air temperatures on Breinosa (max. air temperature during the 2014-2015 winter = -0.8°C) preclude winter precipitation falling as rain at this site. Even if a massive ROS event were to occur on Breinosa, water would percolate into the blocky substrate rather than pool on the blockfield surface.

If rainwater is not reaching the ground surface during ROS events ≤15 mm, it must be trapped within the snowpack. The downward penetration of water in a snowpack is impeded by buried snow crusts and ice layers; water flows laterally along crusts until most of the layer is soaked (Conway and Benedict 1994) (Figure 2.3). Experiments in the Alps demonstrate that ice layers more than double the water storage capacity of the snowpack (Singh et al. 1997). Since the snowpack in central Svalbard is characterized by widespread ice layers and rain crusts (Eckerstorfer and Christiansen 2011), it can be concluded that most wintertime rainfall at the studied landforms freezes in the snowpack and does not reach the ground surface. This does not, however, mean that ROS events less than 20 mm are insignificant. These smaller events can still decrease snow depth (via melting and snow pack densification) and create ice layers within a snow pack that block reindeer from accessing their winter food supply (Hansen et al. 2011; Hansen et al. 2014). In addition, relatively small ROS events (<10 mm) can increase shallow ground temperatures more than dry warm events of the same magnitude; this is addressed in the following, landform specific, discussion sections.

7.2. Ground temperature response to warm events

This section begins with a discussion of ground temperature conditions at each of the landforms, focusing on processes that effect to what degree air temperatures impact ground temperatures. Afterwards, the impact of warm events is considered on the seasonal scale. At the end, the results of this thesis are directly compared to the conclusions of previous Svalbard ROS literature that regards ground temperatures.

7.2.1. Loess terrace

Ground surface temperature at the loess terrace closely follows air temperature because of minimal snow cover at this location; the ground is poorly insulated. In addition, ground surface temperature variation is the highest at this landform. This results from the site's relatively "continental" climate, which exhibits the most extreme air temperature minimums (and occasionally maximums) of the studied locations (Figure 6.6). The loess terrace is comprised of fine-grained mineral soil, making its thermal

conductivity higher than the coarser blockfield but lower than the strandflat bedrock. This is corroborated by the temperature data, as the magnitude of ground temperature fluctuations in the loess terrace is greater than those in the blockfield, but less than those in the strandflat.

Winter warm events cause temperature fluctuations at the ground surface, 1 m, and 2m in this landform. During January and February 2015, multiple spikes in air temperature occurred, some of which were associated with rain. Two of the air temperature spikes were of the same magnitude (18.8°C and 18.7°C), but the first air temperature spike was associated with a 8.6 mm rain event (22 January) while the other was not. Ground temperatures at 1 and 2 m increased more following the rain event than the dry event, indicating that warm events with rain do perturb ground temperatures more than dry events. Ground surface temperature was not constrained near 0°C after this rain event, which indicates there was not a prolonged period of rainwater freezing. Given the moderate quantity of rain (8.6 mm) it is likely that relatively little water, if any, reached the ground surface. In the absence of a thick snowpack, this water froze rapidly, regardless of if it was in the snowpack or at the ground surface. Only the two largest rain events of the investigated winters caused ground surface temperatures at this landform to stabilize near 0°, with temperature stabilization lasting 2-3 days.

7.2.2. Solifluction sheet

Ground surface temperatures at the solifluction sheet exhibit considerably less variation than in the loess terrace or strandflat; this is explained by the thicker snow cover at this site. Snow depth is approximately twice as large at the solifluction sheet than the loess terrace or strandflat. Harris et al. (2011) also found ground thermal regime at this site to be strongly influenced by snow depth and duration, which varies considerably winter-to-winter at this location. Early continuous snow cover at this site can explain the delayed onset of ground cooling in this landform compared to the others. Harris et al. (2011) found that increased snow thickness in late October and November resulted in delay of active layer freeze-back until December. Ice volume is fairly high in this landform (roughly 40-45% between 1 and 2.5 m depth) due to the transient layer (Harris et al. 2011). Increased ice content increases thermal conductivity, but this property is offset by the site's relatively thick snow cover. The smaller rain events (<20 mm) only caused increased temperatures at the ground surface, regardless of event timing. The multi-day rain event in 2010 increased temperatures at 1m, and the large January 2012 rain event was followed by temperature increases at 1 and 2 m depth. This rain event also resulted in the longest near 0°C plateau in ground surface temperature (4 days) of any site over the investigated period. This matches the finding of Westermann et al. (2011) that a thicker snowpack insulates percolated water, drawing out the rainwater

freezing process and thus the release of latent heat. Winter 2013-2014 ground temperatures were considerably warmer than the other winters and showed almost no temperature fluctuations; snow cover is also the best explanation for this scenario. A thick snowpack keeps ground temperatures warmer and greatly impedes heat conduction to the ground, reducing the ability of warm events to impact ground temperatures.

7.2.3. Blockfield

The ground temperatures at the blockfield are the lowest of any of the landforms, and warm events have the shallowest impact in this landform. One major contributing factor is the blockfield's elevation; winter air temperatures on Breinosa were typically 2.5°C lower than in Adventdalen (Figure 6.6). The 2014-2015 mean winter air temperature on Breinosa was -12.0°C, lower than that of the other studied locations. During the 2014-2015 winter, daily mean air temperature never exceeded 0°C, so technically the conditions of a warm event were never met.

In the literature, negative temperature anomalies in blocky material are explained in a number of ways: (i) the abundance of pore space between blocks allows for the downwards convection of cold air and displacement of warmer air (frequently called the Balch effect) (Harris and Pedersen 1998); (ii) the presence of an ice-rich area in the subsurface which has high thermal conductivity hampers summer thaw (Gorbunov et al. 2004); and (iii) blocks protrude through snow creating enhanced conduction (Juliussen and Humlum 2008). What follows is a discussion of the aforementioned explanations for relatively low blockfield temperatures, in relation to known conditions on Breinosa. The Balch effect might cool the blockfield early in the season, but this process ceases with snowpack development, which begins on Breinosa before the start of winter. Also, according to this process, lower temperatures should be found deeper in the blockfield – this is not the case during winter, where temperatures at 1, 2, and 3 m depth increase consecutively. The presence of ice within some of the pore space may contribute to the generally low temperatures, but a high ice content would mean greater thermal conductivity; this would cause an increased coupling of ground and air temperatures, which does not occur at the blockfield. Juliussen and Humlum (2008) found that temperature in the upper 1 m of blockfields in central-eastern Norway was coupled with winter air temperature; their explanation is that blocks protrude through the snow and act as "heat bridges," providing enhanced conduction. At the Breinosa blockfield, the situation is the opposite: ground temperatures show the least coupling with air temperatures of any of the sites, and warm events are reflected at a maximum depth of 1 m.

The significant attenuation of the air temperature signal at the blockfield must result from early, continuous snow cover. Blockfield ground temperatures, which may be driven by the Balch effect before snow cover develops, are sealed off from the atmosphere by the development of a spatially continuous snow cover that covers all blocks around the borehole. The blockfield's air-filled pore space results in a low thermal conductivity for the substrate overall, further mitigating the impact of warm events. This explanation is supported by the study of Juliussen and Humlum (2008), as they found reduced coupling of ground and air temperatures occurred with increased snow depth at blockfield sites in Norway.

7.2.4. Strandflat

Solid rock has a thermal conductivity greater than sediments. Since the entirety of the strandflat borehole is drilled into bedrock where little to snow accumulates, a close coupling of air temperature and ground surface temperature is expected and observed. The air temperature signal penetrates deepest in the ground at this site; temperature at 5 m depth increased after the warmest and rainiest day of the investigated winters (30 January 2012). The milder warm air excursions typically resulted in temperature increases in the upper 3 m of ground. It must be noted that the observed ground temperature perturbations are not representative of the entire strandflat environment, as strandflat beach deposits and have somewhat lower thermal conductivity and thus have different ground temperature profiles (Christiansen et al. 2010).

Analysis of the temperature spikes with and without rain occurring during the 2014-2015 winter (previously discussed in Section 7.2.1 in regards to the loess terrace) shows that air temperature increases of the same magnitude (18.8°C and 18.7°C) were not matched with ground temperature increases of the same magnitude; the air temperature spike occurring with rain increased temperature at 1 m 1.3°C more than the air temperature spike without rain. It is possible the difference in temperature increase at 1 m could be explained by changes in surface conditions, like a reduction in snow thickness. But, since this phenomenon is observed at multiple landforms, it is concluded that warm events with rain typically impact shallow ground temperatures more than warm events without rain.

As has been previously mentioned, Westermann et al. (2011) found that rain events had the largest impact on ground temperatures when a substantial quantity of rain percolates through a thick snowpack. Temperatures and precipitation amounts are greater at Isfjord Radio than Svalbard Lufthavn, so the first condition (of a substantial quantity of rain) is more easily met at this location than at the other inland landforms. However, the Kapp Linné area is regularly snow-blown with thin snow cover, so the freezing of rain water must happen relatively rapidly at this location, as there is not a thick snowpack

to insulate and prolong the freezing process (as described by Westermann et al. 2011). This can be seen in the ground surface temperatures at the strandflat after ROS events, as they remain near 0°C for one or two days as opposed to the four days observed at the solifluction sheet.

7.2.5. Assessment of seasonal and inter-annual impacts of warm events

The mean winter ground temperature profiles of the four warmest winters during the ground temperature series are as warm as or warmer than the 2009-2015 average, indicating that winter air temperature largely controls winter ground temperatures. This, in addition to the role of the snowpack described at each landform, leads to the conclusion that mean winter ground temperatures are primarily controlled by air temperature and the duration and depth of snow cover. At the solifluction sheet, the 2013-2014 mean winter ground temperature profile was significantly warmer than the others; this could be explained by a relatively thick and/or early snow cover that season. This also explains the reduced impact of warm events at the solifluction sheet during the 2013-2014 winter (Figure 6.8), when only the ground surface and 1 m temperatures reacted to changes in air temperature. During the rainiest winter (2009-2010), mean winter ground temperatures were relatively cool, implying that rainfall does not typically impact ground temperatures at the seasonal scale. However, enough consecutive warm events would impact mean winter air temperature, and thus may result in increased mean ground temperatures.

Mean annual ground temperatures at 10 m depth (Figure 6.11) show that permafrost temperatures have been increasing 0.3°C to 0.9°C in all the landforms since the boreholes were drilled. The 10 m temperature trends indicate that any warming arising from intra-seasonal temperature variations or rain events is superimposed on general permafrost warming. Hansen et al. (2014) came to the same conclusion about the January 2012 rain event and permafrost temperatures at Janssonhaugen.

7.2.6. Comparisons with previous studies

At the beginning of this thesis, conclusions from previous Svalbard ROS literature were put forth as hypotheses: (i) strong wintertime rain events impact ground temperatures, and do so most significantly when snow depth is high and a large quantity of rain falls over a short period (Westermann et al. 2011); (ii) wintertime rain events constrain ground surface temperature near 0°C for prolonged periods (Westermann et al. 2011; Hansen et al. 2014); and (iii) extreme warm events with rain cause substantial increase in permafrost temperatures, with ground temperature response lasting weeks to months after the event (Hansen et al. 2014; Isaksen et al. 2000). What follows is a discussion of these points, based on the results presented in this thesis and how they compare to the literature.

The ground temperature response of the landforms to the large January 2010 and 2012 ROS events supports (i), as these events resulted in some of the deepest ground temperature perturbations. ROS events >20 mm tend to constrain ground surface temperatures near 0°C. Smaller ROS events cause peaks in ground surface temperature (not plateaus), but still impact ground temperatures a few meters into the ground. The second portion of statement (i), that ROS event impact is most significant with high snow depth and rapid rain, is supported by ground surface temperature at the solifluction sheet after the extreme January 2012 ROS event. Ground surface temperature remained between 0°C and -1°C for four days despite decreased air temperature after the event, indicating some freezing of rainwater releasing latent heat. The snowpack at the solifluction sheet is roughly twice as thick as at the other low elevation landforms. According to Westermann et al. (2011) large snow depths delay the freezing of infiltrated water, so the increased snow depth at the solifluction sheet explains why ground surface temperature remained near 0°C for a longer period of time at this landform.

This discussion leads directly into point (ii). Westerman et al. (2011) found that ground surface temperature at a site near Ny-Ålesund was constrained near 0°C for several weeks following a period of rain and slush in December 2005 and January 2006. The longest period of near 0°C ground surface temperature observed in the landforms occurred at the solifluction sheet after the January 2012 ROS event, when ground surface temperature remained between 0°C and -1°C for four days. The relatively long period of near 0°C ground surface temperature observed by Westermann et al. (2011) can be explained by the increased snow depths and rainfall in Ny-Ålesund compared to Longyearbyen. In the event described by Westermann et al. (2011), snow depth was around 0.7 m and rainfall totaled 40 mm; snow depth and rainfall was always lower at the studied landforms. Hansen et al. (2014) found that ground surface temperatures at some sites in central Spitsbergen stayed near 0°C for two weeks or more following the January 2012 ROS event. However, the sites where this was observed are in Semmeldalen, a valley approximately 30 km south of Longyearbyen. At Janssonhaugen (a hill on the east end of Adventdalen), ground surface temperature response was of shorter duration (Hansen et al. 2014), matching with the observed length of ground surface temperature response to ROS events studied in the landforms. It can be concluded that ROS events can constrain ground surface temperature near 0°C for prolonged periods, but this requires extreme rainfall and a thick snowpack, conditions that are not typically met in the Longyearbyen area.

The last point (iii), that extreme ROS events cause substantial increase in permafrost temperatures, with ground temperature response lasting weeks to months, is the most subjective.

Hansen et al. (2014) concluded that "a long-lasting extreme warm spell … caused a substantial rise in permafrost temperatures." The authors based their findings on 30-day mean ground temperature to 5 m depth at Janssonhaugen. The 30-day period was adjusted successively with depth to account for phase lag. The resulting figure (Figure 7.1) is somewhat misleading, as a reader could easily think the ground temperatures at all the depths occurred at the same time. By adjusting for phase lag, the 30-day period at 5 m depth occurs more than three months after the 30-day period at the surface (Isaksen et al. 2001). This method averages ground temperatures which are effected by air temperature overall, not just the conditions of the event. The 2011-2012 winter had the highest mean winter temperature (-6.0°C) of the 2009-2015 period. The authors acknowledge the ROS event was part of a two week warm spell, but the averaged ground temperatures are not presented in context of that winter's overall warmth. In addition, Janssonhaugen is a bedrock borehole, so increased ground temperature perturbations are expected given the site's relatively high thermal conductivity. Though the language of Hansen et al. (2014) may overstate the lasting impact of warm events on ground temperatures, the results presented in this thesis confirm that warm events perturb ground temperatures down to 5 m depth in bedrock. The ground substrate is key, as warm events do not impact ground temperatures this deep in other landforms of lower thermal conductivity.

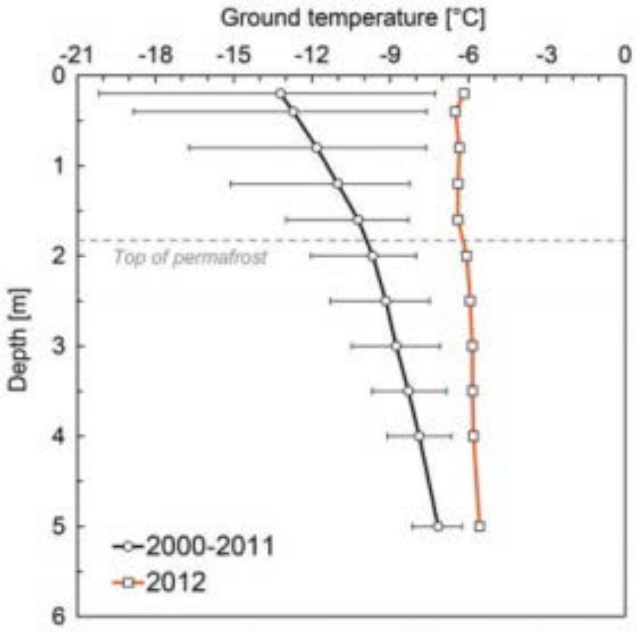

The extreme warm spell and ROS events in January–February 2012 caused dramatic changes in the properties of the permafrost and the snow-pack. (a) 30-Day mean ground temperature centred at 30 January down to 5 m depth at Janssonhaugen (in Adventdalen, close to Longeyarbyen) for 2011–12 (red line) compared to the mean for 2000–11 (black line). Horizontal bars show the absolute variations of the previous years, grey dotted line indicates the top of permafrost. To be representative and detect the full effect of the extreme warm spell that penetrated into the permafrost, the period for the 30-day mean ground temperature values in the series is adjusted successively with depth for the phase lag following calculations made for the study site by Isaksen *et al* (2000).

Figure 7.1. 30-day mean ground temperature centered around the January 2012 ROS event (red line) in Janssonhaugen. From Hansen et al. (2014), shown with the original caption.

8. Conclusions and Perspectives

The main aims of this thesis were to identify and characterize winter ROS and warm events on Svalbard, determine how deep these events perturb ground temperatures, and to compare the impact of warm events with and without rain. Warm events were also examined in the context of seasonal and annual ground temperatures. The investigation of these aims led to the following conclusions:

- Warm events result from low-pressure systems bringing warm, moist air from the south to Spitsbergen's west coast. The activity of these storms is impacted by atmospheric circulation at the synoptic scale, and increases during regimes of increased meridional transport. Both dry and moist winter warm events on Svalbard are hypothesized to increase in frequency in the future, due to increasing trends in both air temperature and precipitation. These increasing trends will result in an increased fraction of precipitation falling as rain during winter (Førland and Hanssen-Bauer 2000), increasing the number of rain-on-snow events in central Svalbard.
- Warm events result in increases in ground temperatures down to 2 m depth in the loess terrace and solifluction sheet, down to 1 m depth in the blockfield, and down to 5 m depth in the strandflat. The end members in terms of detected depth – the blockfield and strandflat – are also the end members in terms of thermal conductivity. Air temperature analysis of the 2014-2015 winter indicated that winter warm events rarely occur at higher elevations like the blockfield on Breinosa.
- ROS events result in higher amplitude ground temperature changes than warm events, though this is only true for ground surface temperature and the uppermost meters of the ground (2 m and above). Rain-on-snow events with more than 20 mm of rainfall have the greatest impact on ground surface temperature, causing temperature to stabilize near 0°C for multiple days. Previous literature has overlooked the impact of dry warm events, which also result in local maxima in ground temperatures.
- Mean winter ground temperatures are primarily controlled by air temperature and the duration and depth of snow cover. Total winter rainfall does not correlate with mean winter ground temperatures. However, the occurrence of enough warm events leads to a relatively high mean winter air temperature, resulting in higher mean winter ground temperatures. Any seasonal warming is superimposed on an observed permafrost warming trend in the studied landforms.

The previous literature on Svalbard ground temperature response to ROS studied ground temperatures in soil with a high mineral content, and bedrock (Westermann et al. 2011; Hansen et al. 2014). These materials have relatively high thermal conductivity compared to other landforms found on Svalbard, like blockfields and solifluction sheets. This thesis has shown the impact of warm events on ground temperatures varies significantly from landform to landform, and thus on the landscape scale. It is concluded that warm events on Spitsbergen impact ground temperatures the most in valleys and coastal plains where air temperatures tend to be higher and where fine-grained landforms and bedrock outcrops can be found. ROS events have the greatest impact on ground temperatures where snow depth and rainfall are high, meaning the dry Longyearbyen area and snow-blown Kapp Linné strandflat are somewhat less impacted by these events than localities with both high snow depth and rainfall, like Ny-Ålesund (Westermann et al. 2011). This spatial, locality-based consideration of warm event impact is absent in the previous literature.

Future research on the impact of winter warm events on ground temperatures should include a more detailed analysis of snow conditions. A simple, regular measurement of snow depth would improve understanding of warm event impact and winter ground thermal regime in general. Ground temperatures are measured in a borehole near Ny-Ålesund; this ground temperature series should be compared to those presented here to confirm the proposed spatial variability in event impact described above. A follow-up study should also be conducted regarding the extreme ROS event that occurred from 29 December 2015 to 3 January 2016 (the resulting icing is depicted in the cover image). During this period, daily mean air temperature reached 5.2°C and 33.5 mm of rain fell (eKlima 2016). Though this amount of rainfall is comparable to ROS events that occurred during the 2009-2015 study period, a warm event of this magnitude (in terms of air temperature) and duration is unprecedented. This event was not considered in this thesis since ground temperature data from this period has not yet been downloaded from the boreholes.

References

Andersland, O.B., and Ladanyi, B. 2004. *Frozen ground engineering* (2 ed.) John Wiley & Sons. 363 pp.

Arctic Council, Conservation of Arctic Flora and Fauna Working Group (CAFF). 2001. *CAFF Map No.18 - Average atmospheric sea-level air pressure in winter and summer 2001.* Image available at: http://library.arcticportal.org/1342/ (Accessed: 05.04.2016)

Åkerman, H.J., and Johansson, M. 2008. Thawing permafrost and thicker active layers in sub-Arctic Sweden. *Permafrost and Periglacial Processes* 19 (3), 279-292.

Baggi, S., and Schweizer, J. 2009. Characteristics of wet-snow avalanche activity: 20 years of observations from a high alpine valley (Dischma, Switzerland). *Natural Hazards* 50 (1), 97-108.

Bartelt, P., and Lehning, M. 2002. A physical SNOWPACK model for the Swiss avalanche warning: Part I: numerical model. *Cold Regions Science and Technology* 35 (3), 123-145.

Bartsch, A. 2010. Ten years of SeaWinds on QuikSCAT for snow applications. *Remote Sensing* 2 (4), 1142-1156.

Benn, D., and Evans, D. 2010. *Glaciers and Glaciation*. London: Hodder Education. 802 pp.

Brown, J., Hinkel, K., and Nelson, F. 2000. The circumpolar active layer monitoring (CALM) program: research designs and initial results. *Polar geography* 24 (3), 166-258.

Bryant, I.D. 1982. Loess deposits in lower Adventdalen, Spitsbergen. *Polar Research* 2, 93-103.

Butt, F.A., Drange, H., Elverhøi, A., Otterå, O.H., and Solheim, A. 2002. Modelling Late Cenozoic isostatic elevation changes in the Barents Sea and their implications for oceanic and climatic regimes: preliminary results. *Quaternary Science Reviews* 21 (14), 1643-1660.

Butt, F., Elverhøi, A., Solheim, A., and Forsberg, C. 2000. Deciphering Late Cenozoic development of the western Svalbard Margin from ODP Site 986 results. *Marine Geology* 169 (3), 373-390.

Christiansen, H.H. 2005. Thermal regime of ice-wedge cracking in Adventdalen, Svalbard. *Permafrost and Periglacial Processes* 16 (1), 87-98.

Christiansen, H.H., Etzelmüller, B., Isaksen, K., Juliussen, H., Farbrot, H., Humlum, O., Johansson, M., Ingeman-Nielsen, T., Kristensen, L., Hjort, J., Holmlund, P., Sannel, A.B.K., Sigsgaard, C., Åkerman, H.J., Foged, N., Blikra, L.H., Pernosky, M.A., and Ødegård, R.S. 2010. The thermal state of permafrost in the Nordic area during the International Polar Year 2007-2009. *Permafrost and Periglacial Processes* 21 (2), 156-181.

Christiansen, H.H., French, H.M., and Humlum, O. 2005. Permafrost in the Gruve-7 mine, Adventdalen, Svalbard. *Norsk Geografisk Tidsskrift-Norwegian Journal of Geography* 59 (2), 109-115.

Christiansen, H.H., and Humlum, O. 2008. Interannual variations in active layer thickness in Svalbard. *Ninth International Conference on Permafrost Proceedings*. Kane, D.L. and Hinkel, K.M. (eds.) Fairbanks, AK, 29 June-3 July 2008. 9, 257-262.

Christiansen, H.H., Humlum, O., and Eckerstorfer, M. 2013. Central Svalbard 2000-2011 meteorological dynamics and periglacial landscape response. *Arctic, Antarctic, and Alpine Research* 45 (1), 6-18.

Cimoli, E. 2015. *Determining Snow Depth Distribution from Unmanned Aerial Vehicles and Digital Photogrammetry*. Master thesis. Department of Civil Engineering, Technical University of Denmark (DTU). 73 pp.

Colbeck, S.C. 1979. Water flow through heterogeneous snow. *Cold Regions Science and Technology* 1 (1), 37-45.

Conway, H., and Benedict, R. 1994. Infiltration of water into snow. *Water Resources Research* 30 (3), 641-649.

Conway, H., Carran, W., and Carran, A. 2009. Rain-on-snow avalanches: forecasting the return to stability. *International Snow Science Workshop.* Davos, Switzerland, 27 September-2 October 2009. 267-270.

Dallmann, W.K. (ed.) 2015. *Geoscience Atlas of Svalbard.* Report Series No. 148. Tromsø: Norsk Polarinstitutt. 292 pp.

Decaulne, A., and Sæmundsson, T. 2006. Geomorphic evidence for present-day snow-avalanche and debris-flow impact in the Icelandic Westfjords. *Geomorphology* 80 (1), 80-93.

Dickson, R., Osborn, T., Hurrell, J., Meincke, J., Blindheim, J., Adlandsvik, B., Vinje, T., Alekseev, G., and Maslowski, W. 2000. The Arctic ocean response to the North Atlantic oscillation. *Journal of Climate* 13 (15), 2671-2696.

Drobot, S., Stroeve, J., Maslanik, J., Emery, W., Fowler, C., and Kay, J. 2008. Evolution of the 2007–2008 Arctic sea ice cover and prospects for a new record in 2008. *Geophysical Research Letters* 35 (19).

Eckerstorfer, M., and Christiansen, H.H. 2011. The "high Arctic maritime snow climate" in central Svalbard. *Arctic, Antarctic, and Alpine Research* 43 (1), 11-21.

Eckerstorfer, M., and Christiansen, H.H. 2012. Meteorology, Topography and Snowpack Conditions causing Two Extreme Mid-Winter Slush and Wet Slab Avalanche Periods in High Arctic Maritime Svalbard. *Permafrost and Periglacial Processes* 23 (1), 15-25.

eKlima. 2016. Free access weather and climate data. Norwegian Meteorological Institute. http://eklima.met.no (Accessed: 11.2015-02.2016)

Elberling, B. 2007. Annual soil CO_2 effluxes in the High Arctic: The role of snow thickness and vegetation type. *Soil Biology and Biochemistry* 39 (2), 646-654.

Etzelmüller, B., Schuler, T., Isaksen, K., Christiansen, H., Farbrot, H., and Benestad, R. 2011. Modeling the temperature evolution of Svalbard permafrost during the 20th and 21st century. *The Cryosphere* 5 (1), 67-79.

Farnsworth, W.R. 2013. *The Topographical and Meteorological Influence on Snow Distribution in Central Svalbard: How the spatial variability of snow influences slope-scale stability, permafrost landform dynamics and regional distribution trends*. Master thesis. Department of Geosciences, University of Oslo. 150 pp.

Fassnacht, S. 2004. Estimating Alter-shielded gauge snowfall undercatch, snowpack sublimation, and blowing snow transport at six sites in the coterminous USA. *Hydrological Processes* 18 (18), 3481-3492.

French, H.M. 2007. *The Periglacial Environment*. John Wiley & Sons. 458 pp.

Furdada, G., Martínez, P., Oller, P., and Vilaplana, J.M. 1999. Slushflows at El Port del Comte, northeast Spain. *Journal of Glaciology* 45 (151), 555-558.

Førland, E.J.(ed.), Benestad, R.E., Flatøy, F., Hanssen-Bauer, I., Haugen, J.E., Isaksen, K., Sorteberg, A., and Ådlandsvik, B. 2009. *Climate development in North Norway and the Svalbard region during 1900–2100*. Tromsø: Norsk Polarinstitutt, Rapportserie Nr. 128. 44 pp.

Førland, E.J., Benestad, R., Hanssen-Bauer, I., Haugen, J.E., and Skaugen, T.E. 2011. Temperature and precipitation development at Svalbard 1900–2100. *Advances in Meteorology* 2011, doi:10.1155/2011/893790. [Online].

Førland, E.J., and Hanssen-Bauer, I. 2000. Increased precipitation in the Norwegian Arctic: True or false? *Climatic Change* 46 (4), 485-509.

Førland, E.J., and Hanssen-Bauer, I. 2003. Past and future climate variations in the Norwegian Arctic: overview and novel analyses. *Polar Research* 22 (2), 113-124.

Førland, E., Hanssen-Bauer, I., and Nordli, P.Ø. 1997. *Orographic precipitation at the glacier Austre Brøggerbreen, Svalbard*. Oslo: Norwegian Meteorological Institute (DNMI), Report 2/97. 45 pp.

Gilbert, G.L. 2014. *Sedimentology and geocryology of an Arctic fjord head delta (Adventdalen, Svalbard)*. Master thesis. Department of Geosciences, University of Oslo. 123 pp.

Gorbunov, A.P., Marchenko, S.S., and Seversky, E.V. 2004. The thermal environment of blocky materials in the mountains of Central Asia. *Permafrost and Periglacial Processes* 15 (1), 95-98.

Grenfell, T., and Putkonen, J. 2008. A method for the detection of the severe rain-on-snow event on Banks Island, October 2003, using passive microwave remote sensing. *Water Resources Research* 44 (3).

Groisman, P.Y., Sun, B., Vose, R.S., Lawrimore, J.H., Whitfield, P.H., Førland, E., Hanssen-Bauer, I., Serreze, M.C., Razuvaev, V.N., and Alekseev, G.V. 2003. Contemporary climate changes in high latitudes of the Northern Hemisphere: daily time resolution. *14th Symposium on Global Change and Climate Variations,* American Meteorological Society. Long Beach, CA, 2003. CD 4.8.

Hansen, B.B., Aanes, R., Herfindal, I., Kohler, J., and Sæther, B. 2011. Climate, icing, and wild arctic reindeer: past relationships and future prospects. *Ecology* 92 (10), 1917-1923.

Hansen, B.B., Isaksen, K., Benestad, R.E., Kohler, J., Pedersen, Å.Ø., Loe, L.E., Coulson, S.J., Larsen, J.O., and Varpe, Ø. 2014. Warmer and wetter winters: characteristics and implications of an extreme weather event in the High Arctic. *Environmental Research Letters* 9 (11), 114021.

Hanssen-Bauer, I., and Førland, E. 1998. Long-term trends in precipitation and temperature in the Norwegian Arctic: can they be explained by changes in atmospheric circulation patterns? *Climate Research* 10 (2), 143-153.

Hanssen-Bauer, I., Solås, M., and Steffensen, E. 1990. *The climate of Spitsbergen*. Oslo: Norwegian Meteorological Institute (DNMI), Report 39/90 Klima. 40 pp.

Harris, S.A., French, H.M., Heginbottom, J.A., Johnston, G.H., Ladanyi, B., Sego, D.C., and van Everdingen, R.O. 1988. *Glossary of permafrost and related ground-ice terms.* Permafrost Subcommittee, National Research Council of Canada. Technical memorandum No. 142. 156 pp.

Harris, C., Kern-Luetschg, M., Christiansen, H.H., and Smith, F. 2011. The role of interannual climate variability in controlling solifluction processes, Endalen, Svalbard. *Permafrost and Periglacial Processes* 22 (3), 239-253.

Harris, C., Mühll, D.V., Isaksen, K., Haeberli, W., Sollid, J.L., King, L., Holmlund, P., Dramis, F., Guglielmin, M., and Palacios, D. 2003. Warming permafrost in European mountains. *Global and Planetary Change* 39 (3), 215-225.

Harris, S.A., and Pedersen, D.E. 1998. Thermal regimes beneath coarse blocky materials. *Permafrost and Periglacial Processes* 9 (2), 107-120.

Held, I.M., and Soden, B.J. 2006. Robust responses of the hydrological cycle to global warming. *Journal of Climate* 19 (21), 5686-5699.

Hinkel, K.M., and Nicholas, J.R. 1995. Active layer thaw rate at a boreal forest site in central Alaska, USA. *Arctic and Alpine Research* 27 (1), 72-80.

Hopsø, I.S. 2013. *Wet snow detection by C-band SAR in avalanche forecasting*. Master thesis. Department of Physics and Technology, University of Tromsø. 79 pp.

Humlum, O. 1997. Active layer thermal regime at three rock glaciers in Greenland. *Permafrost and Periglacial Processes* 8 (4), 383-408.

Humlum, O. 2002. Modelling late 20th-century precipitation in Nordenskiöld Land, Svalbard, by geomorphic means. *Norsk Geografisk Tidsskrift-Norwegian Journal of Geography* 56 (2), 96-103.

Humlum, O., Instanes, A., and Sollid, J.L. 2003. Permafrost in Svalbard: a review of research history, climatic background and engineering challenges. *Polar Research* 22 (2), 191-215.

Ingólfsson, Ó. 2011. Fingerprints of Quaternary glaciations on Svalbard. *Geological Society, London, Special Publications* 354 (1), 15-31.

Ingólfsson, Ó., and Landvik, J.Y. 2013. The Svalbard–Barents Sea ice-sheet–Historical, current and future perspectives. *Quaternary Science Reviews* 64, 33-60.

Isaksen, K., Benestad, R.E., Harris, C., and Sollid, J.L. 2007a. Recent extreme near-surface permafrost temperatures on Svalbard in relation to future climate scenarios. *Geophysical Research Letters* 34 (17).

Isaksen, K., Holmlund, P., Sollid, J.L., and Harris, C. 2001. Three deep Alpine-permafrost boreholes in Svalbard and Scandinavia. *Permafrost and Periglacial Processes* 12 (1), 13-25.

Isaksen, K., Mühll, D.V., Gubler, H., Kohl, T., and Sollid, J.L. 2000. Ground surface-temperature reconstruction based on data from a deep borehole in permafrost at Janssonhaugen, Svalbard. *Annals of Glaciology* 31 (1), 287-294.

Isaksen, K., Sollid, J.L., Holmlund, P., and Harris, C. 2007b. Recent warming of mountain permafrost in Svalbard and Scandinavia. *Journal of Geophysical Research: Earth Surface* 112 (F2).

Jaedicke, C., Høydal, Ø.A., and Midtbø, K.H. 2013. Identification of slushflow situations from regional weather models. *International Snow Science Workshop*. Grenoble, France, 7-11 October 2013. 177-182.

Juliussen, H., Christiansen, H., Strand, G., Iversen, S., Midttømme, K., and Rønning, J. 2010. NORPERM, the Norwegian Permafrost Database–a TSP NORWAY IPY legacy. *Earth System Science Data* 2 (2), 235-246.

Juliussen, H., and Humlum, O. 2008. Thermal regime of openwork block fields on the mountains Elgåhogna and Sølen, central-eastern Norway. *Permafrost and Periglacial Processes* 19 (1), 1-18.

Kattsov, V.M., and Källén, E. 2005. Future Climate Change: Modeling and Scenarios for the Arctic (Chapter 4). *In* Symon, C., Arris, L., and Heal, B. (eds.) *Arctic Climate Impact Assessment*. ACIA Scientific Report. Cambridge University Press, 99-150.

Knies, J., Matthiessen, J., Vogt, C., Laberg, J.S., Hjelstuen, B.O., Smelror, M., Larsen, E., Andreassen, K., Eidvin, T., and Vorren, T.O. 2009. The Plio-Pleistocene glaciation of the Barents Sea–Svalbard

region: a new model based on revised chronostratigraphy. *Quaternary Science Reviews* 28 (9), 812-829.

Kohler, J., and Aanes, R. 2004. Effect of winter snow and ground-icing on a Svalbard reindeer population: results of a simple snowpack model. *Arctic, Antarctic, and Alpine Research* 36 (3), 333-341.

Kudryavtsev, V.A., Garagulya, L.S., Kondrat'yeva, K.A. and Melamed, V.G. 1977. *Fundamentals of Frost Forecasting in Geological Engineering Investigations.* Translated by U.S. Joint Publications Research Service for U.S. Army Cold Regions Research and Engineering Laboratory, Hanover, New Hampshire. 489 pp.

Lachenbruch, A.H., and Marshall, B.V. 1986. Changing climate: geothermal evidence from permafrost in the Alaskan Arctic. *Science* 234 (4777), 689-696.

Landvik, J.Y., Alexanderson, H., Henriksen, M., and Ingólfsson, Ó. 2014. Landscape imprints of changing glacial regimes during ice-sheet build-up and decay: a conceptual model from Svalbard. *Quaternary Science Reviews* 92, 258-268.

Landvik, J.Y., Bondevik, S., Elverhøi, A., Fjeldskaar, W., Mangerud, J., Salvigsen, O., Siegert, M.J., Svendsen, J., and Vorren, T.O. 1998. The last glacial maximum of Svalbard and the Barents Sea area: ice sheet extent and configuration. *Quaternary Science Reviews* 17 (1), 43-75.

Landvik, J.Y., Ingolfsson, O., Mienert, J., Lehman, S.J., Solheim, A., Elverhøi, A., and Ottesen, D. 2005. Rethinking Late Weichselian ice-sheet dynamics in coastal NW Svalbard. *Boreas* 34 (1), 7-24.

Langhamer, D. 2009. *Influence of summer meteorology and local ground conditions on thaw progression for two Circumpolar Active Layer Monitoring (CALM) sites: A comparison between northeast Greenland and central Svalbard.* Diploma thesis. Geographisches Institut (Institute of Geogrpahy), Heidelberg University. 83 pp.

Lemke, P., and Jacobi, H. 2011. *Arctic climate change: the ACSYS decade and beyond.* Springer Science & Business Media. 464 pp.

Marsh, P. 2016. *Flow Fingers, Resolute, NWT*. Available at: http://philipmarsh.ca/?attachment_id=138 (Accessed: 15.05.2016)

McBean, G. 2005. Arctic Climate: Past and Present (Chapter 2). *In* Symon, C., Arris, L., and Heal, B. (eds.) *Arctic Climate Impact Assessment*. ACIA Scientific Report. Cambridge University Press, 21-60.

NOAA (National Oceanic and Atmospheric Administration). 2016. *Teleconnections*. Available at: http://www.ncdc.noaa.gov/teleconnections/ (Accessed: 23.05.2016)

Nordli, P.Ø., Hanssen-Bauer, I., and Førland, E. 1996. *Homogeneity analyses of temperature and precipitation series from Svalbard and Jan Mayen*. Oslo: Norwegian Meteorological Institute (DNMI), Report 16/96 Klima. 41 pp.

Nordli, Ø., Przybylak, R., Ogilvie, A.E., and Isaksen, K. 2014. Long-term temperature trends and variability on Spitsbergen: the extended Svalbard Airport temperature series, 1898-2012. *Polar Research* 33, 21349.

NORPERM (Svalbard). 2016. Ground temperature database hosted by the Geological Survey of Norway. Available at: http://geo.ngu.no/kart/permafrost_svalbard/?lang=English

Norwegian Polar Institute. 2016. *Svalbardkartet*. Available at: http://svalbardkartet.npolar.no/en/ (Accessed: 14.04.2016)

O'Gorman, P.A., and Schneider, T. 2009. The physical basis for increases in precipitation extremes in simulations of 21st-century climate change. *Proceedings of the National Academy of Sciences of the United States of America* 106 (35), 14773-14777.

Osterkamp, T. 2007. Characteristics of the recent warming of permafrost in Alaska. *Journal of Geophysical Research: Earth Surface* 112 (F2).

Overland, J.E., and Wang, M. 2010. Large-scale atmospheric circulation changes are associated with the recent loss of Arctic sea ice. *Tellus A* 62 (1), 1-9.

Przybylak, R. 2003. *The climate of the Arctic.* Springer. 270 pp.

Putkonen, J., Grenfell, T.C., Rennert, K., Bitz, C., Jacobson, P., and Russell, D. 2009. Rain on snow: little understood killer in the north. *Eos, Transactions American Geophysical Union* 90 (26), 221-222.

Putkonen, J., and Roe, G. 2003. Rain-on-snow events impact soil temperatures and affect ungulate survival. *Geophysical Research Letters* 30 (4), 1188.

Rennert, K.J., Roe, G., Putkonen, J., and Bitz, C.M. 2009. Soil thermal and ecological impacts of rain on snow events in the circumpolar Arctic. *Journal of Climate* 22 (9), 2302-2315.

Romanovsky, V., and Osterkamp, T. 1997. Thawing of the active layer on the coastal plain of the Alaskan Arctic. *Permafrost and Periglacial Processes* 8 (1), 1-22.

Schirmer, M., Wirz, V., Clifton, A., and Lehning, M. 2011. Persistence in intra-annual snow depth distribution: 1. Measurements and topographic control. *Water Resources Research* 47, W09516, doi:10.1029/2010WR009426.

Screen, J.A., and Simmonds, I. 2010. The central role of diminishing sea ice in recent Arctic temperature amplification. *Nature* 464 (7293), 1334-1337.

Serreze, M.C., and Barry, R.G. 2014. *The Arctic climate system* (2 ed.) Cambridge University Press. 404 pp.

Serreze, M.C., Carse, F., Barry, R.G., and Rogers, J.C. 1997. Icelandic low cyclone activity: Climatological features, linkages with the NAO, and relationships with recent changes in the Northern Hemisphere circulation. *Journal of Climate* 10 (3), 453-464.

Singh, P., Spitzbart, G., Hübl, H., and Weinmeister, H. 1997. Hydrological response of snowpack under rain-on-snow events: a field study. *Journal of Hydrology* 202 (1), 1-20.

Smith, M., and Riseborough, D. 2002. Climate and the limits of permafrost: a zonal analysis. *Permafrost and Periglacial Processes* 13 (1), 1-15.

Smith, S., Romanovsky, V., Lewkowicz, A., Burn, C., Allard, M., Clow, G., Yoshikawa, K., and Throop, J. 2010. Thermal state of permafrost in North America: a contribution to the international polar year. *Permafrost and Periglacial Processes* 21 (2), 117-135.

Smith, S.L., Wolfe, S.A., Riseborough, D.W., and Nixon, F.M. 2009. Active-layer characteristics and summer climatic indices, Mackenzie Valley, Northwest Territories, Canada. *Permafrost and Periglacial Processes* 20 (2), 201-220.

Stimberis, J., and Rubin, C.M. 2011. Glide avalanche response to an extreme rain-on-snow event, Snoqualmie Pass, Washington, USA. *Journal of Glaciology* 57 (203), 468-474.

Su, H., and Wang, Y. 2012. Using MODIS data to estimate sea ice thickness in the Bohai Sea (China) in the 2009–2010 winter. *Journal of Geophysical Research: Oceans* 117 (C10).

Tsukernik, M., Kindig, D.N., and Serreze, M.C. 2007. Characteristics of winter cyclone activity in the northern North Atlantic: Insights from observations and regional modeling. *Journal of Geophysical Research: Atmospheres* 112 (D3) .

Vorren, T.O., Landvik, J.Y., Andreassen, K., and Laberg, J.S. 2011. Glacial history of the Barents Sea region. *In* Ehlers, J., Gibbard, P.L., and Hughes, P.D. (eds.) *Developments in Quaternary Science*. Quaternary Glaciations – Extent and Chronology: A Closer Look. Vol. 15. 361-372.

Walczowski, W., and Piechura, J. 2011. Influence of the West Spitsbergen Current on the local climate. *International Journal of Climatology* 31 (7), 1088-1093.

Walker, D., Jia, G., Epstein, H., Raynolds, M., Chapin III, F., Copass, C., Hinzman, L., Knudson, J., Maier, H., Michaelson, G., Nelson, F., Ping, C.L., Romanovsky V.E., and Shiklomanov, N. 2003. Vegetation-soil-thaw-depth relationships along a low-arctic bioclimate gradient, Alaska: Synthesis of information from the ATLAS studies. *Permafrost and Periglacial Processes* 14 (2), 103-123.

Waller, R.I., Murton, J.B., and Kristensen, L. 2012. Glacier–permafrost interactions: Processes, products and glaciological implications. *Sedimentary Geology* 255 1-28.

Watanabe, T., Matsuoka, N., and Christiansen, H.H. 2013. Ice-and Soil-Wedge Dynamics in the Kapp Linné Area, Svalbard, Investigated by Two-and Three-Dimensional GPR and Ground Thermal and Acceleration Regimes. *Permafrost and Periglacial Processes* 24 (1), 39-55.

Westermann, S., Boike, J., Langer, M., Schuler, T., and Etzelmüller, B. 2011. Modeling the impact of wintertime rain events on the thermal regime of permafrost. *The Cryosphere* 5, 1697-1736.

Wetherald, R.T., and Manabe, S. 1975. The effects of changing the solar constant on the climate of a general circulation model. *Journal of the Atmospheric Sciences* 32 (11), 2044-2059.

Williams, P.J., and Smith, M.W. 1989. *The Frozen Earth*. Cambridge University Press. 306 pp.

Yoshikawa, K., and Nakamura, T. 1996. Pingo growth ages in the delta area, Adventdalen, Spitsbergen. *Polar Record* 32 (183), 347-352.

Zahn, M., and von Storch, H. 2010. Decreased frequency of North Atlantic polar lows associated with future climate warming. *Nature* 467 (7313), 309-312.

Appendix A

Additional meteorology figures

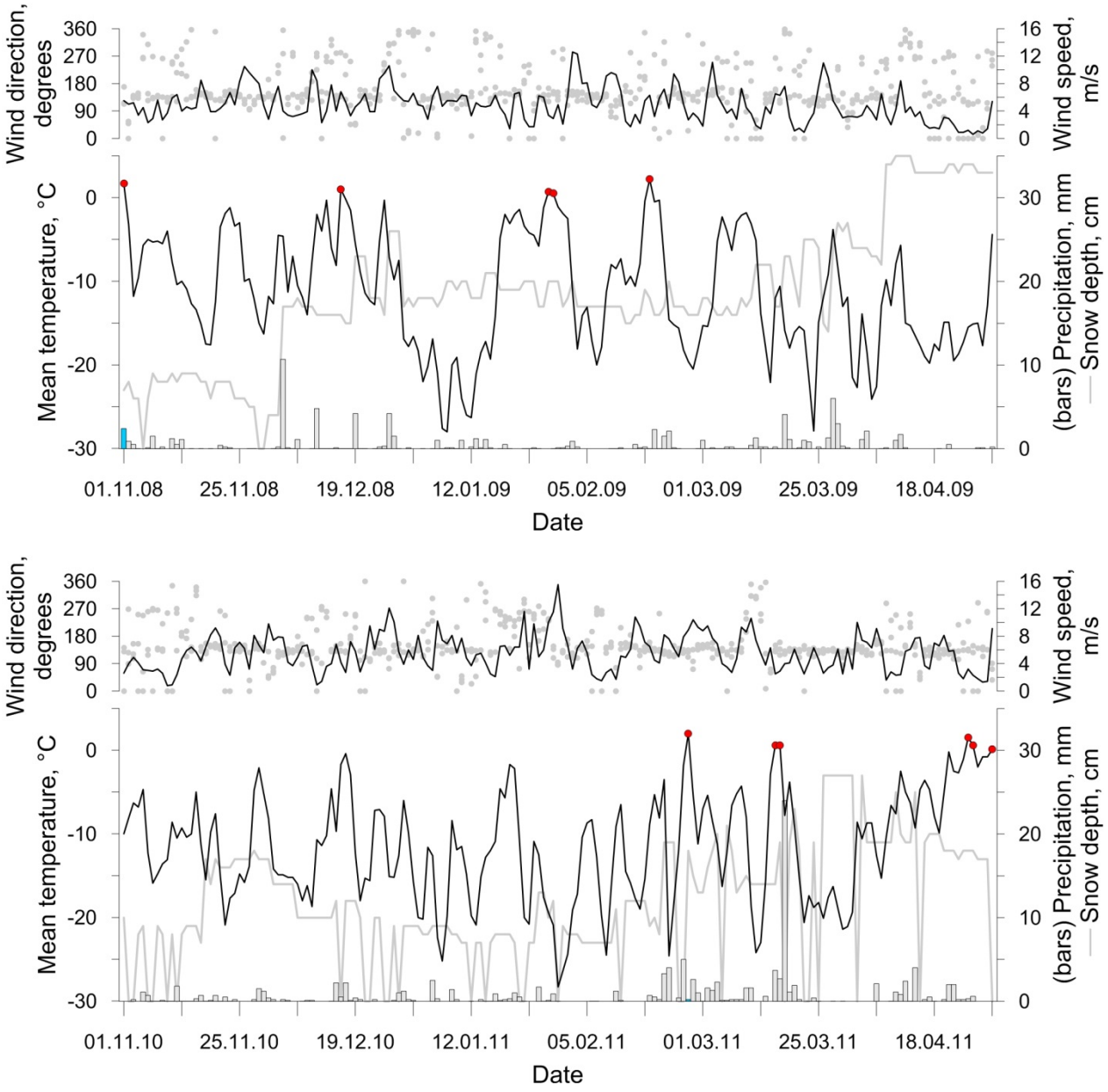

Figure A.1. Meteorology for winters 2008-2009 (top) and 2010-2011 (bottom). Red dots indicate when daily mean air temperature exceeded 0°C, blue bars indicate rain, and gray bars indicate snow. Gray dots indicate wind direction measured at 06, 12, and 18 Coordinated Universal Time (UTC).

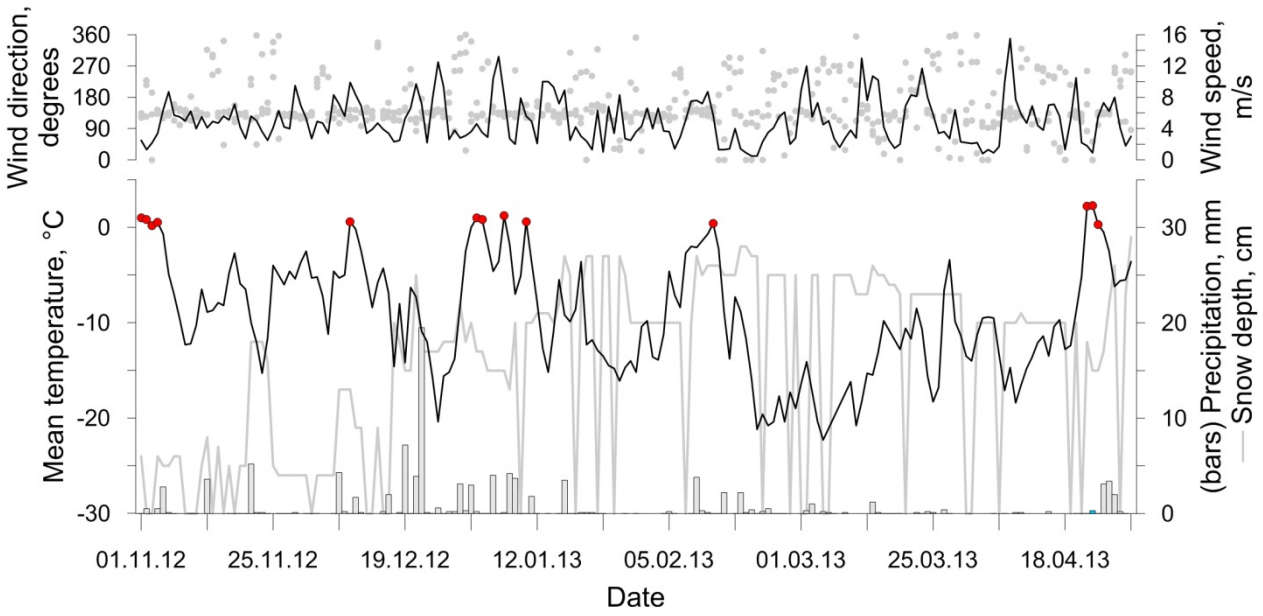

Figure A.2. Meteorology for the 2012-2013 winter. Red dots indicate when daily mean air temperature exceeded 0°C, blue bars indicate rain, and gray bars indicate snow. Gray dots indicate wind direction measured at 06, 12, and 18 Coordinated Universal Time (UTC).

Appendix B

Additional ground temperature figures

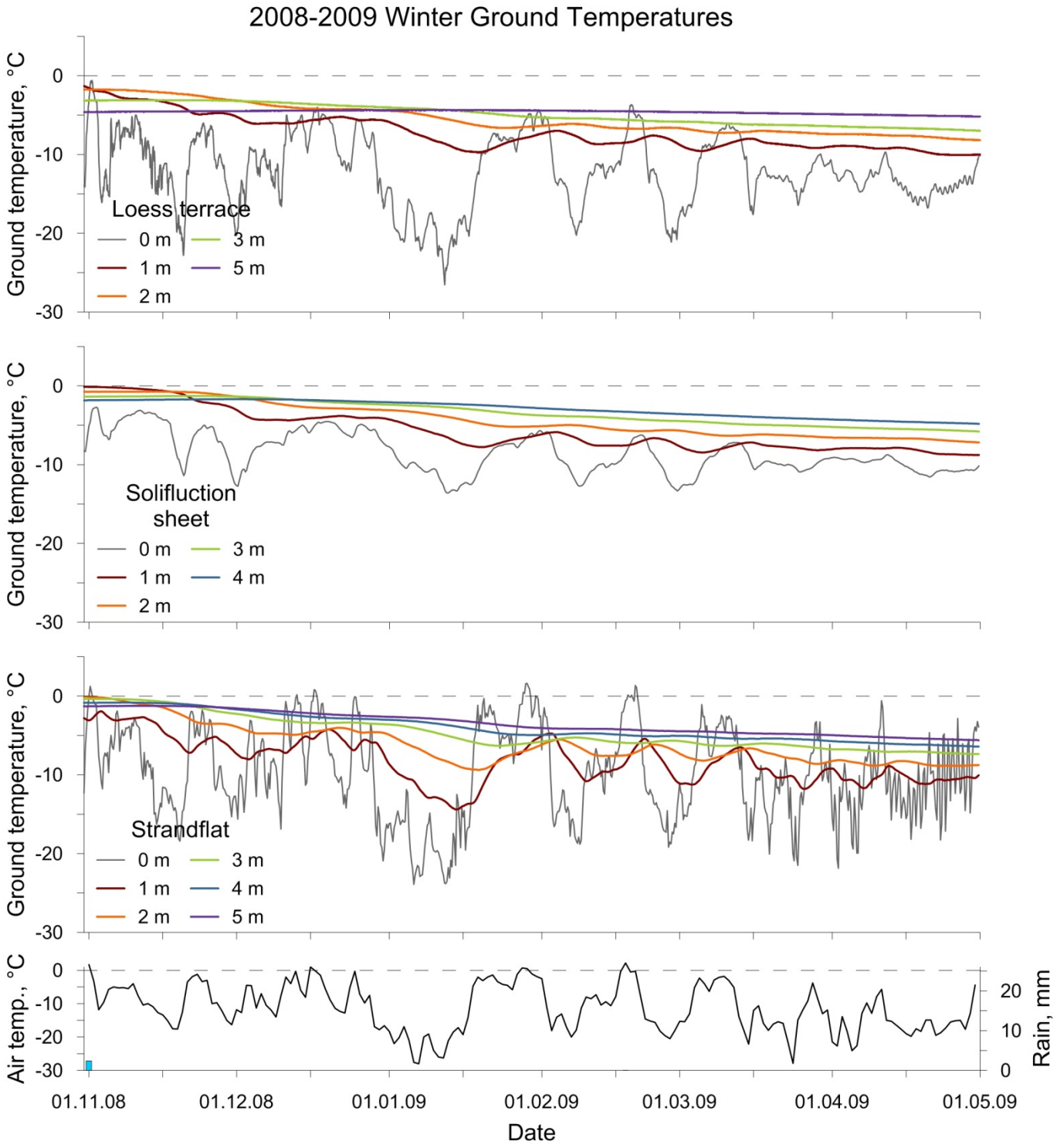

Figure B.1. 2008-2009 winter ground temperatures; line color indicates depth of temperature measurement. Svalbard Lufthavn daily mean air temperature (black line) and daily rain sum (blue bars) is plotted at the bottom.

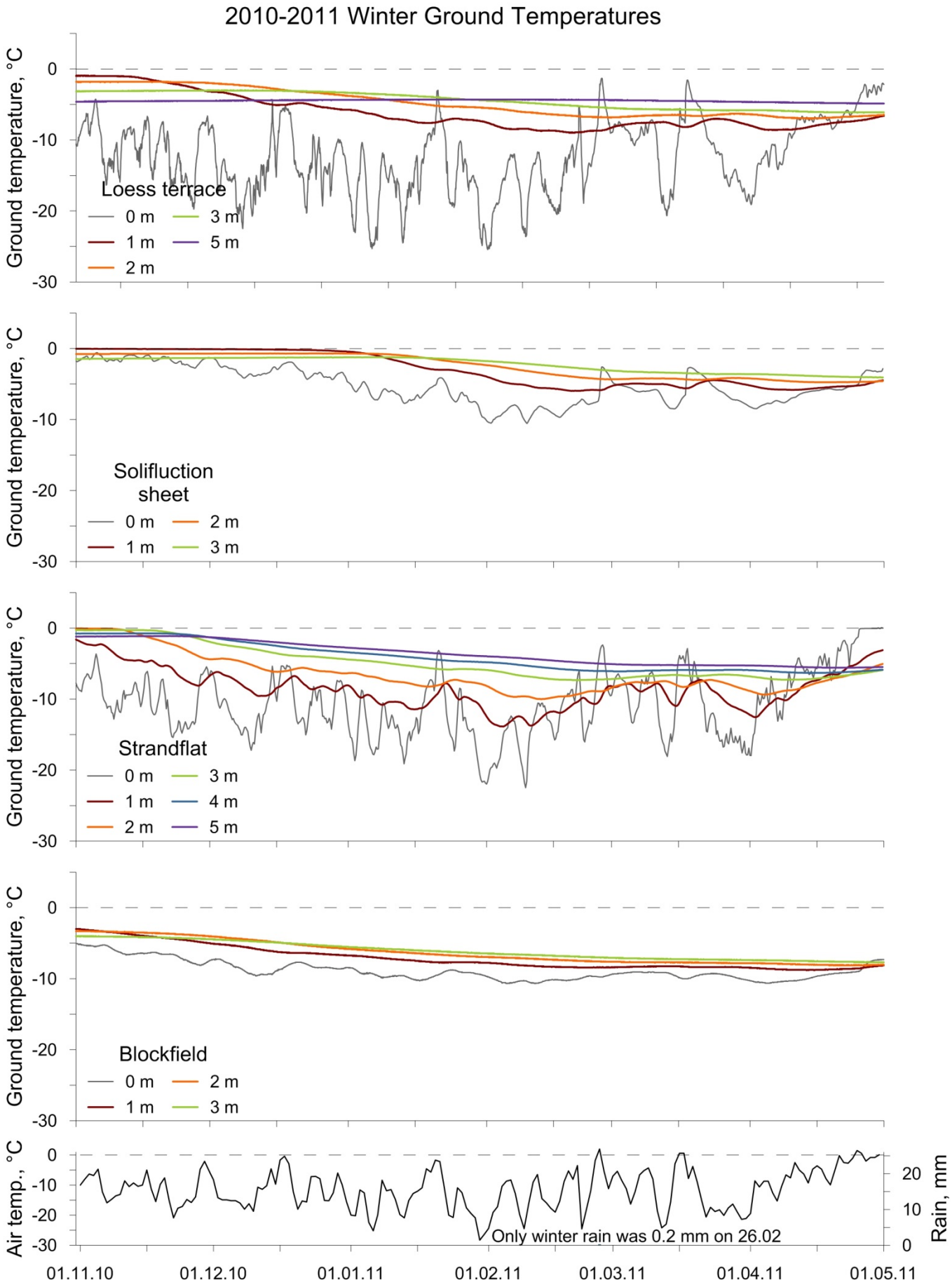

Figure B.2. 2010-2011 winter ground temperatures; line color indicates depth of temperature measurement. Svalbard Lufthavn daily mean air temperature (black line) and daily rain sum (blue bars) is plotted at the bottom.

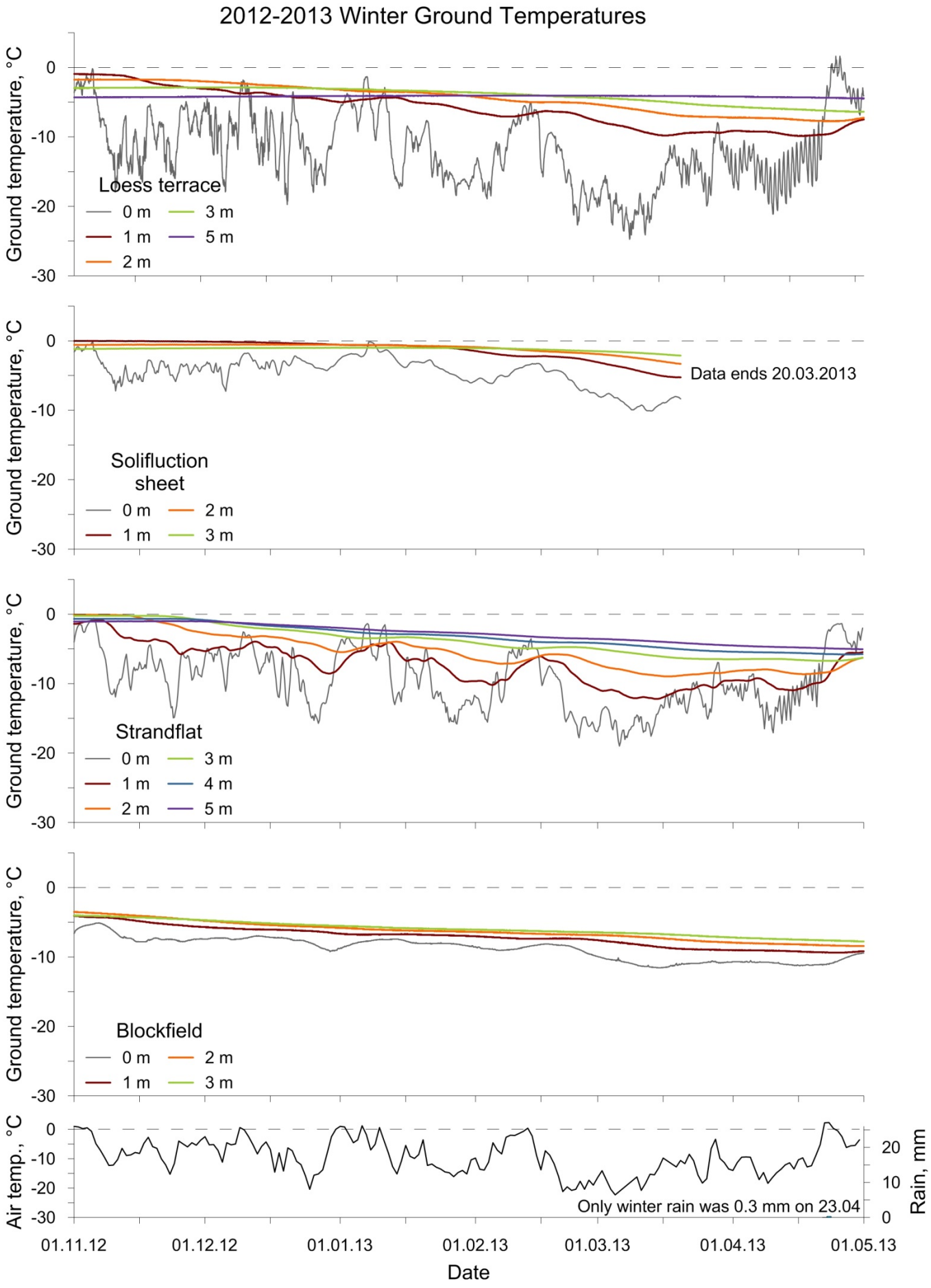

Figure B.3. 2012-2013 winter ground temperatures; line color indicates depth of temperature measurement. Svalbard Lufthavn daily mean air temperature (black line) and daily rain sum (blue bars) is plotted at the bottom.